2007:39

LICENTIATE THESIS

L

Fractionation of the stable silicon isotopes: Analytical method developments and selected applications in geochemistry

Emma Engström

Luleå University of Technology
Department of Chemical Engineering and Geosciences
Division of Applied Geology

2007:39 | ISSN: 1402-1757 | ISRN: LTU-LIC -- 07/39 -- SE

Fractionation of the stable silicon isotopes: Analytical method developments and selected applications in geochemistry

Emma Engström

Division of Applied Geology
Department of Chemical Engineering and Geosciences
Luleå University of Technology
S- 971 87 Luleå, Sweden

Abstract

During the last few decades, variations in the 'natural' isotopic abundances of stable elements (termed 'fractionation') have received considerable interest from the scientific community. Though analytical methods and techniques for the measurement of isotopic abundances with adequate figures of merit have been available for light elements (e.g. B, C, N and O) for some time, and the wealth of data produced has secured maturity status for such applications, relatively modest progress in fractionation studies devoted to high-mass elements has been made until recently, mainly because of constraints of the available analytical techniques. The situation has changed drastically with the advent of multi-collector inductively coupled plasma mass spectrometry (MC-ICP-MS), with the number of reports about natural fractionation of Fe, Cu, Zn, Mo, Cd, Sn increasing exponentially during the recent years.

In spite of the high Si abundance in nature and the importance of the element in many areas of the Earth sciences (focusing on e.g. weathering, the global Si cycle, paleoclimate studies, paleoceanography, and biological uptake), the available information on Si isotope fractionation remains rather limited due to the laborious and hazardous chemical purification procedures associated with the analyses. The focus of this thesis was the development of analytical methods for the precise and accurate measurements of Si isotope ratios, which is an absolute requirement for meaningful fractionation studies, in various matrices. This work involved detailed studies on sample preparation (including matrix separation) and refining the measurement protocol by using high resolution MC-ICP-MS. In the former stages, quantitative analyte recovery, thorough control of contamination levels and purification efficiency were the major targets, while severe spectral interferences and the need for adequate instrumental mass bias corrections challenged the latter. The performance of the method was tested in the first inter-laboratory performance assessment study of its kind with good results.

As limited examples of applications, studies on Si isotope fractionation in aqueous, plant and humus samples were performed utilizing methods developed. The efficient analyte separation, high-resolution capability of the instrument, quantitative Si recovery and accurate mass bias correction using Mg as internal standard, allowed the determination of the Si isotopic composition of natural waters and biological samples with long-term reproducibility, expressed as twice the standard deviation (2σ), equal to or less than 0.10‰ for δ^{29}Si and 0.25‰ for δ^{30}Si. Furthermore, the presence of a challenging spectral interference on ^{29}Si originating from $^{28}SiH^{+}$ was revealed during this study, indicating that instrumental resolution

in excess of 3500 is required for interference-free Si isotopic analyses. However, despite complete removal of N-, O-, and C-containing interferences appearing on the high-mass side of the Si isotopes, it was found that exact matching of both the acid matrix and the Si concentration are mandatory due to tailing from the abundant $^{14}N^{16}O^{+}$ interference on ^{30}Si.

This thesis also includes results from the first study of the Si isotopic homogeneity of major biomass components from a defined area in Northern Sweden covered by boreal forest. Since the potential impact of vegetation on the terrestrial biogeochemical cycle has attracted considerable interest, thorough characterization of the Si isotopic composition of the biomass potentially allows the utilization of this isotope system in the assessment of the relative contributions of biogenic and mineral silica in plants, soil solutions and natural waters (including fresh-, brackish- and marine waters). Isotopic analyses of the biological materials yielded a surprisingly homogenous silicon isotopic composition (relative to the NBS28 Si reference material), expressed as δ^{29}Si (2σ), ranging from (–0.14 ± 0.05)‰ to (0.13 ± 0.04)‰. Furthermore, elemental and isotopic analysis of local airborne particulate matter suggests that vegetation also accumulates silica via incorporation of exogenous Si containing primary and secondary minerals (in addition to root uptake of non-ionic silicic acid), a fact that has been neglected in previously published studies. This strongly indicates that the presence of potential surface contributions must be considered during *in situ* silicon uptake studies via the difference in dissolution kinetics for biogenic and mineral Si.

PREFACE

The thesis is based on the following papers hereafter referred to by their Roman numerals.

I. B. C. Reynolds, J. Aggarwal, L. André, D. C. Baxter, C. Beucher, M. A. Brzezinski, E. Engström, R. B. George, M. Land, M. J. Leng, S. Opfergelt, I. Rodushkin, H. J. Sloane, S. H. J. M. van den Boorn, P. Z. Vroon and D. Cardinal. An inter-laboratory comparison of Si isotope reference materials (2007) *Journal of Analytical Atomic Spectrometry* **22** 561-568.

II. E. Engström, I. Rodushkin, D. C. Baxter and B. Öhlander. Chromatographic purification for the determination of dissolved silicon isotopic compositions in natural waters by high-resolution multicollector inductively coupled plasma mass spectrometry (2006) *Analytical Chemistry* **78** 250-257.

III. E. Engström, I. Rodushkin, B. Öhlander, J. Ingri and D. C. Baxter. Silicon isotopic composition of boreal forest vegetation in Northern Sweden (2007) *Manuscript*

Papers written by the research group but not included in this thesis

A. E. Engström, A. Stenberg, D. C. Baxter, D. Malinovsky, I. Mäkinen, S. Pönni and I. Rodushkin. Effects of sample preparation and calibration strategy on accuracy and precision in the multi-elemental analysis of soil by sector-field ICP-MS (2004) *Journal of Analytical Atomic Spectrometry* 19 858-866.

B. A. Stenberg, H. Andrén, D. Malinovsky, E. Engström, I. Rodushkin and D. C. Baxter. Isotopic variations of Zn in biological materials (2004) *Analytical Chemistry* **76** 3971-3978.

C. E. Engström, A. Stenberg, S. Senioukh, R. Edelbro, B. C. Baxter and I. Rodushkin. Multi-elemental characterization of soft biological tissues by inductively coupled plasma-sector field mass spectrometry (2004) *Analytica Chimica Acta* **521** 123-135.

D. I. Rodushkin, E. Engström, A. Stenberg and D. C. Baxter. Determination of low-abundance elements at ultra-trace levels in urine and serum by inductively coupled plasma-sector field mass spectrometry (2004) *Journal of Analytical and Bioanalytical Chemistry* **380** 247-257.

E. I. Rodushkin, P. Nordlund, E. Engström anad D. C. Baxter. Improved multi-elemental analyses by inductively coupled plasma-sector field mass spectrometry through methane addition to the plasma (2005) *Journal of Analytical Atomic Spectrometry* **20** 1250-1255.

F. A. Stenberg, D. Malinovsky, B. Öhlander, H. Andrén, W. Forsling, L. M. Engström, A. Wahlin, E. Engström, I. Rodushkin and D. C. Baxter. Measurement of iron and zinc isotopes in human whole blood: Preliminary application to the study of HFE genotypes (2005) *Journal of Trace Elements in Medicine and Biology* **19** 55-60.

G. D. C. Baxter, I. Rodushkin, E. Engström and D. Malinovsky. Revised exponential model for mass bias correction using an internal standard for isotope abundance ratio measurements by multi-collector inductively coupled plasma mass spectrometry (2006) *Journal of Analytical Atomic Spectrometry* **21** 427-430.

H. D. C. Baxter, I. Rodushkin, E. Engström, D. Klockare and H. Waara. Methylmercury measurement in whole blood by isotope-dilution GC-ICPMS with 2 sample preparation methods (2007) *Clinical Chemistry* **53** 111-116.

I. I. Rodushkin, T. Bergman, G. Douglas, E. Engström, D. Sörlin and D. C. Baxter. Authentication of Kalix (NE Sweden) vendace caviar using inductively coupled plasma-based analytical techniques: Evaluation of different approaches (2007) *Anaytica Chimica Acta* **583** 310-318

Contents

1. Introduction

Investigations of the natural isotopic composition of the elements have gained considerable interest since the introduction of inorganic mass spectrometry (Becker and Dietze, 2000). Technical development, mainly via the introduction of inductively coupled plasma mass spectrometry (MC-ICP-MS), drastically increased the applicability of measurements of natural isotopic abundances. During the last decade, isotope ratio measurements have been applied for determining the isotopic abundances of unstable and stable isotopes, and hence natural and radioactive fractionations applicable when studying petrogenesis (Ding *et al*., 1996), geochronology (Faure and Mensing, 2005), paleoclimate and paleoooceanography (De La Rocha *et al*., 1997; De La Rocha *et al*., 1998; Webb and Longstaffe, 2000), weathering of primary minerals (Ziegler *et al*., 2005), as well as medical and biological processes (Becker and Dietze, 2000; Stenberg *et al*., 2005).

Silicon is the second most abundant element in the Earth's crust, making up 27% by weight, and is a main constituent in a variety of matrices such as; soils, sediments, phytoplankton, plants, natural waters, primary and secondary minerals. Significant mass-dependent fractionations of the stable isotopes of silicon are expected via the large relative mass difference between the silicon isotopes. Therefore, the combination of high abundance and large mass difference has resulted in a considerable interest for studying the isotopic composition of Si in a variety of terrestrial and extraterrestrial materials during the last five decades (Reynolds and Verhoogen, 1953; Allenby, 1954; Tilles, 1961; Taylor and Epstein, 1970; Molino-Velsko *et al*., 1986; Ding *et al*., 1996; Basile-Doelsch, 2006).

1.1 Scope of the thesis

Despite the widespread interest and great applicability of the stable isotopes of silicon, the investigation of natural fractionation of the silicon isotopes has been limited. The development in the area of stable silicon isotopes has been hampered by the hazardous, time and labour consuming conventional methods for the determination of silicon isotopic composition by inorganic mass spectrometry. The focus of this thesis was the development of more accurate, simpler and less hazardous analytical techniques for highly accurate and precise determination of silicon isotopic abundances in natural waters, biological materials and Si isotope reference materials. The availability of safer techniques for silicon isotope

analyses will hopefully attract more research groups to work in this area (De La Rocha *et al*., 2002), and hence increase the knowledge of the global biogeochemical cycle of silicon.

1.2 Silicon reservoirs

Silicon can be considered as being distributed in two main pools; the primary pool consisting of Si incorporated in primary minerals and the secondary pool consisting of Si released from the primary pool by incongruent and congruent weathering (Basile-Doelsch, 2006). The secondary pool therefore includes dissolved silicic acid in marine and fresh waters, in soil solution, ground waters and also silicon incorporated in secondary minerals (clays), phytoliths, phytoplankton and Si in fresh- and marine water sediments and particulate matter. Weathering of primary silicate minerals accounts for 45 % of the total content of dissolved major and minor elements in river water (Stumm and Wollast, 1990). Furthermore, the weathering of Si containing primary minerals removes atmospheric CO_2 (Berner, 1997), connecting the biogeochemical cycle of silicon with the global C-cycle since soil carbon is consumed and transformed to dissolved hydrogen carbonate during incongruent and congruent weathering.

Vegetation takes up large amounts of non-ionic dissolved silicic acid present in the soil solution during the growing season (Alexandre *et al*., 1997; Derry *et al*., 2005; Farmer *et al*., 2005; Ma and Yamaji, 2006). Transpiration then concentrates the absorbed silicic acid until it polymerizes and forms precipitates of amorphous opal-A, also known as phytoliths or plant stone (Ma and Yamaji, 2006). As a result, vegetation constitutes a large terrestrial biological pool of silicon with a Si concentration ranging from <0.1 to 10% (dry weight). In equatorial forests, approximately 8% of the phytoliths are preserved in the soil profile, forming a stable pool of opal-A (Alexandre *et al*., 1997), which can be used as a tracer of paleoclimate and the paleoenvironment (Kelly *et al*., 1998; Webb and Longstaffe, 2000; Trombold and Israde-Alcantara, 2005). Increased plant resistance to abiotic and biotic stress is exploited in the routine application of Si-containing fertilizers to crops (Ma and Yamaji, 2006). The plant impact of the biogeochemical silicon cycle has been assessed (Alexandre *et al*., 1997; Derry *et al*., 2005; Farmer *et al*., 2005), indicating that most of the silica entering Hawaiian streams has been taken up by vegetation, precipitated as phytoliths and dissolved again (Derry *et al*., 2005). These studies also provide evidence to support that phytoliths are the principal source of released silicon to rivers and streams during events of heavy rains and snowmelt, indicating

that Si entering the ocean has passed through the terrestrial biogenic pool (Farmer *et al*., 2005).

Dissolved silicon in natural water is present as the essentially non-ionic silicic acid, $Si(OH)_4$ (pK_{a1} ~9.8), in neutral to weakly acidic solutions (Iler, 1979). Silicic acid in fresh- and marine waters is essential for the growth of diatoms (a group of phytoplankton with shells composed of amorphous silica) and other silica mineralizing groups such as radiolarians and silicoflagellates, which utilize $Si(OH)_4$ to build their shells composed of opal (amorphous hydrated SiO_2) (De La Rocha *et al*., 1998). It has been concluded that the production and dissolution of biogenic silica dominates the marine silica cycle, in contrast to the river input and sedimentation rates of biogenic silica (Nelson *et al*., 1995). In extreme cases, it has been established that diatoms account for in excess of 90% of the primary production in marine waters, observed during midsummer blooms in the ice edge zone of the Ross Sea, Antarctica (Nelson *et al*., 1995).

1.3 Geochemistry of the stable silicon isotopes

Silicon has three stable isotopes ^{28}Si, ^{29}Si and ^{30}Si, with relative abundances of 92.22, 4.69 and 3.09 % (J. R. De Laeter *et al*., 2003), and a fourth naturally occurring radioactive isotope, ^{32}Si, with a half-life of 140 ± 6 y.

The resulting silicon isotope composition, or fractionation, is usually expressed according to the δ-notation defined as;

$$\delta^{29}Si = \left(\frac{\left({}^{29}Si / {}^{28}Si \right)_{sample}}{\left({}^{29}Si \right)_{NBS\,28}} - 1 \right) \cdot 1000\,‰ \qquad (1)$$

$$\delta^{30}Si = \left(\frac{\left({}^{30}Si / {}^{28}Si \right)_{sample}}{\left({}^{30}Si \right)_{NBS\,28}} - 1 \right) \cdot 1000\,‰ \qquad (2)$$

where the isotopic composition in the sample is expressed relative to the NBS28 quartz reference material (Coplen *et al*., 2002).

The interest in investigating natural variations in the isotopic composition of silicon started early in the 1950s (Reynolds and Verhoogen, 1953; Allenby, 1954; Tilles, 1961). In 1953,

Reynold and Verhoogen detected correlations between the natural isotopic abundances of silicon and the crystallization temperature of the mineral. Further, Allenby (1954) proposed that ^{28}Si tends to concentrate in basic rocks, while the heavier isotopes tend to concentrate in acidic and sedimentary rocks. Since the continental and oceanic crusts are primarily composed of silicate minerals (Faure and Mensing, 2005), it has been suggested that silicon isotopes can be used for investigating the origin of ore deposits and igneous rocks (Ding *et al*., 1996). Silicon is also a main constituent in extraterrestrial rocks (Faure and Mensing, 2005), resulting in considerable interest in investigating the silicon isotopic composition of lunar rocks and meteorites (Taylor and Epstein, 1970; Molino-Velsko *et al*., 1986).

It has been concluded that biological and physical processes cause fractionation of the stable silicon isotopes (De La Rocha *et al*., 1997; Ding *et al*., 2005; Ziegler *et al*., 2005; Opfergelt *et al*., 2006*a*, *b*), opening up the possibility to utilize the silicon isotope system in biological- and environmental studies. The relative mass difference between the silicon isotopes exceeds 3%, indicating that large mass-dependent fractionations are to be expected. However, silicon is always covalently bonded to O in the nature, forming SiO_2 or the stable silicate anion SiO_4^{4-} (e.g. forming dissolved silicic acid or primary minerals with Na, K, Ca when Al^{3+} has substituted Si^{4+} to form the aluminosilicate anion), decreasing the relative mass difference between the isotopomers. In 2005, Zeigler *et al.* concluded that weathering of basalt preferentially releases ^{28}Si, while secondary mineral formation preferentially removes ^{28}Si from solution, resulting in depletion of ^{28}Si in soil solution in comparison to the secondary minerals. This opens up the possibility to use stable silicon isotopes for tracing silicon pathways from the primary to the secondary pool.

It has been demonstrated that diatoms preferentially take up ^{28}Si during formation of biogenic silica (De La Rocha *et al*., 1997), resulting in an isotopic fractionation of approximately 1.0‰. This discrimination against ^{29}Si and ^{30}Si successively enriches the reservoir of dissolved silicic acid in the heavier isotopes assuming steady-state conditions, suggesting that increased utilization of silicic acid results in diatom opal shells with heavier silicon isotopic composition, allowing Si isotopic information to be applied in paleoclimatic and paleooceanographic studies (De La Rocha *et al*., 1997; De La. Rocha *et al*., 1998).

In a thorough study by Opfergelt *et al.* (2006*b*), it has been proposed that plants fractionate silicon isotopes during uptake of dissolved silicic acid present in the soil solution, discriminating against the heavier isotopes similar to diatoms (Opfergelt *et al*., 2006*b*). Further, intra-plant variations in the silicon isotopic composition have been detected, with

successive enrichment of heavier isotopes higher up in the vascular plants, allowing the utilization of silicon isotope information in studies of biological uptake of dissolved silicic acid (Opfergelt *et al*., 2006*a*, *b*; Ding *et al*., 2005). Moreover, similar to O-isotopes, it has been proposed by Ding *et al*. in 2005 that the stable pool of hydrated opal-A (phytoliths), deposited in the soil profile, has a potential to be used in paleoclimatic studies.

Since the assessment of the plant impact on the biogeochemical silicon cycle has attracted considerable attention during the last decade (Alexandre *et al*., 1997, Derry *et al*., 2005, Farmer *et al*., 2005), thorough characterization of the silicon isotopic composition of the terrestrial biogenic Si reservoir would potentially open up the possibility for using Si isotope information in the assessment of the relative contribution from biogenic and mineral silicon in soil solution, ground water, biogenic Si and in natural waters and plants. However, the use of vegetal Si isotopic information in the assessment is hampered by the inhomogeneity in the Si isotopic composition of the phytoliths (Basile-Doelsch, 2006). So far, the homogeneity of the biogenic silicon in a defined area has been scarcely investigated.

The number of publications about silicon isotopes in plants is still limited, which might be a result of the extensive sample preparation procedure required for the isotopic analyses (consisting of four or more separate steps) (Ding *et al*., 2005; Opfergelt *et al*., 2006*a*, *b*). Previous studies of the silicon isotopic composition in plants have been focused on the uptake mechanism of silicic acid via the root system and have therefore been limited to include only one species (Opfergelt *et al*., 2006*a*, *b*; Ding *et al*., 2005).

The accumulated silicon in plants originates from two distinct sources; dissolved silicic acid in the soil solution (Ma and Yamaji, 2006) and silicon containing exogenous material partly consisting of primary silicates, quartz and clays (Wyttenbach and Tobler, 1998). The exogenous material is present in plants as surface contaminations incorporated in the structure (Wyttenbach and Tobler, 1998). Thorough speciation is of the utmost importance in the assessment of the plant impact on the biogeochemical silicon cycle, since the dissolution kinetics of the exogenous particles and the plant phytoliths differs significantly.

Since secondary mineral formation and the formation of biogenic silicon by diatoms and plants preferentially remove ^{28}Si from the reservoir of dissolved silicic acid, natural waters are enriched in heavier isotopes (De La Rocha *et al*., 2000; Ding *et al*., 2004; Cardinal *et al*., 2005; Basile-Doelsch, 2006). Silicon isotopic information in natural waters can potentially be applied when tracing the origin (biogenic or mineral) of the dissolved silicic acid in soil or surface water, increasing the knowledge of the global biogeochemical silicon cycle (George *et*

al., 2006). Characterization of the silicon isotopic composition of river water is of significance via the large amounts of dissolved silicic acid and particulate matter transported by the rivers to the world oceans (Treguer *et al*., 1995; George *et al*., 2006). The silicon isotopic composition of marine waters is therefore very sensitive to changes in those of river water (George *et al*., 2006).

Silicon isotopic compositions in the primary and secondary Si pools are summarized in Figure 1.

1.4 Mass spectrometric analyses of silicon isotopic abundances

For decades, gas source isotope ratio mass spectrometry (IRMS) has been the predominant technique for the determination of silicon isotopic compositions, and has been applied to a variety of sample matrices, such as primary and secondary minerals, natural waters, diatoms and phytoliths (Douthitt, 1982; De La Rocha *et al*., 1997; De La Rocha *et al*., 1998; Ding *et al*., 2004; Ding *et al*., 2005), with satisfactory precision ranging from 0.1 to 0.2 ‰. However, the determinations of silicon isotopic compositions using this technique have required the use of hazardous preparation methods, which has limited development in this research area (De La Rocha *et al*., 1996). The most widely applied protocols consist of precipitating amorphous silica followed by (laser-driven, De La Rocha *et al*., 1996) fluorination where SiO_2 is reacted with purified F_2 or BrF_5 to form SiF_4 in gaseous form (Douthitt, 1982; De La Rocha *et al*., 1996, De La Rocha *et al*., 2000; Ding *et al*., 2004; Ding *et al*., 2005). The SiF_3^+ ion intensities at *m*/*z* 85, 86 and 87 are then monitored. However, analytical developments in the field of IRMS have eliminated the use of the hazardous compounds F_2 or BrF_5 to produce SiF_4 (g) (also a very toxic substance by inhalation and corrosive to eyes and skin (Air Liquide)) (M. Brezezinski et al., 2006).

The introduction of multi-collector inductively coupled plasma mass spectrometry (MC-ICPMS) offered important advantages over the conventional methods, such as more time-efficient, safer sample preparation techniques and higher sample throughput (De La Rocha, 2002). However, the use of MC-ICPMS has been associated with difficulties in accurately measuring ^{30}Si (De La Rocha, 2002, Cardinal *et al*., 2003), due to the presence and magnitude of the polyatomic interference consisting of $^{14}N^{16}O$ on the ^{30}Si isotope and also analytical difficulties originating from potential matrix effects during the isotopic analyses. Despite the latter analytical disadvantages associated with silicon isotopic analysis by MC-ICP-MS, it constitutes presently the most widely applied technique during the last few years.

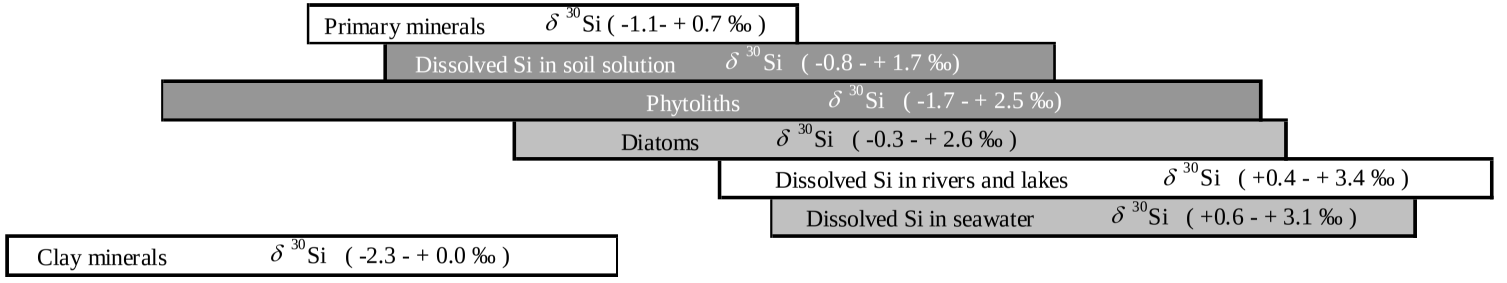

Figure 1. Summary of the reported silicon isotopic composition of selected primary and secondary silicon reservoirs from I. Basile-Doelsch 2006 .

1. 5 Major principles of MC-ICP-MS

1.5.1 Single- versus multi-collector ICP-MS

The requirement for more accurate and precise, as well as more sensitive, mass spectrometric techniques within nuclear, geological, environmental, biological and medical industries, motivated the development of multi-collector inductively coupled plasma mass spectrometers (Platzner, 1997; Becker and Dietze, 2000). The thermal ionization mass spectrometric technique (TIMS), has dominated isotopic analyses of solutions over the last decade. However, the analyses are associated with laborious- and time consuming chemical preparation procedures, as well as analytical difficulties in measuring elements with high first ionization energies (Platzner, 1997). The introduction of the inductively coupled plasma (ICP) in the 1970s was a significant contribution to the field of multielement trace analysis, because of its high detection power and rapid sample throughput without requiring extensive sample preparation (Platzner, 1997). In brief, the plasma is formed when energetic electrons, generated by a rf current, are supplied to an Ar gas stream (termed 'plasma gas') flowing through a plasma torch. The incoming species are vaporized, atomized, excited and ionized in the plasma prior to introduction to the mass spectrometer (Montaser, 1998). In comparison to other ionization sources, the ICP offers high sensitivity for almost all elements, even those with high first ionization potentials (>7.0 eV) (e.g. Si, Fe and Hf) (Wieser and Schwieters, 2005). Temporal fluctuations in the plasma source as a result of variations in the plasma temperature, aerosol characteristics or sample matrix, to mention a few, limit the precision during isotope ratio measurements using conventional single collector instruments, where each isotope is measured sequentially. Instruments capable of measuring the studied isotopes simultaneously were therefore developed, significantly improving the precision of the isotope ratio measurement (Wieser and Schwieters, 2005). In magnetic sector mass spectrometers, the ions are separated when a constant magnetic field is applied to the ion beam, allowing the unique possibility of detecting the isotopes individually in the focal plane of the mass spectrometer (Wieser and Schwieters, 2005). Isotope ratio measurements using single-collector instruments are performed by varying the magnetic field strength applied to the ion beam, and thereby sequentially measuring each isotope of interest in a single detector with a fixed position. In a multi-collector magnetic sector field instrument, the isotopes are measured simultaneously, in up to sixteen static and/or variable detectors. Further, the significantly reduced measuring time using multi-collectors allows analysis of smaller sample volumes. The first generation of multi-collector instruments had static detectors, limiting the

applicability due to the large relative mass difference for lighter elements. Multi-collector instruments, where the positions of the detectors are adjustable with micrometer precision along the focal plane of the mass spectrometer, allow isotopic analyses of a wider range of isotope systems (Wieser and Schwieters, 2005).

1.5.2 Low- versus high-resolution MC-ICP-MS

The increasing interest in isotope systems with masses ranging from approximately 24-60 (e.g. Ca, Fe, Mg and Si), motivated the development of high-resolution multi-collector mass spectrometers. Bradshaw *et al*. described the first high-resolution mass spectrometer combined with an ICP as ion source in 1989. Highly accurate and precise isotope analyses require removal of isobaric interferences appearing at the high- and low-mass sides of the isotopes of interest (high resolution spectra acquired using the single-collector high-resolution sector-field ICP-MS Element2 are shown in Figure 2 (a), (b) and (c) in Paper II). Polyatomic interferences originating from the sample matrix or the ionization source generally have a mass below 90 amu, therefore appearing at the same nominal mass as the isotopes of interest (e. g. $^{14}N^{16}O^{+}$ on $^{28}Si^{+}$, $^{40}Ar^{16}O^{+}$ on $^{56}Fe^{+}$) (Weyer and Schwieters, 2003).

Single-collector instruments with high-resolution capability include two slits (termed ‘entrance’ and ‘exit’ slit) of equal width, producing sharp triangular peaks. The isobaric interferences therefore appear as separated peaks on the low- or high-mass sides of the isotope of interest. However, flat-topped peaks are a requirement for high precision isotope ratio measurement, since small fluctuations in the mass calibration, magnet field or the ICP source would otherwise severely affect the precision for single-collector instruments (Weyer and Schwieter,s 2003). The requirements for high precision, i.e. wide flat-topped peaks and quantitative removal of isobaric interferences, are achieved in multi-collector instruments by using a narrow entrance slit and a wider exit slit. The double focusing multiple-collector sector-field ICP-MS Neptune, utilized for isotope ratio determinations throughout this study, is presented in Figure 2.

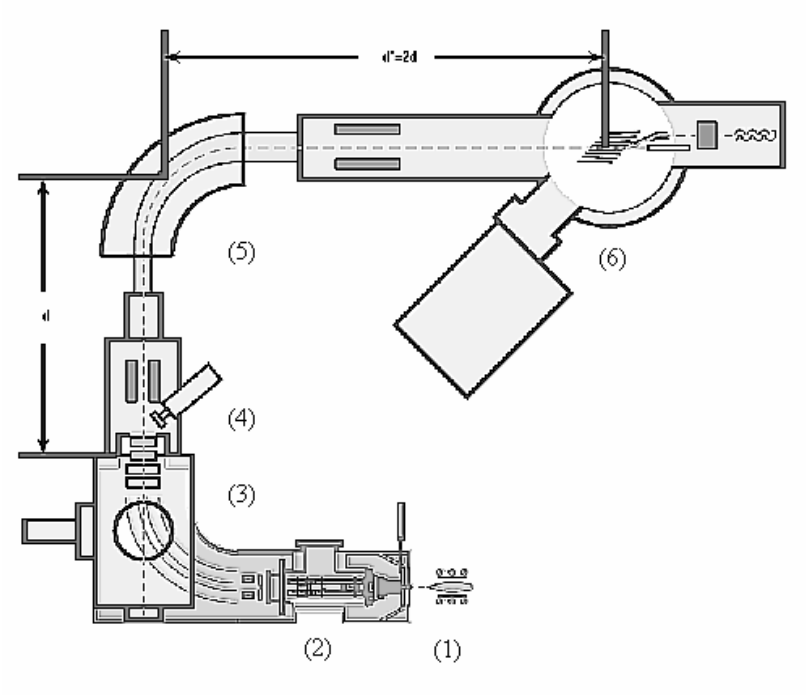

Figure 2. Schematic presentation of the high-resolution MC-ICP-SFMS Neptune; (1) Plasma region; (2) interface region and transfer optics; (3) electrostatic analyzer (termed 'ESA'); (4) analyzer gate; (5) magnetic analyzer; (6) detector.

Since the kinetic energy distribution of the ions entering the mass spectrometer is broad, a magnetic analyzer (5) alone is not sufficient for achieving high mass resolution (Gäbler, 2002). Instead, the ions are focused with respect to kinetic energy in the electrostatic analyzer (termed 'ESA') (3), located after the three switchable entrance slits (Gäbler, 2002). The Neptune has a forward Nier-Johnson geometry (the magnet is positioned after the ESA), allowing individual detection of the isotopes on the focal plane of the instrument (Gäbler 2002). The analyzer gate on the Neptune (4) is positioned between the high-vacuum part and the detector side of the instrument with two ion getter pumps further enhancing the vacuum.

The eight moveable detectors (Faraday cups L4, L3, L2, L1, H1, H2, H3 and H4) (6) can be positioned along the focal plane with μm precision, since four of them are equipped with motors (L3, L1, H3, L1). An additional fixed detector (the center cup, C, equipped with a Faraday cup and an secondary electron multiplier) is positioned between L1 and H1. The maximum relative mass range for the outermost detectors L4 and H4 is 17 % (Weyer and

Schwieters, 2003). More detailed descriptions of the Neptune are given elsewhere (Weyer and Schwieters, 2003; Wieser and Schwieters, 2005). Isotopic analyses using the Neptune can be performed in low-, medium- and high-resolution modes using entrance slits of decreasing slit width (250, 30 and 16 μm) (Weyer and Schwieters, 2003). Changing the slit width from 16 to 30 μm increases the sensitivity by a factor of approximately two, and the sensitivity in low-resolution mode (slit width 250 μm) is increased by a factor of approximately 3-3.5 in comparison to medium resolution. The exit slits on the Neptune physically consist of the detector edges, producing flat-topped peaks with sharp edges. The interferences therefore appear as distinct steps on the flat-topped peaks (mass scans of the silicon isotopes are presented in Figure 2 (d) in Paper II). However, it should be noted that isobaric interferences appearing at the low-mass side of the isotopes (e.g. $^{58}Fe^{++}$ on ^{29}Si) will not be separated using this approach. Instead, chemical purification is required for removal of doubly charged species (Weyer and Schwieters, 2003).

The resolution, *R*, of a mass spectrometer is defined according to;

$$R = m / \Delta m \qquad (3)$$

where *m* and Δm represent the average mass and the mass difference between two adjacent peaks, respectively (Montaser, 1998; Vanhaecke and Moens, 2004). Different definitions of the mass difference, Δm, have been applied to multi- and single-collector mass spectrometers. For single-collector instruments (conventional approach), the mass difference, Δm, is defined as the full width of the peak at 5 % of its height (Montaser, 1998, Vanhaecke and Moens, 2004). Since multi-collector instruments produce flat-topped peaks, the conventional approach cannot be used. Instead, Weyer and Schwieters (2003) have proposed an alternative approach where the *resolving power* is calculated by defining, Δm^*, as the mass difference between 5 % and 95 % of the peak height. In comparison, the resolving power exceeds the resolution by a factor of 2 or more. The Neptune has a maximum resolving power of 9000-10000 (Wieser and Schwieters, 2005).

1.5.3 Isotope ratio measurements and mass bias effects in MC-ICP-MS

Ions are subjected to mass bias effects originating before the entrance slit and favouring transmission of heavier ions. One source of mass bias effects results from space charge effects in the skimmer cone region, caused by repulsive forces acting within the ion beam. Lighter

isotopes are therefore predominantly lost from the central ion beam, resulting in a positive deviation in the measured isotope ratio $^{x}m/^{y}m$, assuming $x > y$ (e.g. $^{29}Si/^{28}Si$). Typically, mass bias of >10 %, 2% and <1% is observed for Li, Fe and U, respectively (Andrén *et al.*, 2004, Weyer and Schwieters, 2003), but the absolute magnitude is dependent on factors such as sample matrix, plasma instability, sample gas flow rate, or the sample introduction (Andrén *et al.*, 2004). The magnitude of the mass bias is often more than 10 times greater than isotopic fractionation of stable isotopes in nature, and therefore accurate correction is mandatory for achieving high quality isotopic ratio analyses.

There are two main approaches for correction of these effects; (1) internal and (2) external normalization (Platzner 1997). Internal normalization can be used for elements with three or more isotopes and is based on correction of the ratio of interest with another isotope pair of the same element, e.g. the Sr and Nd isotope systems. However, this approach is not applicable when determining the total isotopic abundance of an element or for elements with natural variation in all of the isotope pairs, e.g. Pb where three of its four isotopes are produced by radioactive decay. Instead, it has been proposed that an element with similar mass and chemical, as well as physical characteristics can be used for the correction, e.g. correction of Pb isotope ratios using Tl (Rehkämper and Mezger, 2000).

Recently, Baxter *et al.* (2006) have developed a revised model for external normalization using an internal standard, first proposed by Woodhead (2002). In this approach, the measurements solutions (samples, as well as standards) are spiked with a known amount of an internal standard with similar chemical and physical properties as the element of interest. The purpose of adding an internal standard to the samples is to correct for time-, matrix- or instrumental variations in mass bias. Using this protocol, it is mandatory that the isotopes of the internal standard are free from isobaric interferences and that the element used as internal standard is not present in the sample. The accuracy of the resulting isotope ratios is established by using a standard-bracketing technique (Baxter *et al.*, 2006), where the standard consists of a reference material with known isotopic composition.

2. Achieving highly precise and accurate determinations of the silicon isotopic composition by high-resolution multi-collector inductively coupled plasma mass spectrometry

2.1 Development of a measurement protocol for high-quality determinations of silicon isotopic ratios $^{29}Si/^{28}Si$ and $^{30}Si/^{28}Si$

The first step towards achieving accurate and precise isotopic analyses consists of optimizing the instrumental sensitivity. Increased sensitivity reduces the relative impact of the background noise on the instrumental signal, improving the propagated instrumental precision. Further, higher sensitivity allows isotopic measurement of samples with lower silicon concentrations and sample volumes, as well as higher dilutions of the measurement solutions, minimizing potential matrix effects. To this end, if properly implemented, more efficient ion transmission can be achieved by using a platinum guard electrode (CD system activated) (Appelblad *et al*., 2000) and Ni skimmer X-cone. Moreover, daily tuning of sample gas flow, ion lenses and zoom optics is required prior each measurement sessions. In paper II included in the present thesis, a measurement protocol for silicon isotope ratio determinations was developed and presented. Since there are severe isobaric interferences on all of the silicon isotopes (^{28}Si, ^{29}Si and ^{30}Si), the isotopic measurements were conducted in high-resolution mode, i.e. a *resolving power* of approximately 8 000-10 000 depending on the condition of the high-resolution entrance slit. The instrumental sensitivity of the Neptune operating in high-resolution achieved for ^{28}Si was superior to that obtained using Nu Plasma MC-ICP-MS in low resolution (De La Rocha, 2002) with conventional introduction system and comparable to that obtained for the same instrument equipped with a desolvating nebulizer device (Cardinal *et al*., 2003).

Identification of mono- and polyatomic interferences appearing at the low- or high-mass sides of the silicon isotopes is of the utmost importance for achieving highly accurate and precise isotope ratio measurements. There are a number of polyatomic N-, O- and C-containing interferences appearing at the high-mass side of the silicon isotopes (detailed in Table 3 in Paper II). According to calculations based on the exact masses and the conventional definition of resolution (Vanhaecke and Moens, 2004), a *resolving power* in excess of 3200 (corresponding to a resolution of approximately 1600) is sufficient for quantitative removal of the latter polyatomic interferences. However, high-resolution spectra of a single element Si-

standard, acquired using the Element2 (presented in Figure 2 (a), (b) and (c) in Paper II), revealed the presence of two challenging polyatomic interferences appearing at the high-mass sides of ^{29}Si and ^{30}Si, which have been identified by their exact masses to originate from $^{28}SiH^+$ and $^{29}SiH^+$. The insufficiency of using matrix-matched blanks to correct for spectral interferences becomes evident when the most challenging interferences originate from the analyte itself. Due to the small mass difference between the silicon isotopes and the corresponding hydrides, it is required that the positions of the Faraday cups are adjusted for exact alignment of the rising edges of the peaks for the purpose of maximizing the width of the interference free plateau. The deviation in accuracy caused by these interferences is determined by the magnitude of the variations in the hydride formation. Preliminary experiments have shown that the bias in $\delta^{29}Si$ introduced by the $^{28}SiH^+$ interference in some cases might exceed 0.4 ‰, which is not negligible compared to a range of isotopic fractionations observed in nature. However, the high-resolution capability of >3510 using the conventional definition of resolution (Vanhaecke and Moens, 2004) of the Neptune is sufficient for performing interference-free isotopic measurements. Further, since the isotopic abundance for ^{29}Si is approximately 20 times lower than the corresponding value for ^{30}Si, the contribution from $^{29}SiH^+$ on ^{30}Si is within the instrumental precision (~0.2 ‰) for the ratio $^{30}Si/^{28}Si$. The magnitude of the polyatomic interference on ^{30}Si originating from $^{14}N^{16}O^+$ and analytical difficulties in measuring $^{30}Si/^{28}Si$ has been reported previously (De La Rocha, 2002; Cardinal *et al*., 2003). Despite the fact that the instrumental high-resolution capability is sufficient for complete removal of this interference, tailing might be a problem due to the high concentration levels of $^{14}N^{16}O^+$. Further, the use of the Pt guard electrode has been reported to be associated with increased levels of oxide formation (P. K. Appelblad *et al*., 2000), potentially leading to more pronounced difficulties measuring the $^{30}Si/^{28}Si$ isotope ratio. Further, the reduced level of oxide formation by the use of desolvating nebulizer systems (Montaser, 1998), such as that employed by Cardinal *et al*. (2003), would be beneficial in order to attenuate the major source of the interference, although minor formation would still be expected as a result of air entrainment into the plasma. It should also be mentioned that Cardinal *et al*. (2003) did not detect the $^{28}SiH^+$ interference on $^{29}Si^+$ (Fig. 3 in Paper II), although it is unclear whether this resulted from minimization of precursor H-radicals *via* desolvation, or due to resolution limitations of the mass spectrometer. In either case, it is always beneficial to thoroughly investigate the potential occurrence of spectral interferences during method development for MC-ICP-MS using an instrument providing complete separation of adjacent masses, such as the Element2 exploited in this study.

Even though the high-resolution capability of the Neptune can overcome the majority of the interferences appearing at the same nominal mass to charge ratio, *m*/*z*, as the analyte of interest, there are still a number of unresolved spectral interferences appearing at the low-mass side of ^{28}Si, ^{29}Si and ^{30}Si (see section 1.5) consisting of doubly charged ^{56}Fe, ^{58}Fe, ^{58}Ni and ^{60}Ni. These elements must be chemically removed prior to the instrumental isotopic analyses (with reference to section 2.2).

Accurate and precise mass bias corrections are an absolute requirement for achieving high-quality silicon isotope ratio determinations. Since the addition of an internal standard offers the possibility of sample-specific on-line mass bias corrections, this approach is recommended for silicon isotope ratio determinations. Magnesium possesses the physical, as well as chemical, characteristics required of an internal standard for on-line corrections during silicon isotopic analyses. The magnesium isotopes, ^{25}Mg and ^{26}Mg, exhibit similar isotopic masses and are virtually interference free, confirmed by acquiring high resolution spectra using the double-focusing sector-field Element2 (not shown), with a maximum mass resolution of 10 000 calculated using the conventional approach (Vanhaecke and Moens, 2004). Additionally, the isotopes ^{25}Mg and ^{26}Mg are present at relatively high abundances (10.00 and 11.01 %, respectively) (De Laeter *et al*., 2003). De La Rocha first proposed the use of magnesium for on-line mass bias correction in 2002, but the observed difference in the transmission of Si and Mg implied that the level of mass discrimination would not be similar. However, Cardinal *et al*. demonstrated the potential of Mg doping for accurate correction for mass bias in a thorough study in 2003. The maximum contribution from the potentially interfering $^{24}MgH^+$ has theoretically been estimated to be 0.02‰ as a result of variations in the level of hydride formation, which can be considered as negligible. The efficiency of the on-line mass bias correction was thoroughly evaluated in Paper II.

The relative mass difference between ^{25}Mg and ^{30}Si contributes with instrumental difficulties in performing truly simultaneous measurements (Weyer and Schwieters, 2003), since the mass difference between ^{25}Mg and ^{30}Si exceeds 17 % (maximum allowed by the Neptune). The isotopic measurements must therefore be performed in multi-dynamic mode where the magnet mass is changed between measurement of Mg and Si isotopes. As a result, the cup configuration for the Neptune consisted of a main cup configuration where ^{28}Si, ^{29}Si and ^{30}Si are monitored in H1, L1 and L2, and where the magnesium isotopes, ^{25}Mg and ^{26}Mg, were monitored using cups L2 and the center cup (sub configuration). This approach is less effective than truly simultaneous measurements for correction of temporal variations in mass

bias, but equally effective for correction of non-spectral interferences. Further, the time required for the isotopic analyses increased by approximately a factor of two. However, De La Rocha (2002) experienced a required total measuring time, in some cases, in excess of 40 min during isotope analyses using the Nu Plasma MC-ICP-MS instrument in wet plasma mode, exceeding our estimation by a factor of 2-3 (reported in Paper II and III).

Paper I presents the results of a unique inter-laboratory comparison of silicon isotopic abundances in reference materials consisting of amorphous and crystalline quartz. Eight different research groups participated in the inter-laboratory comparison, of which two groups used gas-source IRMS for isotope analyses. The research groups, together with the corresponding sample preparation techniques and instrumentation employed during the present study, are presented in Table 1 in Paper I.

The comparison programme included samples that were virtually matrix free after dissolution of the solid material using HNO_3/HF, implying that chemical or physical purification procedures are not an absolute requirement for accurate and precise isotopic analyses using MC-ICP-MS following acid dissolution. The samples were distributed by the program coordination (Ben C. Reynolds) to avoid potential systematic errors as a result of inter-batch differences in the silicon isotopic composition of the reference materials. The samples included in the inter-laboratory comparison programme were the NBS28 quartz sand (used as the isotopic standard, i.e. δ^{29}Si and δ^{30}Si = 0‰), the silicon isotopic reference material IRMM018 (solid SiO_2), a highly fractionated sample denoted Big Batch and a purified diatomite sample (Diatomite). The major aim of the study was to detect instrumental- and/or method specific systematic variations in the resulting silicon isotopic abundances between different research groups, it being especially important to detect inter-laboratory differences when new studies are based on previously published results.

The silicon isotopic compositions of the distributed reference materials have been reported previously by Carignan *et al*. (2004) and Ding *et al*. (2005). The latter study presents results for IRMM018 (relative to the primary reference material for Si isotopes, NBS28) by IRMS following the SiF_4-method (Ding *et al*., 2004). The measured δ^{29}Si (-0.03 ‰) and δ^{30}Si (-0.05 ‰) implies that the isotopic composition of NBS28 and IRMM018 do not differ significantly. Results reported by The Royal Museum for Central Africa (Damien Cardinal *et al*.) and University of South California, Santa Barbara, (Karen Ziegler and Mark Brezinski) (Carignan *et al*., 2004) for the Big Batch sample, δ^{29}Si of (-5.29 ±0.08)‰ (2σ) and (–5.39

±0.18)‰ (2σ), respectively, indicate that the silicon isotopic composition of the reference material is highly fractionated.

The resulting δ^{29}Si and δ^{30}Si -values reported for Diatomite, Big Batch and IRMM018 are summarized in Figure 3. The reported results reveal a good agreement between the datasets provided by the participating research groups, excluding the possibility of large instrument (IRMS versus MC-ICPMS) or method (acid dissolution versus fusion and/or ion-exchange versus precipitation techniques) specific systematic errors. For all of the samples included in the comparison, the resulting δ^{29}Si ± 1σ and δ^{30}Si ± 1σ reported by the participating group fall within the overall average δ-values ± 1σ. Using the quartile range for individual isotopic measurements, the resulting differences between the average values reported for δ^{29}Si and δ^{30}Si are limited to 0.13‰ and 0.20‰, respectively.

Statistical analysis of the datasets has been performed by the program coordinator (Ben C. Reynolds) to test for significant differences between the reported mean values, and the results are thoroughly discussed in Paper I. In summary, there were no significant differences found for Big Batch or Diatomite excluding mean values with limited number of replicates ($n < 6$). However, several differences were found for IRMM018. The results reported by Group 5 (using IRMS) significantly differ from the results reported by Groups 1, 3 and 8, potentially indicating that there are significant instrument specific differences between the reported mean values. Considering the agreement for the other reference materials, this is suggested to most likely be a result of heterogeneity or contamination of the IRMM018 standard material. Further, we have noticed a difference in the chemical behaviour of this particular material during the preparation, where IRMM018 appears to be more reactive than the other two samples, potentially leading to detectable method specific systematic errors.

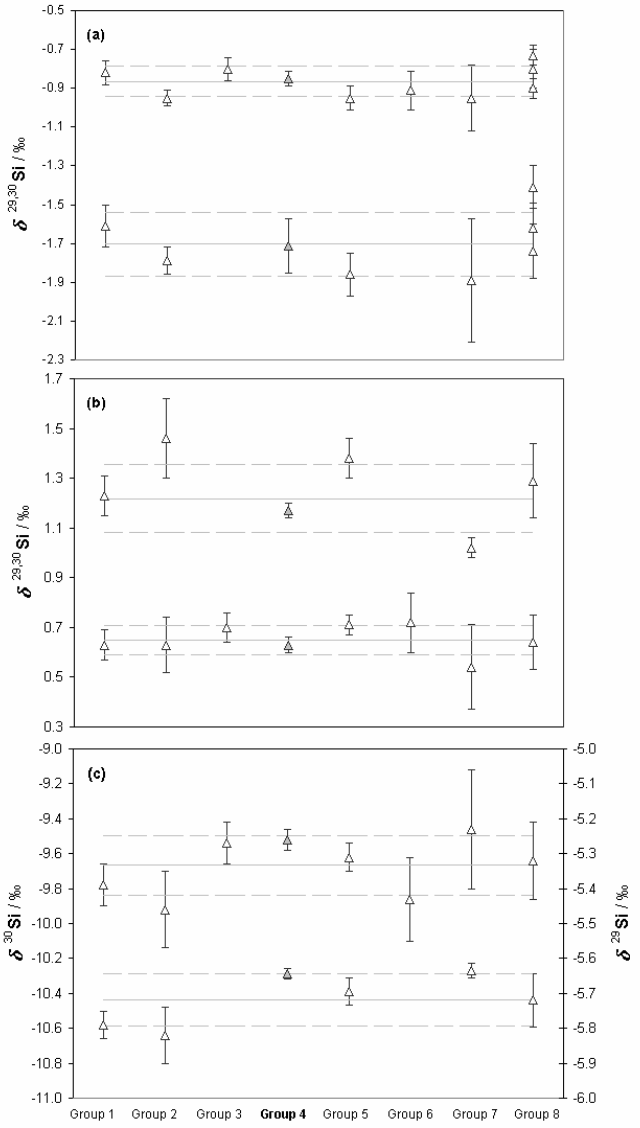

Figure 3. Graphical presentation of the reported δ^{29}Si and δ^{30}Si values for (a) IRMM018, (b) Diatomite and (c) the highly fractionated material Big Batch included in the Si-isotope inter-laboratory comparison, the uncertainty bars correspond to 2σ, the grey lines represent the average δ^{29}Si- and δ^{30}Si values, and the dashed lines denote $\pm 1\sigma$ uncertainty boundaries. The δ^{29}Si and δ^{30}Si values reported by ALS Analytica AB / Luleå University of Technology (Group 4) are presented as grey triangles. In (c), the uppermost dataset represent the reported δ^{29}Si values for Big Batch.

The silicon isotopic composition for IRMM018 reported by the research groups participating in the inter-laboratory comparison (ILC) and those reported by Ding *et al*. (2004) exhibit large discrepancies, for which we have no explanation.

The reported δ^{29}Si and δ^{30}Si -values reported for Diatomite, Big Batch and IRMM018 are presented in a three-isotope plot constructed according to the approach proposed by Young *et al*. (2002) (Figure 4), where it is concluded that analytical precision (< 0.1‰) allows the differentiation between kinetic and equilibrium mass-dependent fractionation. The scales have been reduced to include only results for IRMM018 and Diatomite for the purpose of graphically emphasizing potential deviations from the true mass-dependent fractionation line. Kinetic fractionation is a result of molecular or isotopic movement (and therefore takes consideration of the elemental speciation), while the resulting equilibrium fractionation depends on the isotopic masses alone. Theoretical slopes of the linear function can be calculated using the relationships presented in Young *et al*. (2002). These experimental slopes are thereafter compared with the experimental slope, preferentially determined using linear regression with weighting of both axes. The calculated slopes for silicon are equal to 1.931 and 1.964 (1.984 for SiO_2) for equilibrium and kinetic fractionation, respectively. In natural systems, e.g. diffusion studies or when studying temporal variation in the isotopic composition, it might be very valuable to differentiate between the two types of mass-dependent fractionation. However, in purely analytical studies the calculated slopes can be used to test the robustness of the data. Analytical problems are easily detected since unresolved interferences or inaccurate mass bias corrections cause deviations from the mass-dependent fractionation line. Since the samples included in the present study significantly differ in chemical and physical characteristics, the purpose of using this approach is to test whether the analytical data represent a purely mass-dependent fractionation slope. The theoretical slopes are therefore used as inner and outer slope limits. The slope and intercept of the linear function of the experimental data has been determined to 1.95±0.01 and -0.01±0.04, respectively, which is within the theoretical boundaries set by kinetic and equilibrium mass-dependent fractionation.

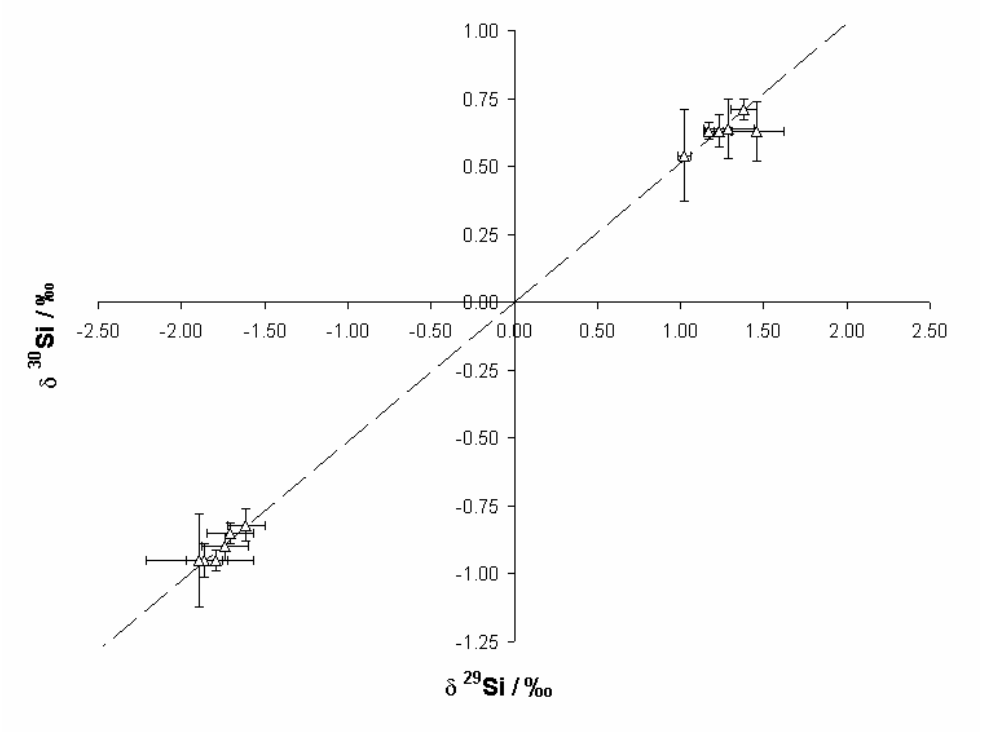

Figure 4. Three isotope plot of IRMM018, Diatomite and Big Batch included in the inter-laboratory comparison programme for Si isotope ratios, constructed according to the relationships proposed by Young *et al.* (2002). The scales have been reduced to only include values for IRMM018 and Diatomite.

2.2 Chemical purification for the determination of silicon isotopic composition in natural samples

2.2.1 Chemical separation and pre-concentration of dissolved silicon in natural waters

Natural samples require chemical purification prior to highly precise Si isotopic analyses, due to the presence of potentially interfering elements in the sample matrix and comparatively low concentrations of dissolved silicon in the samples. The sample matrix may cause severe non-spectral interferences if not completely removed prior to the isotopic analyses. Additionally, the presence of magnesium, iron and nickel deteriorate the measurement accuracy during the analyses, due to analytical difficulties in resolving interferences appearing at the low-mass side of the analyte and inaccurate mass bias corrections (since Mg is used for on-line mass bias correction). Another important advantage of applying chemical purification procedures is the possibility of pre-concentrating the analyte of interest.

With reference to the introduction section, the hazardous nature of silicon isotopic analyses has limited the applicability to natural systems. Conventional preparation techniques briefly consist of converting solid SiO_2 to the gaseous SiF_4, which is toxic by inhalation and corrosive to eyes, skin and respiratory system (Air Liquide). In 1996, De La Rocha and Brezesinski presented a widely applied method for the measurement of Si isotope abundances based on laser-driven fluorination of SiO_2 by F_2 (or BrF_5 (Ding *et al*., 2004)), producing SiF_4 (g) introduced to the mass spectrometer. The solid samples or dissolved silicic acid in natural waters are converted to SiO_2 by a four-step procedure consisting of HF dissolution, precipitation of dissolved Si using triethylmolybdate (Ding *et al*., (2004) used dilute polyethylene oxide instead), filtration and combustion of the retained precipitate (De La Rocha and Brzezinski, 1996).

The introduction of MC-ICPMS, especially when combined with ion-exchange chromatography, for silicon isotope ratio determinations offers the possibility of performing safer analyses and more time- and labour efficient sample preparation procedures for natural samples. Preparation methods based on ion-exchange chromatography represent the most widely applied measuring protocol for isotope ratio determinations in solutions, and offers high selectivity and rapid sample throughput in a safer manner.

Natural waters are a relatively complex matrix with generally high concentrations of the major elements, depending on the origin (marine-, brackish- or freshwater). However, natural

waters contain low levels of organic matter, eliminating the requirement for acid decomposition or fusion. With reference to section 1.2, dissolved silicon is present as the essentially non-ionic silicic acid, $Si(OH)_4$ in natural waters. Dissolved silicic acid, also referred to as *reactive silica*, is in equilibrium with the silicate anion, $H_3SiO_4^-$, and is a very weak acid with a $pK_a \sim 9.8$. At concentration levels exceeding 60 mg l^{-1}, silicic acid starts to polymerize forming non-ionic colloidal silica (Iler, 1979, Ali *et al*., 2004). The non-ionic character of silicic acid hampers the use of ion-exchange chromatography for its separation in natural waters, since the method is based on retention of ions oppositely charged to the stationary phase. Using cation exchange chromatography, it is possible to separate the silicic acid from the cationic matrix components by allowing the silicic acid to run right through the column (George *et al*., 2006). This approach is frequently applied for silicate materials following alkali fusion/dissolution (see Paper I; Van den Boorn *et al*., 2006). However, the main disadvantage of this approach is the fact that silicon is not separated from the anionic matrix components, restricting the applicability of this technique to freshwater samples (George *et al*., 2006). According to the equilibrium between silicic acid and the silicate anion, it is possible to completely convert the former to the latter form by pH adjusting the sample to pH >10. However, this approach is hampered by contamination problems associated with the addition of alkaline reagents to the sample and is therefore not recommended.

In Paper II, a chemical purification procedure for natural waters is presented and evaluated. The technique is based on the use of strong base anion-exchange chromatography, where the resin is pre-conditioned with 2 M NaOH according to the procedure proposed by Ali *et al*. (2004) for silica removal. The non-ionic silicic acid is dissociated to the silicate anion on the strongly alkaline surface of the resin and quantitatively retained (silicon can also be loaded to the column in the form of SiF_6^{2-} as proposed by Wickbold in 1959). Using this approach, the dissolved silicic acid is separated from the cations present in the sample load stage by allowing them to pass through the column without exhibiting retention. To achieve quantitative separation of silicon and interfering elements, such as Fe and Ni (forming doubly charged ^{56}Fe, ^{58}Fe, ^{58}Ni and ^{30}Ni appearing at the same nominal mass as ^{28}Si, ^{29}Si and ^{30}Si), it is required to divide the elution procedure in two separate steps, introducing analytical difficulties. Preliminary experiments showed that silicon in the form of the divalent SiF_6^{2-} appeared to exhibit higher selectivity in comparison to Cl^- and the potentially interfering elements. Elution of the interfering elements was therefore performed using a solution containing dilute hydrochloric acid with traces of hydrofluoric acid. Hydrofluoric acid was

added to the solution for the purpose of converting the retained $H_3SiO_4^-$ to SiF_6^{2-}, the latter exhibiting higher selectivity to the resin due to its divalent character. Silicon is finally eluted with dilute nitric acid with traces of hydrofluoric acid. Since NO_3^- exhibits very high retention to the anion-exchange resin, silicon is quantitatively eluted (recovery in excess of 97 %), excluding the possibility of inducing artificial isotopic fractionation. The complete elution profile of silicon, as well as potentially interfering and major elements, is shown and thoroughly discussed in connection with Figure 1 in Paper II.

Since a variety of physical and biological processes cause natural fractionation of the silicon isotopes, it is of the utmost importance to ensure that that the ion-exchange separation does not induce isotopic fractionation that affects the result of the analysis. It is therefore recommended to subject a single-element standard to the proposed procedure prior to the isotopic analyses.

2.2.2 Modified chemical purification procedure for the determination of silicon isotopic composition in plant and humus samples by MC-ICPMS

Plant samples represent a very challenging matrix, due to the low silicon concentration with a typical concentration level for Swedish vegetation being 97-442 mg kg^{-1}, dry weight (Reimann *et al*., 2001), and complex composition of organic and inorganic constituents.

It is well documented that silicon in plants exists as amorphous silica with a well-defined species-specific form (Ding *et al*., 2005; Opfergelt *et al*., 2006*a*, *b*), exhibiting relatively high solubility in comparison to crystalline silica (quartz). With reference to the *Introduction*, it has been proposed that silicon may be present as surface contamination incorporated in the plant structure (Wyttenbach and Tobler, 1998; Reimann *et al*., 2001) and that organic solvents are required for complete removal of the latter. The exogenous material includes primary and/or secondary minerals, often containing high levels of silicon, exhibiting significantly different dissolution kinetics. When determining the concentration of biogenic silica in suspended matter after wet-alkaline digestion (Ragueneau *et al*., 2005), resulting in complete dissolution of biogenic silicon and partly dissolution lithogenic silicon, the Si concentration is corrected for mineral interference using Al normalization. However, this approach is not applicable when determining the silicon isotopic composition in plant material, and it is therefore crucial that the sample preparation procedures for silicon isotopic compositions in plants offer complete dissolution of amorphous silica, as well as of silicon incorporated in crystalline minerals.

In previously published studies by Ding *et al*. (2005) and Opfergelt *et al*. (2006*a*, *b*) preparation procedures comprising at least four separate stages have been employed, including removal of organic matter by ashing (Ding *et al*., 2005) or acid decomposition (Opfergelt *et al*., 2006*a*, *b)*, precipitation of SiO_2 using dilute polyethylene oxide solution (Ding *et al*., 2005) or TEA-molybdate (Opfergelt *et al*., 2006*a*, *b*), followed by combustion at 1000ºC. Opfergelt *et al*., (2006*a*, *b*) dissolved the residue in HCl-HF prior to the silicon isotopic analyses, while Ding *et al*., 2005 employed the SiF_4 method where SiO_2 is reacted with BrF_5 in a vacuum line to form SiF_4 (Ding *et al*., 2004). With respect to the latter description, the development of a more labour- and time efficient preparation procedure would facilitate analyses of the silicon isotopic composition in plant material. Furthermore, reducing the number of separate preparation steps would make it easier to control the overall Si recovery and blank contribution.

In Paper III, an modified preparation procedure for the determination of silicon isotopic composition in plant and humus samples by MC-ICPMS is presented. The method includes three separate steps; removal of organic matter in a muffle furnace at 550ºC, hydrofluoric acid dissolution of the residue followed by chemical purification based on anion-exchange chromatography. Since induced fractionation might be introduced during the sample dissolution if Si is lost as SiF_4 (g) (Iler, 1979; De La Rocha and Brezezinski, 1996), the added amount of hydrofluoric acid must be carefully chosen. A procedure for the calculation of the added amount of hydrofluoric acid during the dissolution of biological acid is presented and evaluated in Paper III, based on the concentration of the major elements and aluminium.

3. Silicon isotopic composition of natural samples

In Paper II, the isotopic composition of the commercially available FIJI Natural Artesian Water with high concentration of silica was investigated. This material has been selected for quality control and performance assessment in an ongoing, informal, inter-laboratory comparison program. The resulting isotopic composition relative to the IRMM018 reference material of $\delta^{29}Si_{IRMM018}$ = (1.34 ± 0.12) ‰, with the uncertainty expressed as 2σ, approximately corresponds to $\delta^{29}Si_{NBS28}$ = (2.19 ± 0.16). The depletion of ^{28}Si was expected based on the isotopic fractionation caused by weathering and formation of secondary minerals (Ziegler *et al*., 2005), as well as the fractionation caused by potential uptake of silicic acid by vegetation (Opfergel *et al*., 2006*b*). During this study, the Si isotopic composition of a representative brackish water sample from the Northern area of the Bay of Bothnia was investigated (results shown in Paper III). The resulting $\delta^{29}Si_{NBS28}$ of 0.99 ± 0.05 ‰ (1σ), was also expected due to the silicon isotopic signature of the incoming river water and also due to utilization of dissolved silicic acid by diatoms (De La Rocha *et al*., 1997; De La Rocha *et al*., 1998) during the summer, as well as early spring (Sobek *et al*., 2004). Further, the silicon isotopic composition was well consistent with previously reported results for natural waters (De La Rocha *et al*., 2000; Ding *et al*., 2004; Basile-Doelsch, 2006).

The silicon isotopic composition of representative biomass in a boreal forest in Northern Sweden was investigated and presented in Paper III. The potential use of silicon isotopes in the assessment of the plant impact on the biogeochemical cycle of silicon requires thorough characterization of the silicon isotopic composition of vegetation, along with knowledge of the forms of silicon present in the plant material. Silicon isotopic analyses of the representative biomass from a region with bedrock consisting of dolomitic limestone and soil of sandy till (the local till is composed of quartz, feldspar, biotite and amphibole), yielded surprisingly homogenous δ^{29} Si in vegetation, ranging from (–0.14 ± 0.05)‰ (2σ) to (0.13 ± 0.04)‰ corresponding to a maximum difference of 0.27 ‰ in the autumn. Since previously published studies of the silicon isotopic composition of plants have been limited to include only one plant species (Ding *et al*., 2005; Opfergelt *et al*., 2006*a*, *b*), our study is the first investigating the homogeneity of plant material from a restricted area.

The accumulated dissolved silicic acid forming phytoliths (Wyttenbach and Tobler, 1998) with a characteristic form, and the exogenous silicon existing as crystalline surface

contaminations, exhibit very different dissolution kinetics, implying that investigation of the Si forms present in plants is of great significance for understanding the biogeochemical cycle of silicon. It has previously been proposed that the concentration of Al, as well as of Ti, Fe, Zr, Th and Sc, can be used for assessing the soil contribution to the elemental content in plants (Wyttenbach and Tobler, 1998; Riemann *et al*., 2001), indicating that the elemental ratio Si/Al in the airborne particulate matter and in the plant material can be used for estimating the surface contribution. The elemental ratio Si/Al in the airborne particulate matter was determined by multi-elemental analysis of local epiphytic lichens, exhibiting only atmospheric uptake of metals (Loppi *et al*., 1999). The estimated Si surface contributions to the plant samples ranged from 0.3 to 74 %, the exact species-specific data being detailed in Table 3 in Paper III), demonstrating that the presence of exogenous Si must be carefully considered during *in situ* uptake studies. It should be mentioned that the presence of codeposits of Al and Si in conifers have been suggested (Hodson and Sangster, 1998; Hodson and Sangster, 1999), implying that the estimated surface contribution using Al as normalizing element could be overestimated. The interactions between Si and Al have attracted substantial interest, since it has been proposed that Si might have a detoxifying effect of Al that has been mobilized during events of acid precipitation (Hodson and Sangster, 1998; Hodson and Sangster, 1999). However, solid Al was mainly found in the epidermis of the needles, implying that the observed Al could be of exogenous origin. Further, since the area has carbonaceous bedrock, the soil is expected to be well buffered and it is therefore not likely that Al toxicity will occur (Hodson and Sangster, 1999). Nevertheless, for the purpose of verifying the resulting surface contributions, corresponding calculations were preformed using Ti (Wyttenbach and Tobler, 1998; Reimann *et al*., 2001), yielding equivalent results.

Isotopic analyses of lyme grass (*Leymus arenarius*), a species native to the sandy border between the Bay of Bothnia and the forest and sampled in both the spring and the autumn 2006, revealed a successive enrichment of the heavier isotopes during the growth period.

4. Overall conclusions

This thesis demonstrates that highly precise and accurate Si isotopic analyses of natural waters and plant samples are now achievable in an expedient and less hazardous manner, due to the high resolving power of the MC-ICP-MS instrument, the development of efficient chemical purification methods and the accurate correction of instrumental mass discrimination using a simultaneously monitored internal standard. The accuracy of the silicon isotopic analyses has been assessed in an inter-laboratory comparison programme with satisfying results, revealing the absence of instrument- and method specific differences in the isotopic compositions determined in the participating laboratories. The presented chemical purification methods for natural waters and plant materials, based on anion-exchange chromatography, provide quantitative recovery of silicon without inducing artificial fractionation, and complete removal of potentially interfering elements. The removal of Fe, Ni and Mg during the separation is of prime importance since Mg is used for on-line mass bias correction and because Fe and Ni would appear as doubly charged ions on the low-mass sides of the Si ion beams. The high-resolution capability of the Neptune offers complete removal of the remaining N-, C- and O-containing polyatomic interferences, as well as $^{28}SiH^{+}$ and $^{29}SiH^{+}$, appearing on the high-mass sides of the silicon isotopes. However, despite quantitative resolution of the $^{14}N^{16}O^{+}$-interference on ^{30}Si, some tailing problems seem to persist, as revealed by repeated analyses of measurement solutions with varying Si- and HNO_3 concentrations. This implies that the use of a desolvating nebulizer to reduce the solvent load and hence the formation of polyatomic species, would be advantageous in future studies.

This thesis provides compelling evidence that the silicon isotopic composition of plant material from a restricted sampling area is relatively homogenous, implying that Si isotope information in the biogenic output potentially can be used for tracing biogeochemical processes in nature. Furthermore, the predominant enrichment of the heavier isotopes during the growing season in leaf blades of lyme grass (*Leymus arenarius*) collected in the sandy border between the forest area and the Bothnian Bay, certainly deserves further investigation.

5. Future studies

Despite considerable interest in investigating the global biogeochemical cycle of silicon, the number of studies presenting silicon isotope information of minerogenic and biological samples is still limited. In addition, the majority of the studies are limited to include only one specific matrix. In order to accurately studying local biogeochemical transfers of silicon, it is required that methods are available for a variety of matrices such as; natural waters, soil solutions, sediments, soils, primary minerals and biogenic silicon. Furthermore, since natural silicon isotopic compositions exhibit significant local variations, Si isotope ratio determinations of soils, soil solutions, ground waters, biogenic silica and primary minerals from a restricted area, are required for accurately studying the silicon cycle. Therefore, method development should continue to be an important part in the future research. Moreover, further investigations of the magnitude of Si isotopic fractionations caused by natural processes (e.g. *in situ* formation of phytoliths, dissolution of re-deposited phytoliths and local weathering) would facilitate interpretations of e.g. seasonal variations in the silicon isotopic composition of soil solutions and natural waters.

The lack of accuracy of previously reported silicon isotopic information has been stressed. Therefore, certified silicon isotopic reference materials available for primary minerals, clays, natural waters, sediments, soils and biogenic silica (phytoliths and diatoms) would be beneficial for quality assurance purposes.

The silicon isotopic composition of freshwater diatoms, podsol profiles and human biological samples have never been studying, the latter representing a very challenging matrix.

Acknowledgements

First of all, I would like to send my gratitude to my supervisors Ilia Rodushkin, Douglas Baxter and Björn Öhlander for their encouragement and critical reviewing of my work.

Ilia has taught me everything I know about practical mass spectrometry, for which I am very grateful. His knowledge and experience of ICP-MS is outstanding and invaluable. I am also grateful for all the work he has spent on this study, for patiently answering my questions and for constructive criticisms. I also would like to thank him for his friendship and his support, and for his advices throughout these years.

I would like to thank Björn Öhlander for his constant encouragement and support during this work, and for sharing his great knowledge. Björn and Johan Ingri introduced me to the field of geochemistry, for which I am grateful.

Douglas is acknowledged especially for help with English grammar and spelling and for his friendship, but also for his invaluable help with chemistry, statistics and mathematics.

This work is a team effort, whereby I wish to thank everyone that has been involved in this study. In addition to the above-mentioned persons, I especially would like to thank Christer Pontér for introducing me to Björn, and Anna Stenberg who sadly left us for studying in Stockholm. Furthermore, I would like to thank and my friend Dieke for helping me with sample preparations. I am also grateful to the personnel of Analytica for technical and financial assistance, and especially the service team for all reparations of the Neptune. In addition, I would also like to express my gratitude to my colleagues at the Division of Applied Geology for interesting discussions, Magnus Land for providing IRMM-018 and to Milan Vnuk for helping me with the technical preparation of this thesis.

This work was supported by the European Unions structural fund for objective 1 Norra Norrland. Purchase of the Neptune (MC-ICP-MS) was facilitated by a grant from Kempestiftelserna.

Last but not least, I would like to thank my Erik for always supporting and encouraging me, and for lightening up my life!

References

Air Liquide, Safety data sheets, (http://encyclopedia.airliquide.com/sds/en/108_AL_EN.pdf) (0706021)

M. B. S. Ali, B. Hamrouni, S. Bouguecha, M. Dahbi. Silica removal using ion-exchange resins (2004) *Desalination* **167** 273-279.

R. J. Allenby. Determination of the isotopic ratios of silicon in rocks (1954) *Geochim. Cosmochim. Acta* **5** 40-48

H. Andrén, I. Rodushkin, A. Stenberg, D. Malinovsky , D. C. Baxter. Sources of mass bias and isotope ratio variation in multi-collector ICP-MS: optimization of instrumental parameters based on experimental observations (2004) *J. Anal. Atom. Spectrom.* **19** 1217-1224

P. K. Appelblad, I. Rodushkin, D. C. Baxter. The use of Pt guard electrode in inductively coupled plasma sector field mass spectrometry: advantages and limitations (2000) *J. Anal. Atom. Spectrom.* **15** 359-364.

I. Basile-Doelsch. Si stable isotopes in the Earth´s surface: A review (2006) *J. Geochem. Explor.* **88** 252-256.

D. C. Baxter, I. Rodushkin, E. Engström, D. Malinovsky. Revised exponential model for mass bias correction using an internal standard for isotope abundance ratio measurements by multi-collector inductively coupled plasma mass spectrometry (2006) *J. Anal. Atom. Spectrom.* **21** 427-430.

J. S. Becker, H.-J. Dietze. Precise and accurate isotope ratio measurements by ICP-MS (2000) *Fresenius J. Anal. Chem.* **368** 23-30.

R. A. Berner. The rise of plants and their effect on weathering and atmospheric CO_2 (1997) *Science* **276** 544-545.

N. Bradshaw, E. F. H. Hall, N. E. Sanderson. Inductively coupled plasma as an ion source for high-resolution mass spectrometry (1989) *J. Anal. Atomic. Spectrom.* **4** 801-803.

M. A. Brzezinski, J. L. Jones, C. P. Beucher, M. S. Demarest, H. L. Berg. Automated determination of silicon isotope natural abundance by the acid decoposition of cesium hexafluosilicate (2006) *Anal. Chem.* **78** 6109-6114.

D. Cardinal, L. Alleman, J. De Jong, K. Ziegler, L. André. Isotopic composition of silicon measured by multicollector plasma source mass spectrometry in dry plasma mode (2003) *J. Anal. At. Spectrom.* **18** 213-218.

D. Cardinal, L. Alleman, F. Dehairs, N. Saviye, T. W. Trull, L. André. Relevance of silicon isotopes to Si-nutrient utilization and Si-source assessment in Antarctic waters (2005) *Glob. Biogeochem. Cycles* **19** doi:10.1029/2004GB002364

J. Carignan, D. Cardinal, A. Eisenhauer, A. Galy, M. Rehkämper, F. Wombacher, N. Vigier. A reflection on Mg, Cd, Ca, Li and Si isotopic measurements and related reference materials (2004) *Geostand. Geoanal. Res.* **28** 139-148.

T. B. Coplen, J. A. Hopple, J. K. Böhlke, H. S. Peiser, S. E. Reider, H. R. Krouse, K. J. R. Rosman, T. Ding, R. D. Vocke, K. M. Revesz, A. Lamberty, P. Taylor, P. De Bievre Compilation of Minimum and Maximum Isotope Ratios of Selected Elements in Naturally Occuring Terrestrial Materials and Reagents (2002) *U. S. Geological Survey*, Reston, Virginia, pp. 45-50.

J. R. De Laeter, J. K. Böhlke, P. De Bièvre, H. Hidaka, H. S. Peiser, K. J. R. Rosman, P. D. P. Taylor. Atomic weights of the elements. Review 2000 (IUPAC Technical Report) (2003) *Pure Appl. Chem.* **75** 683-800

C. L. De La Rocha, M. A. Brzezinski. Purification, recovery, and laser-driven fluorination of silicon from dissolved and particulate silica for the measurement of natural stable isotope abundances (1996) *Anal. Chem***. 68** 3746-3750.

C. L. De La. Rocha, M. A. Brzezinski, M. J. DeNiro. Fractionation of silicon isotopes by marine diatoms during biogenic silica formation (1997) *Geochim. Cosmochim. Acta* **61** 5051-5056.

C. L. De La Rocha, M. A. Brzezinski, M. J. DeNiro, A. Shemesh. Silicon-isotope composition as an indicator of past oceanic change (1998) *Nature* **395** 680-683.

C. L. De La Rocha, M. A. Brzezinski, M. J. DeNiro. A first look at the distribution of the stable isotopes of silicon in natural waters (2000) *Geochim. Cosmochim. Acta* **64** 2467-2477.

C. L. De La Rocha. Measurement of silicon stable isotope natural abundances via multicollector inductively coupled plasma mass spectrometry (MC-ICP-MS) (2002) *Geochem. Geophys. Geosyst.* (*G*^{3}) **3** ISSN: 1525-2027.

T. Ding, S. Jiang, D. Wan, Y. Li, J. Li, H. Song, Z. Liu, X. Yao. Silicon Isotope Geochemistry (1996) Geological Publishing House, Beijing.

T. P. Ding, D. Wan, C. Wang, F. Zhang. Silicon isotope compositions of dissolved silicon and suspended matter in the Yangtze River, China (2004) *Geochim. Cosmochim. Acta* **68** 205-216.

T. P. Ding, G. R. Ma, M. X. Shui, D. F. Wan, R. H. Li. Silicon isotope study on rice plants from the Zhejiang province, China (2005) *Chem. Geol.* **218** 41-50.

C. B. Douthitt. The geochemistry of the stable isotopes of silicon (1982) *Geochim. Cosmochim. Acta* **46** 1449-1458.

V. C. Farmer, E. Delbos, J. D. Miller. The role of phytolith formation and dissolution in controlling concentrations of silica in soil solutions and streams (2005) *Geoderma* **127** 71-79

H.-E. Gäbler. Applications of magnetic sector ICP-MS in geochemistry (2002) *J. Geochem. Explor.* **75** 1-15

G. Faure, T. M. Mensing. Isotopes Principles and Applications. 3rd edition (2005) John Wiley & Sons, Inc., Hobonken, New Jersey.

R. B. George, B. C. Reynolds, M. Frank, A. N. Halliday. Mechanisms controlling the silicon isotopic composition of river waters (2006) *Earth Planet. Sci. Letter* **249** 290-306.

R. B. George, B. C. Reynolds, M. Frank, A. N. Halliday New sample preparation technique for the determination of Si isotopic composition using MC-ICPMS (2006) *Chem. Geol.* **235** 95-104.

M. J. Hodson, A. G. Sangster. Mineral deposition in the needles of white spruce [*Picea glauca* (Moench.) Voss] (1998) *Ann. Bot.* **82** 375-385.

M. J. Hodson, A. G. Sangster. Aluminium/silicon interactions in conifers (1999) *J. Inorg. Biochem.* **76** 89-98.

R. Iler. The chemistry of silica (1979) Wiley, New York.

E. F. Kelly, S. W. Blecker, C. M. Yonker, C. G. Olson, E. E. Wohl, L. C. Todd. Stable isotope composition of soil organic matter and phytoliths as paleoenvironmental indicators (1998) *Geoderma* **82** 59-81.

S. Loppi, S. A. Pirintos, V. De Dominicis. Soil contribution to the elemental composition of epiphytic lichens (Tuscany, Central Italy) (1999) *Environ. Monitor. Assess.* **59** 121-131.

J. F. Ma, N. Yamaji. Silicon uptake and accumulation in higher plants (2006) *Trends Plant Sci*. **11**, 392-397.

C. Molino-Velsko, T. K. Mayeda, R. N. Clayton. Isotopic composition in meteorites (1986) *Geochim. Cosmochim. Acta* **50** 2719–2726

A. Montaser. Inductively coupled plasma mass spectrometry (1998), John Wiley & Sons Ltd, New York.

D. M. Nelson, P. Tréguer, M. A. Brezezinski, A. Leynaert, B. Quéguiner. Production and dissolution of biogenic silica in the ocean: Revised global estimates, comparison with regional data and relationship to biogenic sedimentation (1995) *Global Biogeochem. Cycles* **9** 359-372.

S. Opfergelt, D. Cardinal, C. Henriet, L. André, B. Delavaux. Silicon isotope fractionation between plant parts in banana: In situ vs. in vitro (2006*a*) *J. Geochem. Explor.* **88** 224-227.

S. Opfergelt, D. Cardinal, C. Henriet, X. Draye, L. André, B. Delvaux. Silicon isotopic fractionation by banana (*Musa* spp.) grown in a continuous nutrient flow device (2006*b*) *Plant Soil* **285** 333-345.

I. T. Platzner. Modern isotope ratio mass spectrometry, Chemical analysis, Vol 145 (1997) John Wiley & Sons Ltd, West Sussex.

O. Ragueneau, N. Savoye, Y. Del Amo, J. Cotton, B. Tardiveau, A. Leynaert. A new method for the measurement of biogenic silica in suspended matter of coastal waters: using Si:Al ratios to correct for mineral interference (2005) *Continent. Shelf Res.* **25** 697-710.

C. Riemann, F. Koller, B. Frengstad, G. Kashulina, H. Niskavaara, P. Englmaier. Comparison of the element composition in several plant species and their substrate from a 1 500 000-km^2 area in Northern Europe (2001) *Sci. Total Environ.* **278** 87-112.

M. Rehkämper, K. Mezger. Investigation of matrix effects for Pb isotope ratio measurements by multiple collector ICP-MS: verification and application pf optimized analytical protocols (2000) *J. Anal. At. Spectrom.* **15** 1451-1460.

J. H. Reynolds, J. Verhoogen. Natural variations in the isotopic composition of silicon (1953) *Geochim. Cosmochim. Acta* **3** 224-234.

B. C. Reynolds, R. B. George, F. Oberli, U. Wiechert, A. N. Halliday. Re-assessment of silicon isotope reference materials using high-resolution multi-collector ICP-MS (2006) *J. Anal. At. Spectrom*. **21** 266-269.

A. Sobek, Ö. Gustafsson, S. Hajdu, U. Larsson. Particle-water partitioning of PCBs in the Phoyic Zone: A 25-month study in the Open Baltic Sea (2004) *Environ. Sci. Technol.* **38** 1375-1382.

A. Stenberg, D. Malinovsky, B. Öhlander, H. Andrén, L.-M. Engström, A. Wahlin, E. Engström, I. Rodushkin, D. C. Baxter. Measurement of iron and zinc isotopes in human whole blood: Preliminary application to the study of HFE genotypes (2005) *J. Trace Elem. Med. Biol.* **19** 55-60

W. Stumm, R. Wollast. Coordination chemistry of weathering (1990) *Rev. Geophys.* **28** 53-69.

H. P. Taylor, S. Epstein. Oxygen and silicon isotope ratios of the Lunar rock 12013* (1970) *Earth Planet. Sci. Letter* **9** 208-210.

D. Tilles. Natural variations in isotopic abundances of silicon (1961) *J. Geophys. Res.* **66** 3003-3014.

P. Treguer, D. M. Nelson, A. J. Van Bennekom, D. J. DeMaster, A. Leynaert, B. Queguiner. The silica balance in the world ocean: A reestimate (1995) *Science* **268** 375-379.

C. D. Trombold and I. Israde-Alcantara. Paleoenvironment and plant cultivation on terraces at La Quemada, Zacatecas, Mexico: the pollen, phytolith and diatom evidence (2005) *J. Archaeol. Sci.* **32** 341-353.

S. H. J. M. Van den Boorn, P. Z. Vroon, C. C. Van Belle, B. van der Wagt, J. Schwieters and M. J. van Bergen. Determination of silicon isotope ratios in silicate materials by high-reslution MC-ICP-MS using a sodium hydroxide sample digestion method (2006) *J. Anal. Atom. Spectrom.* **21** 734-742.

F. Vanhaecke, L. Moens. Overcoming spectral overlap in isotopic analysis via single and multi-collector ICP-mass spectrometry (2004) *Anal. Bioanal. Chem.* **378** 232-240.

E. A. Webb, F. J. Longstaffe. The oxygen isotopic composition of silica phytoliths and plant water in grasses: Implications for the stuffy of paleoclimate (2000) *Geochim. Cosmochim. Acta* **64** 767-780.

R. Wickbold. (In german) (1959) *Fresenius Z. Anal. Chem.* **171** 81-91.

M. E. Wieser, J. B. Schwieters. The development of multiple collector mass spectrometry for isotope ratio measurements (2005) *Int. J. Mass. Spectrom.* **242** 97-115.

J. Woodhead. A simple method for obtaining highly accurate Pb isotope data by MC-ICP-MS (2002) J. Anal. Atom. Spectrom. 17 1381-1385.

A. Wyttenbach, L. Tobler. Effect of surface contamination on results of plant analysis (1998) *Commun. Soil Sci. Plant Anal.* **29** 809-823.

E. D. Young, A. Galy, H. Nagahara Kinetic and equilibrium mass dependent isotope fractionation laws in nature and their geochemical and cosmochemical significance (2002) *Geochim. Cosmochim. Acta.* **66** 1095-1104.

K. Ziegler, O. Chadwick, M. A. Brzezinski, E. F. Kelly. Natural variations of $\delta\ ^{30}Si$ ratios during progressive basalt weathering (2005) *Geochim. Cosmochim. Acta* **69** 4597-4610.

I

An inter-laboratory comparison of Si isotope reference materials

Journal of Analytical Atomic Spectrometry **22** *(2007) 561-568*

B. C. Reynolds, J. Aggarwal, L. André, D. C. Baxter, C. Beucher, M. A. Brzezinski, E. Engström, R. B. George, M. Land, M. J. Leng S. Opfergelt, I. Rodushkin, H. J. Sloane, S. H. J. M. van den Boorn, P. Z. Vroon and D. Cardinal

An inter-laboratory comparison of Si isotope reference materials

Ben C. Reynolds,*[a] Jugdeep Aggarwal,[b] Luc André,[c] Douglas Baxter,[d] Charlotte Beucher,[e] Mark A. Brzezinski,[e] Emma Engström,[df] R. Bastian Georg,[ag] Magnus Land,[h] Melanie J. Leng,[ij] Sophie Opfergelt,[ck] Ilia Rodushkin,[df] Hilary J. Sloane,[i] Sander H. J. M. van den Boorn,[l] Pieter Z. Vroon[m] and Damien Cardinal[c]

Received 17th November 2006, Accepted 26th January 2007
First published as an Advance Article on the web 27th February 2007
DOI: 10.1039/b616755a

Three Si isotope materials have been used for an inter-laboratory comparison exercise to ensure reproducibility between international laboratories investigating natural Si isotope variations using a variety of chemical preparation methods and mass spectrometric techniques. These proposed standard reference materials are (i) IRMM-018 (a SiO_2 standard), (ii) Big-Batch (a fractionated SiO_2 material prepared at the University of California Santa Barbara), and (iii) Diatomite (a natural diatomite sample originally deposited as marine biogenic opal). All analyses are compared with the international Si standard NBS28 (RM8546) and are in reasonable agreement ($< \pm 0.22$‰ $1\sigma_{SD}$ δ^{30}Si) given the different measurement techniques involved. These methods include both acid and alkaline dissolution/fusion, Si separation using cation exchange, selective co-precipitation, and gas-source *versus* plasma-ionization (high and low resolution) mass-spectrometric techniques. The average δ^{30}Si for Diatomite, IRMM-018, and Big-Batch are $+1.26$‰, -1.65‰ and -10.48‰, respectively, with corresponding δ^{29}Si values of $+0.64$‰, -0.85‰ and -5.35‰ for the same standards, respectively. For the most fractionated standard (Big-Batch), results demonstrate a kinetic mass-dependent fractionation effect for atomic Si (*i.e.*, $\delta^{29}\text{Si} \sim 0.51 \times \delta^{30}\text{Si}$). There is almost no statistical difference between the mean values obtained by each participating laboratory, with the notable exception of the IRMM-018 standard. This effect could be caused by heterogeneity or contamination of this standard. The results for the other two standards indicate that data sets produced using any of the methods employed in this study will have similar precision and differences are limited to 0.2‰ in mean δ^{30}Si values for a given sample between laboratories, or differences of 0.13‰ in mean δ^{29}Si values.

[a] *IGMR, Erdwissenschaften, Clausiusstrasse 25ETH Zürich, CH-8092 Zürich, Switzerland. E-mail: reynolds@erdw.ethz.ch, georg@erdw.ethz.ch*
[b] *Keck Isotope Laboratory, Department of Earth Sciences, University of California, Santa Cruz, USA. E-mail: jaggarwal@pmc.ucsc.edu*
[c] *Department of Geology, Musée Royal de l'Afrique Centrale, Leuvensesteenweg 13, Tervuren, Belgium. E-mail: lucandre@africamuseum.be, damien.cardinal@africamuseum.be, opfergelt@sols.ucl.ac.be*
[d] *Analytica AB, Aurorum 10, S-977 75 Luleå, Sweden. E-mail: douglas.baxter@analytica.se, emma.engstrom@analytica.se, ilia.rodushkin@analytica.se*
[e] *Department of Ecology Evolution and Marine Biology and the Marine Science Institute, University of California, Santa Barbara, CA, USA. E-mail: brzezins@lifesci.ucsb.edu, beucher@lifesci.ucsb.edu*
[f] *Division of Applied Geology, Luleå University of Technology, S-971 87 Luleå, Sweden. E-mail: emma.engstrom@analytica.se*
[g] *Department of Earth Sciences, University of Oxford, UK. E-mail: bastian.georg@earth.ox.ac.uk*
[h] *Department of Geology and Geochemistry, Stockholm University, and Laboratory for Isotope Geology, Swedish Museum of Natural History, Stockholm, Sweden. E-mail: per.andersson@nrm.se*
[i] *NERC Isotope Geosciences Laboratory, British Geological Survey, Keyworth, Nottingham, UK. E-mail: mjl@nigl.nerc.ac.uk, h.sloane@nigl.nerc.ac.uk*
[j] *School of Geography, University of Nottingham, Nottingham, UK. E-mail: mjl@nigl.nerc.ac.uk*
[k] *Soil Science Unit, Université catholique de Louvain, Place Croix du Sud Belgium. E-mail: opfergelt@sols.ucl.ac.be*
[l] *Department of Earth Sciences, Utrecht University, Budapestlaan 4, Utrecht, The Netherlands. E-mail: boorn@geo.uu.nl*
[m] *Department of Petrology, FALW, Vrije Universiteit, De Boelelaan 1085, Amsterdam, The Netherlands. E-mail: pieter.vroon@falw.vu.nl*

Introduction

Recently, there has been a renewed interest in the measurement of silicon (Si) isotope variations in natural samples because of the importance of Si in global biogeochemical cycles,[1] and its importance as the most abundant non-volatile element in the solar system. Naturally occurring variations in the isotopic composition of Si can be caused by mass-dependent fractionation processes, either kinetic or thermodynamic isotope effects, *via* chemical and biological reactions, or by non-mass-dependent processes from stellar nucleosynthesis and the incorporation of pre-solar grains (see ref. 2 and references cited therein). This makes the ability to measure very slight variations in the relative abundances of the three naturally occurring stable isotopes (^{28}Si, ^{29}Si, and ^{30}Si have abundances of 92.23%, 4.67%, and 3.10%, respectively[3]) of interest to a broad range of geoscientific disciplines.[4]

Stable isotope variations of Si were first measured over 50 years ago by Reynolds and Verhoogen[5] and Allenby,[6] who converted the siliceous minerals into gaseous SiF_4 and assayed this gas in a Nier-type mass spectrometer. These authors used different techniques for the production of the purified gas, measured as SiF_3^+, with a precision of $>0.3‰$ ($2\sigma_{SD}$). Since these early experiments, the natural variability of the terrestrial Si isotope composition has been inadequately investigated, due mainly to analytical difficulties and the poor reproducibility compared with small natural variations in the $^{30}Si/^{28}Si$ ratio of only 3.5‰ for terrestrial, igneous and metamorphic rocks, and 6‰ for biogenic opal,[7] with an error of $\pm 0.2‰$ $2\sigma_{SD}$.[4] Furthermore, unlike with oxygen isotopes, careful studies of meteorites and lunar material could not evidently show visible isotopic anomalies, *e.g.* ref. 8, with all of the measured samples falling close to a single mass-fractionation line, although small pre-solar SiC grains contain very anomalous Si isotope compositions.[9] The relatively small variations observed, as compiled by Douthitt,[7] showed that Si isotopes were probably of little significance in the understanding of igneous processes, whilst the fractionation of aqueous or biological precipitates was limited by an inability to measure dissolved Si isotope compositions. Hence, in the following decade, little work was done to further investigate Si isotope fractionations, see ref. 10. However, the application of Si isotope variations to investigate geochemical cycles has been enhanced by two separate developments. Firstly, the ability to measure the Si isotope composition on a wide range of samples: dissolved and biogenic Si from marine and freshwaters environments,[11–19] soils and plants[20–22] as well of altered rocks and soils.[11,15,23–26] Secondly, improved gas source isotope ratio mass spectrometer (IRMS) techniques[27] and the advancement of multi-collector inductively coupled plasma mass spectrometry (MC-ICP-MS)[28,29] now provide the precision required to better constrain these biogeochemical systems.

The exploitation of MC-ICP-MS offers two major advantages over IRMS: firstly, faster analytical protocols (both chemical processing and analysis time), including repeated analyses, and secondly, much smaller sample sizes. However, MC-ICP-MS also has disadvantages, including lower internal precision on isotopic measurement compared with dual-inlet IRMS, potential 'matrix effects' and significant polyatomic interferences resulting from the plasma source. Few comparisons of Si isotope variations between IRMS and MC-ICP-MS analyses have been made[28] but they show agreement between methods of *ca.* 0.2‰. The present paper demonstrates that, despite recent problems concerning the composition of IRMM-018,[29–31] $\delta^{30}Si$ and $\delta^{29}Si$ compositions measured using a wide variety of chemical preparation methods and mass-spectrometric techniques all give consistent results and that there is no systematic bias induced by measurement instrumentation.

Stable isotope fractionation can be assessed using only two isotopes, but different mass-dependent fractionation laws apply for kinetic, equilibrium, and experimentally observed instrumental mass-fractionation. However, to resolve differences between these fractionation laws, as observed for oxygen, iron and magnesium,[32–35] there must be considerable mass-fractionation and three isotopes must be measured to extremely high precision. Hence, most natural Si isotope variations can be reported as variations in either $^{30}Si/^{28}Si$ or $^{29}Si/^{28}Si$ (or even $^{30}Si/^{29}Si$), and are expressed in δ-notation; variations relative to the international Si standard NBS28 (RM8546) in per mille (‰). For mass-dependent fractionation, the enrichment of ^{30}Si is almost twice the enrichment of ^{29}Si when normalised to ^{28}Si, resulting in the fact that $\delta^{30}Si$ variations are roughly twice those of $\delta^{29}Si$, for any given fractionation. Given similar precisions on the measured $^{30}Si/^{28}Si$ and $^{29}Si/^{28}Si$ ratios, the relative error on $\delta^{30}Si$ variations are less than those of $\delta^{29}Si$, which is why natural Si isotope variations are typically expressed as $\delta^{30}Si$. However, the analyses of $^{30}Si/^{28}Si$ ratios using some MC-ICP-MS are problematic due to more pronounced polyatomic interferences on mass 30, so a number of laboratories can only determine the $\delta^{29}Si$ values. Precision for MC-ICP-MS methods are comparable to that obtained by IRMS.

Samples and methods

In order to compare stable Si isotope variations between different laboratories and measurement techniques, it was decided that three materials should be used so that variations could be observed for natural samples which were both distinctly light and distinctly heavy compared with the international Si isotope standard reference material NBS28 (RM8546), and also highly fractionated. To ensure easy distribution and similar sample preparation protocols of all the standards, the chosen standards were required to be distributed as powdered SiO_2, just like NBS28. Although several laboratories have their own in-house standards (typically a commercially available Si powder), these were not used as they had $\delta^{30}Si$ values similar to NBS28. The three materials chosen were (i) IRMM-018, a SiO_2 standard, (ii) a natural diatomite sample termed "Diatomite", and (iii) a highly fractionated SiO_2 material termed "Big-Batch".[27,28] Although the European Si standard IRMM-018 was commercially available, in order to address the possibility of sample heterogeneity given a large discrepancy between previously published $\delta^{30}Si$ values,[4,29–31] sub-samples of IRMM-018 were distributed from ETH Zürich to all the participating laboratories (under verbal agreement from IRMM). The previously published results for the highly fractionated standard Big Batch were initially prepared by Christina De La Rocha and Mark Brzezinski at the Marine Science Institute of the University of California Santa Barbara, as precipitated triethylamine silicomolybdate from a dissolved sodium metasilicate.[36] For the inter-comparison exercise, a new batch of powdered SiO_2 was produced, and distributed by Mark Brzezinski, from multiple combustions and subsequent crushing and mixing of the same precipitated triethylamine silicomolybdate. Unfortunately, the combustion does not fully remove all the molybdate, and the Big Batch standard actually contains about 1.5 ppm Mo,[23] which may not be separated from Si during the chemical preparation during dissolution or cation-exchange chromatography and thus lead to potential matrix effects (see later). The Diatomite Standard was also prepared and distributed by Mark Brzezinski, and from a 1 kg sample of purified diatomite

Table 1 Summary of the different methods used by each group for the preparation of the standard materials and the mass-spectrometric techniques for determining the relative Si isotope composition

Group. no.	Group	Authors	Ion source	Mass spectrometry	Preparation technique	References
1	IGMR, ETH Zürich	Ben C. Reynolds and R. Bastian Georg	ICP	NuPlasma 1700	Alkali fusion and ion-exchange	11,16,18,29
2	Keck Labs, UCSC	Jugdeep Aggarwal	ICP	Neptune	See ref. 29	
3	MRAC, Belgium	Damien Cardinal, Sophie Opfergelt, Luc André	ICP	NuPlasma (low-res.)	HCl–HF dissolution, dry plasma, Mg doping	14,15,19,20,22,28
4	Analytica AB, Luleå, Sweden	Douglas Baxter, Emma Engström, Ilia Rodushkin	ICP	Neptune	HNO_3–HF dissolution	12
5	Marine Science, UCSB	Mark Brzezinski, Charlotte Beucher	Duel-inlet gas-source	Kiel III MAT 252	HF dissolution, then $CsSiF_6$ precipitation	17,25,26,36,40–42
6	Stockholm, Sweden	Magnus Land	ICP	IsoProbe (low-res.)	$LiBO_2$ fusion and HCl dissolution	
7	NERC Isotope Labs, UK	Melanie Leng, Hilary Sloane	Gas-source	Finnigan MAT 253	Based on O_2 method	37
8	FALW, VU, Netherlands	Sander van den Boorn, Pieter Vroon	ICP	Neptune	Alkali dissolution and ion-exchange	23

with the trade name Celpure®, donated by the Celite Corporation of Lompoc, California. The three distributed standards are all relatively pure SiO_2, but with variable amounts of water, so are not crystographically identical. Additional milligram sized samples of the Big Batch and Diatomite standards are available from Mark Brzezinski.

In terms of sample and standard preparation, each group has developed its own techniques and protocols suitable for its own instrumentation, as shown in Table 1. We will use the term group rather than laboratory as, although only one mass-spectrometer has been used in each case, workers participating within each group may come from several laboratories. The details for all of these analytical methods are published elsewhere, see Table 1. However we will briefly review the advances in chemical preparation and mass-spectrometric techniques.

Advances in mass spectrometry

IRMS

Silicon isotope analysis by IRMS usually involves conversion of the sample to SiF_4 gas,[7,8,10,36] for example using fluorine compounds, and heat to convert SiO_2 to O_2 and SiF_4, as also used for the measurement of silica oxygen, see ref. 37. The SiF_4 is converted to beams of SiF_3^+ ions by electron bombardment in the ion source of the mass spectrometer, the intensities of which are measured at 85, 86, 87 m/z. The procedure is difficult because of the use of dangerous fluorine based compounds, but once samples are prepared analysis by dual inlet IRMS is highly reliable and has high internal precision. The results for IRMS analyses in this paper were produced using the fluorination method (BrF_5) and a MAT 253 isotope ratio mass spectrometer (at NIGL, Nottingham) and the Cs_2SiF_6 method (UCSB, California) using a modified Kiel III carbonate device attached to a MAT 252 isotope ratio mass spectrometer.

The new IRMS method eliminates the need to use F_2 or BrF_5 to produce SiF_4.[27] Samples are converted to solid $CsSiF_6$ using simple chemical procedures and SiF_4 is a product of the acid decomposition of $CsSiF_6$. Several commercially available inlet systems operate on the principle of acid decomposition of solids for the analysis of carbonates. Minor modification of these systems can make them suitable for the analysis of isotopes of Si.[27] Cs_2SiF_6 is loaded directly into these systems with the acid decomposition performed mechanically, allowing for relatively rapid automated analysis.

MC-ICP-MS

Initial measurements of Si isotopes using MC-ICP-MS used a 'wet-plasma' sample introduction technique, with 0.25 M HF.[38] Unfortunately, this technique produced very poor sensitivity, poor temporal stability of instrumental mass-bias and severe memory effects, so that the analytical precision was poor. Relative Si isotope variations are measured using a standard–sample–standard bracketing technique that requires identical conditions in the measurement solutions and plasma-source between samples and standards, and minimum drift in the instrumental mass-bias with time. Failure to ensure identical conditions, for instance the presence of additional cations in the analyte, can lead to 'matrix-effects' and incorrect determination of relative isotopic compositions. However, when correctly implemented, this bracketing technique effectively eliminates the errors from instrumental background and amplifier corrections, since these should affect both sample and standard in an identical manner. A refined analytical technique was developed by Cardinal *et al.* (2003), with a 'dry-plasma' sample introduction using a desolvating nebulization system and Mg external doping for mass bias correction.[28] This technique introduced very dilute acids, with HF below 0.01 M, in order to increase the sensitivity and stabilize instrumental mass-bias over time.

Under normal operating conditions, as well as the efficient ionization of cations, there is also the production of interfering polyatomic ions, either within the plasma or in the interface region. Assuming a typical $^{28}Si^+$ intensity of 60 pA on an instrument equipped with a desolvating nebulizer,[11,28] the polyatomic species $^{14}N_2H^+$ and $^{14}N^{16}O^+$ would typically result in signals corresponding to at least 0.7% and 5% of the $^{29}Si^+$ and $^{30}Si^+$ ion beams, respectively. For instruments

using conventional 'wet-plasma' sample introduction systems,[12] the magnitude of these spectral interferences on the silicon isotopes would be even more pronounced. Although some of these interferences can be corrected for,[28] the polyatomic interference on mass 30 prevents accurate measurement of $^{30}Si/^{28}Si$ ratios compared with $^{29}Si/^{28}Si$. However, polyatomic ions are slightly heavier than atomic ions of the same nominal mass in this region of the mass spectrum, a fact that can be exploited using high-resolution ion optics to separate the Si^+ ion beams from potential polyatomic interferences.[2] This requires the ability to resolve ion beams which differ by less than 1‰ in mass (usually expressed as requiring a mass-resolution ($m/\Delta m$) in excess of 1000), and has been demonstrated for Si isotope analyses using higher resolution MC-ICP-MS instruments[12,29] utilized by groups participating in this study. A new chemical preparation technique has also been developed independently by two groups to avoid HF in sample solutions, which has been shown to enhance sensitivity and minimize mass-bias variations.[11,23,29]

Results

There are a variety of ways to compare different isotope results generated within and between laboratories, and so we will first describe the statistical approach taken here. For Si isotope analyses, the internal errors on individual measurements are much lower than the reproducibility among measurements. For the standard–sample–standard bracketing approach used in MC-ICP-MS analysis there are a number of ways in which to propagate measurement error on the standard and sample, leading to discrepancies between reported internal errors. A simplified approach is taken here; we assume that the errors for individual measurements of $\delta^{30}Si$ and $\delta^{29}Si$ values are much smaller than the measurement reproducibility and that they are equal for all measurements from all groups. While this is not strictly true, it is a fair approximation as it does not lead to a significant bias in the distribution of the reproducibility reported for each group, or the collectively pooled data.

The collected data from the eight groups taking part (Table 1) are shown in Fig. 1 and Table 2. Note that when a silica dissolution step is required (*i.e.*, when using MC-ICP-MS), each group has performed at least three separate dissolutions for every reference material. The measured Si isotope composition for single analyses of Diatomite range from +0.47 to +0.85‰ $\delta^{29}Si$ or +0.99 to +1.70‰ $\delta^{30}Si$, whilst for IRMM-018 the $\delta^{30}Si$ and $\delta^{29}Si$ values range from −1.13 to −2.16‰ and −0.61 to −1.10‰, respectively. However, ranges are biased by the inclusion of statistical outliers (or anomalies), and thus do not reflect how well the measured values may be compared between laboratories. Despite the wide range from

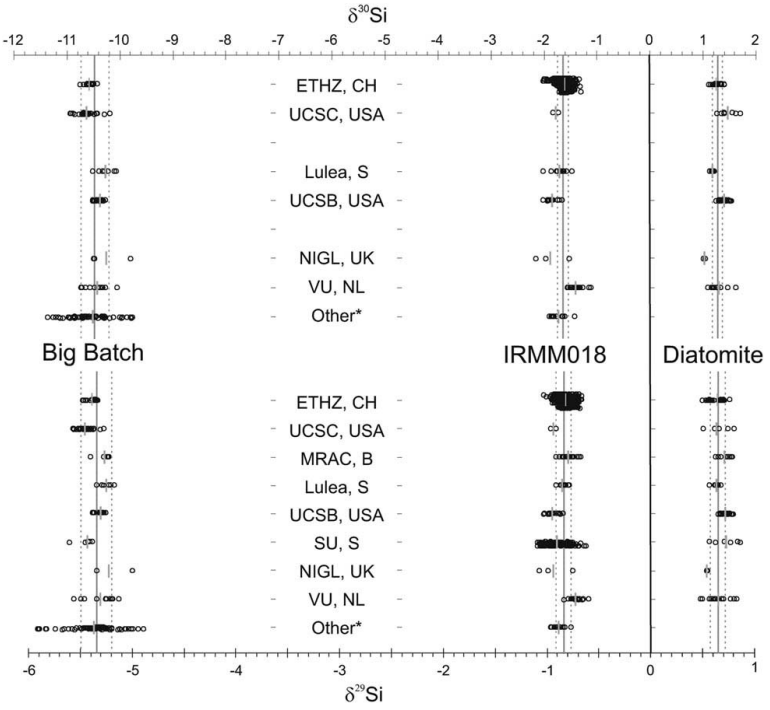

Fig. 1 Summary of all of the results from each group, upper panel for $\delta^{30}Si$ and lower panel for $\delta^{29}Si$, scaled to allow direct correlation between these two units. There is no $\delta^{30}Si$ data available from MRAC and SU-NRM due to the mass spectrometry used. *Other refers to previously analysed preparation of Big Batch (see Table 2) and for a different sample of IRMM-018 obtained by and run at VU, Amsterdam. Grey lines mark the pooled mean values (solid) and plus/minus 1 σ_{SD} from the mean (broken), see Table 2.

Table 2 Summary of all of the results from each group, in rank order of mean δ^{29} Si value for each standard. Pooled data is weighted according to the precision of the 95% confidence limit (c.l.). Data shown in grey when the number of measurements (n) was small ($n < 6$), which leads to 95% c.l. $\ll 1\ \sigma_{SD}$ (one standard deviation of the mean), and a mean value that is poorly constrained. * Denotes results from a previously analysed preparation of Big Batch, and a separate supply of IRMM-018 to VU

Standard	Group no.	**Group**	Rank	δ^{30}**Si**	95% c.l. SEM	$1\sigma_{SD}$	n	δ^{29}**Si**	95% c.l. SEM	$1\sigma_{SD}$	n
IRMM-018	5	UCSB	1	**−1.86**	0.07	0.11	14	**−0.95**	0.03	0.06	14
IRMM-018	7	NIGL	2	**−1.89**	0.81	0.32	3	**−0.95**	0.42	0.17	3
IRMM-018	2	UCSC	3	**−1.79**	0.59	0.07	2	**−0.95**	0.35	0.04	2
IRMM-018	6	SU-NRM	4	n/a				**−0.91**	0.02	0.10	157
IRMM-018	4	Luleå	5	**−1.71**	0.09	0.14	12	**−0.85**	0.03	0.04	12
IRMM-018	1	ETHZ	6	**−1.61**	0.01	0.11	493	**−0.82**	0.01	0.06	493
IRMM-018	3	MRAC	7	n/a				**−0.80**	0.03	0.06	21
IRMM-018	8	VU	8	**−1.41**	0.05	0.11	25	**−0.73**	0.03	0.05	24
IRMM-018*	8	VU, new		**−1.74**	0.08	0.14	14	**−0.90**	0.03	0.05	14
IRMM-018	8	VU, both		**−1.62**	0.04	0.13	39	**−0.80**	0.03	0.10	39
IRMM-018	Pooled			**−1.65**	0.01	0.11	563	**−0.85**	0.01	0.07	740
Diatomite	7	NIGL	1	**+1.02**	0.32	0.04	2	**+0.54**	1.53	0.17	2
Diatomite	2	UCSC	2	**+1.46**	0.15	0.16	7	**+0.63**	0.10	0.11	7
Diatomite	4	Luleå	3	**+1.17**	0.03	0.03	6	**+0.63**	0.03	0.03	8
Diatomite	1	ETHZ	4	**+1.23**	0.03	0.08	31	**+0.63**	0.02	0.06	30
Diatomite	8	VU	5	**+1.29**	0.09	0.15	13	**+0.64**	0.07	0.11	13
Diatomite	3	MRAC	6	n/a				**+0.70**	0.04	0.06	11
Diatomite	6	SU-NRM	7	n/a				**+0.72**	0.12	0.12	6
Diatomite	5	UCSB	8	**+1.38**	0.04	0.08	23	**+0.71**	0.04	0.04	23
Diatomite	Pooled			**+1.26**	0.02	0.10	82	+0.64	0.02	0.07	**100**
Big batch	2	UCSC	1	**−10.64**	0.05	0.15	38	**−5.46**	0.02	0.06	42
Big batch	6	SU-NRM	2	n/a				**−5.43**	0.11	0.10	6
Big batch	1	ETHZ	3	**−10.58**	0.04	0.07	18	**−5.39**	0.02	0.05	18
Big batch	5	UCSB	4	**−10.39**	0.04	0.07	23	**−5.31**	0.04	0.04	23
Big batch	8	VU	5	**−10.44**	0.13	0.20	12	**−5.32**	0.09	0.15	12
Big batch	3	MRAC	6				n/a	**−5.27**	0.07	0.07	6
Big batch	4	Luleå	7	**−10.29**	0.12	0.14	8	**−5.26**	0.06	0.07	8
Big batch	7	NIGL	8	**−10.27**	0.98	0.40	3	**−5.23**	0.52	0.21	3
Big batch*	3	MRAC		n/a				**−5.29**	0.02	0.04	23
Big batch*	5	UCSB		**−10.56**	0.07	0.17	23	**−5.39**	0.04	0.09	23
Big batch*	1	ETHZ		**−10.48**	0.18	0.50	34	**−5.39**	0.11	0.31	34
Big batch		Pooled		**−10.48**	0.04	0.27	**159**	**−5.35**	0.02	0.15	**198**

individual data points, the mean results from each group are in good agreement (Fig. 1), with a marked overlap in the measured isotope ratios for each standard from each group.

The data can be compiled to form a probability density function (pdf), so that the shape of the distribution can be easily observed, as is shown in Fig. 2. However, this can be realized in two separate ways, either (i) by weighting all the data points equally or (ii) by weighting the averages for each group equally. The results of both approaches are illustrated in the figure. For the large number of analyses obtained, we would expect the data to be normally distributed around an average value, and in describing the data and reproducibility in terms of standard deviations (σ_{SD}) and standard errors (σ_{SEM}, standard error of the mean) one would be defining this to be the case. However, as is shown in Fig. 2, the data are not normally distributed in a Gaussian or bell-shaped curve, so the modal and arithmetic mean (or average) of each population is not exactly the same. That is to say, the peak in the pdf is not in the middle of the distribution. Thus, by describing the data in terms of a mean, plus/minus a standard deviation, we are not accurately reflecting the underlying data, and the given values can be somewhat biased by the way the data is amassed. A better approach would be to quantify the quartile or 90% confidence limits of the observed distributions in order to quantify the reproducibility of the Standards (Table 3). For Big Batch these δ^{30}Si ranges are from −10.77 to −10.23‰, and −10.64 to −10.38‰ for the 90% range and 50% (quartile) range, respectively, weighting each point equally, or from −10.81 to −10.04‰, and −10.60 to −10.29‰ for the 90% range and 50% (quartile) range, respectively, weighting each

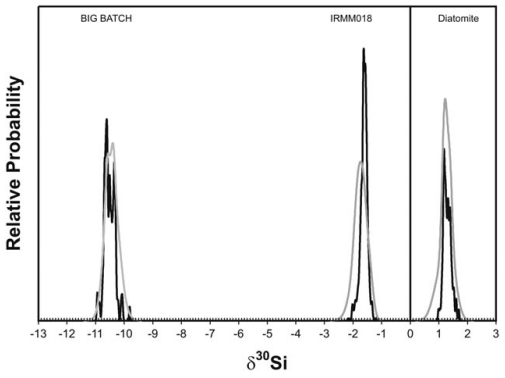

Fig. 2 Probability density function (pdf) of the δ^{30}Si results from all groups for all 3 standards, using both equal weighting for each data point (black line) and equal weight for each group (grey line).

Table 3 Summary of the collective distribution of δ^{30}Si and δ^{29}Si values for each standard, based on either weighting all the data points equally or by weighting the averages for each group equally

Standard	Equal Weighting	Composition	Modal value	Quartile range		90% range	
				Lower	Upper	Lower	Upper
IRMM-018	Datapoints	δ^{30}Si	−1.61	−1.68	−1.54	−1.85	−1.44
IRMM-018	Groups	δ^{30}Si	−1.73	−1.88	−1.58	−2.12	−1.36
IRMM-018	Datapoints	δ^{29}Si	−0.84	−0.90	−0.79	−1.01	−0.72
IRMM-018	Groups	δ^{29}Si	−0.88	−0.96	−0.80	−1.10	−0.70
Diatomite	Datapoints	δ^{30}Si	+1.27	+1.19	+1.38	+1.11	+1.54
Diatomite	Groups	δ^{30}Si	+1.25	+1.13	+1.39	+0.85	+1.61
Diatomite	Datapoints	δ^{29}Si	+0.66	+0.61	+0.71	+0.51	+0.79
Diatomite	Groups	δ^{29}Si	+0.65	+0.58	+0.72	+0.47	+0.85
Big batch	Datapoints	δ^{30}Si	−10.53	−10.64	−10.38	−10.77	−10.23
Big batch	Groups	δ^{30}Si	−10.45	−10.60	−10.29	−10.81	−10.04
Big batch	Datapoints	δ^{29}Si	−5.38	−5.46	−5.30	−5.55	−5.20
Big batch	Groups	δ^{29}Si	−5.34	−5.43	−5.25	−5.56	−5.10

group equally. The modal δ^{30}Si value, or average, is between −10.53 and −10.45‰, depending upon the weighting used, as is shown in Table 3. Even for this highly fractionated standard, all groups have data within these relatively narrow quartile ranges.

As the number of measurements (n) is not the same between groups, the mean can be biased to either the groups from which more data has been analysed or those which have produced less. Rather than use either of these extremes for creating an average or mean δ-value, we have weighted the contribution from each group by their individual reproducibility (the 95% confidence-limit (c.l.) of each group's dataset). The error on this mean δ-value is estimated using normal theory, where the total pooled variance (σ_p^2) is the sum of the variance from within each group normalized to the degrees of freedom (n–1). Statistical differences between the means from each group and each other group, and the overall mean (termed pooled value) are evaluated using Scheffé adjustment on a Bonferroni method at the 95% c.l. ($p < 0.05$), see Table 2.[39] This corrects for the likelihood that given enough comparisons there is likely to be some significant difference arising from the application of simple pair-wise comparisons (like the Student's T-test).

Discussion

As shown in Fig. 1 and Table 2, the average results from each group are typically within 1 standard deviation (σ_p) of the pooled mean, implying that all groups obtained consistent results for both δ^{30}Si and δ^{29}Si values for all three standards. As these groups employ distinctive methods (including acid/alkaline dissolution/fusion, Si separation using cation exchange, selective co-precipitation, as well as fluorination techniques) there does not appear to be any significant mass-fractionation associated with any of the methods. Furthermore, the good agreement between gas-source and plasma-ionization (both in high and low resolution) mass spectrometric techniques excludes the possibility of a systematic bias in the determined Si isotope composition induced by measurement instrumentation. This confirms the previously published conclusion that there is no systematic offset between MC-ICP-MS and IRMS.[28] The published data from a previous comparison of Big Batch are presented in Table 2 (denoted by Big Batch*) along with the unpublished results from the analysis of the same sample solution at ETH, which further illustrates the agreement between instruments.

An indicator of data quality is given by the correlation between measured δ^{30}Si and δ^{29}Si values, as unresolved interferences or problems in the Si isotope analyses should cause isotope ratios to be shifted away from that expected from terrestrial mass-dependent fractionation. As is shown in Fig. 3, there is an excellent correlation between δ^{30}Si and δ^{29}Si values for all the mean values reported from each group (R^2 = 0.999 96, excluding Diatomite from UCSC, which appears to have an interference problem, discussed below). Furthermore, the slope of this line depends upon the fractionation process: for an equilibrium fractionation the gradient should equal 0.518, whilst for kinetic fractionation it would depend upon the Si species considered and gives values from 0.509 for Si atoms to 0.505 for SiO_2. The best-fit line, with an intercept of zero, has a gradient of 0.511 which is principally controlled by the composition of Big Batch, and implies that the fractionation induced in the formation of this standard was kinetically controlled and did not take place under equilibrium

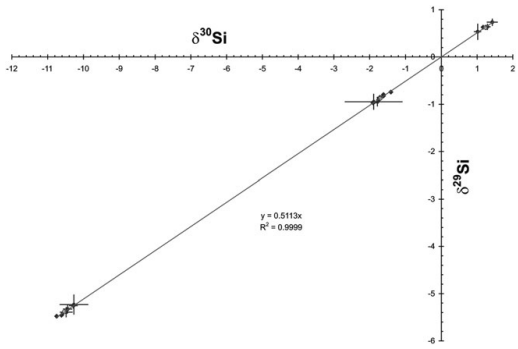

Fig. 3 Three isotope plot of δ^{29}Si *versus* δ^{30}Si (error bars are 1 σ_{SD}). Means from all groups for all standards fall along a mass-dependent fractionation array (excluding Diatomite from UCSC), with a slope of 0.511, in close agreement with kinetic isotope fractionation of Si of 0.5092.

conditions. This is expected as the equilibrium conditions generally lead to smaller isotope fractionation effects.

However, despite the generally good agreement, in detail there is some divergence in the mean results from each group beyond the internal reproducibility of the data. This lower reproducibility between groups compared with within groups is typical for most analytical measurements, but it ultimately limits the reliability of comparing datasets published by different groups. Even though published internal precisions may be below 0.1‰, there may remain problems with comparing data from different groups to this level of accuracy. From this inter-laboratory comparison, using the quartile range from individual measurements, it would appear that differences between reported results should be limited to 0.20‰ δ^{30}Si for a given sample and 0.13‰ for δ^{29}Si.

We can quantify the statistical significance of the apparent offsets between participating groups by applying a Bonferroni method to test for significant differences between the mean values reported from each group. Mean results are significant at the 0.05 (or 95% confidence) level if they differ by more than the following (see Table 2): IRMM-018 δ^{30}Si >0.18‰, δ^{29}Si >0.11‰; Big Batch δ^{30}Si >0.44‰, δ^{29}Si >0.22‰; Diatomite δ^{30}Si >0.20‰, δ^{29}Si >0.13‰. Excluding means based on a small number of duplicate analyses ($n < 6$), there are no statistical differences between groups for either the Big Batch or Diatomite standard, apart from one notable exception. This exception is the mean δ^{30}Si value of Diatomite from UCSC compared with Lulea, but given that both groups report exactly the sample δ^{29}Si values and that the high δ^{30}Si values from UCSC do not fit on the terrestrial mass-dependent fractionation array shown in Fig. 3, this UCSC δ^{30}Si data can be clearly seen as anomalous (probably due to a small interference problem on mass 30).

There are several statistical differences in the mean value of IRMM-018 between groups including two different analyses of IRMM-018 from one participating group (VU), see also ref. 23. The statistical differences are unlikely to result from a systematic error, given the agreement for the other two standards, and are possibly due to contamination by dust during handling or heterogeneity within the standard material itself. The mean from UCSB is distinct from the means VU, ETHZ and MRAC, which could be taken to suggest a slight discrepancy in the result between gas-source mass spectrometry and MC-ICP-MS techniques, but may equally be simply due to chance. We thus recommend against future use of IRMM-018 as a calibration standard. Indeed, given that IRMM has stopped selling IRMM-018 and replaced it with IRMM-018a, which may be similar to NBS28, this standard is essentially obsolete. Therefore, NBS28 should remain the primary reference material for Si isotope studies (δ^{30}Si = δ^{29}Si = 0) and we recommend the use of Big Batch and Diatomite as secondary reference materials to check accuracy of methods and new analytical studies.

Conclusions

All chosen methods for both sample preparation and mass-spectrometric techniques give consistent results for both δ^{30}Si and δ^{29}Si values for the samples Diatomite and Big Batch distributed by Mark Brzezinski (UCSB). These methods include dissolution/fusion, cation exchange, co-precipitation and decomposition, and fluorination techniques: in addition, we have used two different types of mass spectrometry, plasma-ionization (both in high and low resolution) and gas-source. Published data can be reliably compared between laboratories at the 0.2‰ accuracy for δ^{30}Si values (2 σ_{SD}), although internal reproducibility within each participating laboratory is generally better than this. Statistical differences between the mean values reported by each group for neither Big Batch nor Diatomite are significant (excluding poorly constrained data). However, they are significant for the IRMM-018 standard. As the Si isotopic compositions of the other standards are in agreement, this difference is unlikely to be a systematic error and is possibly due to heterogeneity of the powder or laboratory contamination of the IRMM-018 standard.

The calibration between δ^{30}Si and δ^{29}Si values are in complete agreement with a mass-dependent fractionation between the standards, with $\delta^{29}\text{Si} = 0.51 \times \delta^{30}\text{Si}$ (or $\delta^{30}\text{Si} = 1.96 \times \delta^{29}\text{Si}$), allowing for easy calculation of δ^{30}Si values from given δ^{29}Si values and *vice versa*. The mean δ^{30}Si values from the collectively pooled data for the three standards are +1.26‰, −1.65‰ and −10.48‰ for Diatomite, IRMM-018 and Big-Batch, respectively.

Acknowledgements

We would like to thank the following for their contributions to various parts of this inter-laboratory comparison: the Celite Corporation of Lompoc, California, USA, for donating the purified diatomite used in this study; from ETH Zürich, Felix Oberli, Martin Frank, and Alex Halliday (for help in instigating Si isotope analyses), and the funding from SNF and STOPFEN EU TMR network; the Belgian group thank their colleagues N. Mattielli and J. de Jong, and the funding agencies BELSPO (EV/37/7C), FNRS (FRFC 2.4.512.00F), and the EC (EVK-CT-2000-00057); the SU-NRM group would like to thank Per Andersson, Hans Schoberg and the Swedish Research Council (VR-621-2001-2619); the VU group would like to thank J. C. van Belle and B. van der Wagt for their help; and the Dutch MC-ICP-MS facility is supported by a grant (no. 175.107.404.01) from the Netherlands Organisation for Scientific Research (NWO/ALW).

References

1 I. Basile-Doelsch, *J. Geochem. Explor.*, 2006, **88**, 252–256.
2 A. N. Halliday, C. H. Stirling, P. A. Freedman, F. Oberli, B. C. Reynolds and R. B. Georg, in *Encyclopedia of Mass Spectrometry*, Elsevier Science Ltd., Amsterdam, The Netherlands, vol. 5, in the press.
3 I. L. Barnes, L. J. Moore, L. A. Machlan, T. J. Murphy and W. R. Shields, *J. Res. Natl. Bur. Stand., Sect. A*, 1975, **79**, 727–735.
4 T. B. Coplen, J. K. Bohlke, P. De Bievre, T. Ding, N. E. Holden, J. A. Hopple, H. R. Krouse, A. Lamberty, H. S. Peiser, K. Revesz, S. E. Rieder, K. J. R. Rosman, E. Roth, P. D. P. Taylor, R. D. Vocke and Y. K. Xiao, *Pure Appl. Chem.*, 2002, **74**, 1987–2017.
5 J. H. Reynolds and J. Verhoogen, *Geochim. Cosmochim. Acta*, 1953, **3**, 224–234.
6 R. J. Allenby, *Geochim. Cosmochim. Acta*, 1954, **5**, 40–48.

7 C. B. Douthitt, *Geochim. Cosmochim. Acta*, 1982, **46**, 1449–1458.
8 S. Epstein and H. P. Taylor, Jr, *Science*, 1970, **167**, 533–535.
9 A. Besmehn and P. Hoppe, *Geochim. Cosmochim. Acta*, 2003, **67**, 4693–4703.
10 T. Ding, in *Handbook of Stable Isotope Analytical Techniques*, ed. P. A. de Groot, 2004, vol. 1, pp. 523–537.
11 R. B. Georg, B. C. Reynolds, M. Frank and A. N. Halliday, *Chem. Geol.*, 2006, **235**, 95–104.
12 E. Engstrom, I. Rodushkin, D. C. Baxter and B. Ohlander, *Anal. Chem.*, 2006, **78**, 250–257.
13 D. E. Varela, C. J. Pride and M. A. Brzezinski, *Global Biogeochem. Cycles*, 2004, **18**, doi:10.1029/2003GB002140.
14 L. Y. Alleman, D. Cardinal, C. Cocquyt, P.-D. Plisnier, J.-P. Descy, I. Kimirei, D. Sinyinza and L. André, *J. Great Lakes Res.*, 2005, **31**, 509–519.
15 L. André, D. Cardinal, L. Y. Alleman and S. Moorbath, *Earth Planet. Sci. Lett.*, 2006, **245**, 162–173.
16 R. B. Georg, B. C. Reynolds, M. Frank and A. N. Halliday, *Earth Planet. Sci. Lett.*, 2006, **249**, 290–306.
17 C. L. De La Rocha, M. A. Brzezinski and M. J. DeNiro, *Geochim. Cosmochim. Acta*, 2000, **64**, 2467–2477.
18 B. C. Reynolds, M. Frank and A. N. Halliday, *Earth Planet. Sci. Lett.*, 2006, **244**, 431–443.
19 D. Cardinal, L. Y. Alleman, F. Dehairs, N. Savoye, T. W. Trull and L. André, *Global Biogeochem. Cycles*, 2005, **19**, doi:10 1029/2004GB002364.
20 S. Opfergelt, D. Cardinal, C. Henriet, L. André and B. Delvaux, *J. Geochem. Explor.*, 2006, **88**, 224–227.
21 T. P. Ding, G. R. Ma, M. X. Shui, D. F. Wan and R. H. Li, *Chem. Geol.*, 2005, **218**, 41–50.
22 S. Opfergelt, D. Cardinal, C. Henriet, X. Draye, L. André and B. Delvaux, *Plant Soil*, 2006, **V285**, 333–345.
23 S. H. J. M. van den Boorn, P. Z. Vroon, C. C. van Belle, B. van der Wagt, J. Schwieters and M. J. van Bergen, *J. Anal. At. Spectrom.*, 2006, **21**, 734–742.
24 I. Basile-Doelsch, J. D. Meunier and C. Parron, *Nature*, 2005, **433**, 399–402.
25 K. Ziegler, O. A. Chadwick, M. A. Brzezinski and E. F. Kelly, *Geochim. Cosmochim. Acta*, 2005, **69**, 4597–4610.
26 K. Ziegler, O. A. Chadwick, A. F. White and M. A. Brzezinski, *Geology*, 2005, **33**, 817–820.
27 M. A. Brzezinski, J. L. Jones, C. P. Beucher, M. S. Demarest and H. L. Berg, *Anal. Chem.*, 2006, **78**, 6109–6114.
28 D. Cardinal, L. Y. Alleman, J. de Jong, K. Ziegler and L. André, *J. Anal. At. Spectrom.*, 2003, **18**, 213–218.
29 B. C. Reynolds, R. B. Georg, F. Oberli, U. H. Wiechert and A. N. Halliday, *J. Anal. At. Spectrom.*, 2006, **21**, 266–269.
30 T. Ding, D. Wan, R. Bai, Z. Zhang, Y. Shen and R. Meng, *Geochim. Cosmochim. Acta*, 2005, **69**, 5487–5494.
31 S. Valkiers, K. Russe, P. Taylor, T. Ding and M. Inkret, *Int. J. Mass Spectrom.*, 2005, **242**, 319–321.
32 M. F. Miller, *Geochim. Cosmochim. Acta*, 2002, **66**, 1881–1889.
33 A. Galy, M. Bar-Matthews, L. Halicz and R. K. O'Nions, *Earth Planet. Sci. Lett.*, 2002, **201**, 105–115.
34 E. D. Young, A. Galy and H. Nagahara, *Geochim. Cosmochim. Acta*, 2002, **66**, 1095–1104.
35 D. Malinovsky, A. Stenberg, I. Rodushkin, H. Andren, J. Ingri, B. Ohlander and D. C. Baxter, *J. Anal. At. Spectrom.*, 2003, **18**, 687–695.
36 C. L. De La Rocha, M. A. Brzezinski and M. J. DeNiro, *Anal. Chem.*, 1996, **68**, 3746–3750.
37 M. J. Leng and P. A. Barker, *Earth-Sci. Rev.*, 2006, **75**, 5–27.
38 C. L. De La Rocha, *Geochem. Geophys. Geosyst.*, 2002, **3**, art. no.-1045.
39 D. G. Uitenbroek, 1997, at http://home.clara.net/sisa/.
40 C. L. De La Rocha, M. A. Brzezinski and M. J. DeNiro, *Geochim. Cosmochim. Acta*, 1997, **61**, 5051–5056.
41 C. L. De La Rocha, M. A. Brzezinski, M. J. DeNiro and A. Shemesh, *Nature*, 1998, **395**, 680–683.
42 M. A. Brzezinski, C. J. Pride, V. M. Franck, D. M. Sigman, J. L. Sarmiento, K. Matsumoto, N. Gruber, G. H. Rau and K. H. Coale, *Geophys. Res. Lett.*, 2002, **29**, 1564, doi:1510.1029/2001GL014349.

II

Chromatographic purification for the determination of dissolved silicon isotopic compositions in natural waters by high-resolution multicollector inductively coupled plasma mass spectrometry

Analytical Chemistry 78 (2006) 250-257

Engström, I. Rodushkin, D. C. Baxter and B. Öhlander

Anal. Chem. **2006,** *78,* 250−257

Chromatographic Purification for the Determination of Dissolved Silicon Isotopic Compositions in Natural Waters by High-Resolution Multicollector Inductively Coupled Plasma Mass Spectrometry

Emma Engström,*,† Ilia Rodushkin,‡ Douglas C. Baxter,‡ and Björn Öhlander†

Division of Applied Geology, Luleå University of Technology, S-971 87 Luleå, Sweden, and Analytica AB, Aurorum 10, S-977 75 Luleå, Sweden

A procedure is described for accurate Si isotope ratio measurements by multicollector inductively coupled plasma mass spectrometry (MC-ICPMS). Dissolved silicon was preconcentrated and separated from other elements present in natural surface waters using anion-exchange chromatography. The optimized procedure provides virtually complete elimination of major inorganic constituents while maintaining Si recovery in excess of 97%. High-resolution capabilities of MC-ICPMS used in this study allow interference-free measurements of ^{28}Si and ^{29}Si isotopes using conventional solution nebulization sample introduction without aerosol desolvation. Owing to the magnitude of polyatomic ion contributions in the region of mass 30, mostly from $^{14}N^{16}O^+$, measurements of the ^{30}Si isotope can be affected by tailing of the interference signals, making exact matching of analyte and nitric acid concentrations in all measurement solutions mandatory. Isotope abundance ratio measurements were performed using the bracketing standards approach and on-line correction for mass-bias variations using an internal standard (Mg). Uncertainties, expressed as 95% confidence intervals, for replication of the entire procedure are better than ±0.18‰ for δ^{29}Si and ±0.5‰ for δ^{30}Si. For the first time with MC-ICPMS, the quality of Si isotope abundance ratio measurements could be verified using a three-isotope plot. All samples studied were isotopically heavier than the IRMM-018 Si isotopic reference material.

Silicon is one of the most common elements in the Earth's crust, making up 27% by weight, and it is present in large amounts in a variety of matrixes, such as soil, water, plants, plankton, sediments, minerals, and rocks.[1] Diatoms largely control the cycling of silicon in the oceans,[2] with minor contributions from other silica mineralizing groups such as radiolarians and silicoflagellates, and dissolved silica is essential for their growth.[3] Fractionation of silicon isotopes by marine diatoms during biogenic silica formation has been observed[4,5] which opened up the possibility for Si isotopes to be used as an oceanographic tracer.[5,6] As in diatoms, formation of biogenic opal (amorphous hydrated silica) in plants causes fractionation.[7] These facts imply that silicon isotope composition also can be used for paloeclimatic[6] and agricultural studies.[7]

Dissolved silicon in natural waters is essentially nonionic in neutral and weakly acidic solutions and is, according to the established terminology, called monosilicic acid, $Si(OH)_4$. The latter is a very weak acid ($pK_a = 9.8$) and is in equilibrium with the silicate anion $H_3SiO_4^-$; ∼5% exists in the silicate form in marine water.[1] Monosilicic acid is often referred to as "reactive" silica, due to its tendency to react with molybdic acid to form molybdosilicic acid, and polymerizes rapidly at concentration levels higher than 60 mg L^{-1}, the saturation level with respect to amorphous silica, to polymeric species (colloidal silica) with virtually no ionic character.[1,8]

Despite widespread interest and great applicability, the number of publications on natural silicon isotope systems over the last 50 years remains rather limited.[9] Hazardous, laborious, and expensive chemical preparation of the analyte, frequently used for silicon isotopic analysis in the past, has certainly limited development in this area. Conventional sample purification methods for dissolved silicon in water consist of a combined precipitation step followed by a reaction with purified F_2 or BrF_5 to form SiF_4 gas.[4,7,10−12] For

* Corresponding author: (e-mail) emma.engstrom@analytica.se.
† Luleå University of Technology.
‡ Analytica AB.

(1) Iler, R. K. *The Chemistry of Silica*; Wiley: New York, 1979.
(2) Tréguer, P.; Nelson, D. M.; Van Bennekom, A. J.; DeMaster, D. J.; Leynaert, A.; Quéguiner, B. *Science* **1995**, *268*, 375−379.
(3) Perry, C. C. *Rev. Mineral. Geochem.* **2003**, *54*, 291−327.
(4) Douthitt, C. B. *Geochim. Cosmochim. Acta* **1982**, *46*, 1449−1458.
(5) De La Rocha, C. L.; Brzezinski, M. A.; DeNiro, M. J. *Geochim. Cosmochim. Acta* **1997**, *61*, 5051−5056.
(6) De La Rocha, C. L.; Brzezinski, M. A.; DeNiro, M. J.; Shemesh, A. *Nature* **1998**, *395*, 680−683.
(7) Ding, T. P.; Ma, G. R.; Shui, M. X.; Wan, D. F.; Li, R. H. *Chem. Geol.* **2005**, *218*, 41−50.
(8) Ali, M. B. S.; Hamrouni, B.; Bouguecha, S.; Dhahbi, M. *Desalination* **2004**, *167*, 273−279.
(9) De La Rocha, C. L. *Geochem. Geophys. Geosyst.* **2002**, *3* (8), 0.1029/2002GC000310.
(10) De La Rocha, C. L.; Brzezinski, M. A.;. DeNiro, M. J. *Anal. Chem.* **1996**, *68*, 3746−3750.

10.1021/ac051246v CCC: $33.50
Published on Web 11/25/2005

decades, isotope ratio mass spectrometry (IRMS) has been the predominant technique for studying Si isotopic compositions, but multicollector inductively coupled plasma mass spectrometry (MC-ICPMS), especially combined with high-resolution capabilities, may offer important advantages. The latter technique may require less demanding, time-efficient, and safer sample preparation,[13] hopefully without extensively sacrificing measurement precision compared with IRMS.

In this study, we present a one-pass separation procedure for dissolved silicon in natural waters prior to isotopic analysis by MC-ICPMS, based on strong-base anion-exchange chromatography with a maximum of 0.1% hydrofluoric acid included in the elution steps. The dissolved silicon can be loaded on the resin either in $Si(OH)_4$ form[8] (in equilibrium with $H_3SiO_4^-$) or in the form of SiF_6^{2-} as proposed by Wickbold in 1959,[14] depending on the sample matrix. Both species exhibit high affinity to the resin in hydroxide form. The silicon separation procedure has been tested on representative water samples with different chemical characteristics, resulting in quantitative recovery, and shown not to induce detectable fractionation. We have also revealed the presence of a nonnegligible isobaric interference on m/z 29 attributable to $^{28}SiH^+$, the level of which suggests that particular attention must be taken in order to achieve accurate isotope abundance ratio measurements. Additionally, the high-resolution capability of the instrument employed offers accurate measurements of $\delta^{30}Si$ to a propagated precision of better than $\pm 0.5‰$, enabling the first combined measurements of $\delta^{29}Si$ and $\delta^{30}Si$ values by MC-ICPMS to be presented.

EXPERIMENTAL SECTION

Instrumentation. The single-collector, double-focusing, sector field ICPMS (ICP-SFMS) instrument used in this study was the Element2 (ThermoElectron, Bremen, Germany). Typical operating conditions and measurement parameters are given elsewhere.[15,16]

Isotopic analyses were performed by MC-ICPMS using a Neptune (ThermoElectron) in high-resolution mode.[17] A platinum guard electrode (CD-system activated) and Ni skimmer X-cone served to maximize the ion transmission. The introduction system consisted of a tandem quartz spray chamber arrangement (cyclone + Scott type double pass), low-flow PFA microconcentric nebulizer (Elemental Scientific Inc., Omaha, NE) together with a peristaltic pump (Perimax 12, SPETEC, Erding, Germany) operating at a flow rate of ~0.25 mL min^{-1}. Instrumental operating conditions and measurement parameters for MC-ICPMS are given in Table 1. After ignition of the plasma, the instrument was left to stabilize for ~2 h before making any measurements.

Since the mass difference between ^{25}Mg and ^{30}Si slightly exceeds 17% (maximum allowed by the detector array of the Neptune[17]), the isotopic analyses were conducted in multidynamic mode, changing the magnet setting between measurement of the Mg and Si isotopes. Though certainly less effective than truly simultaneous measurements for correcting short-term mass-bias variations, this approach is useful for matrix-induced effects. Silicon isotopes at m/z 28, 29, and 30 were monitored using the main cup configuration including Faraday cups L1, H1, and H2; magnesium isotopes at m/z 25 and 26 were collected in L2 and the center cup using a subconfiguration. Each sample measurement consisted of four 1.049-s integrations, five cycles, and five blocks. A 3-s idle time was incorporated in the method to allow the magnet to stabilize after changing cup configuration in each cycle. A plateau test[17] of the measured $^{29}Si/^{28}Si$ ratio using only the main cup configuration was conducted prior to each measurement session to locate the interference-free plateau (see Figure 2d).

Table 1. Instrumental Operating Conditions and Measurement Parameters for the Neptune MC-ICPMS Instrument

forward power	1200 W
accelerating voltage	−10000 V
sampler cone	nickel, 1.1-mm orifice diameter
skimmer X-cone	nickel, 0.8-mm orifice diameter
coolant	16 L of Ar min^{-1}
auxiliary	0.60 L of Ar min^{-1}
nebulizer	~1.15 L of Ar min^{-1} (optimized daily)

Reagents and Samples. The strong-base anion- exchange resin used in this study was Dowex 1 × 8, mesh 100−200 (Serva Feinbiochemica, Heidelberg, Germany). All calibration and internal standard solutions for external calibrations and element spiking used were prepared by diluting single-element standard solutions from SPEX Plasma Standards (Edison, NJ) or, in the case of silicon, Ultra Scientific (North Kingstown, U.K.). Analytical-reagent grade nitric acid (Merck, Darmstadt, Germany) was utilized after additional purification by sub-boiling distillation in a quartz still. The resulting silicon blank from HNO_3 is routinely tested and has not been found to represent a significant contribution to overall blank levels. The hydrofluoric (40%, Suprapure grade; Merck) and hydrochloric (30%, analytical plus grade; Fluka, Steinheim, Germany) acids, as well as granular NaOH (analytical grade; Merck), were used as supplied.

The dilution of samples and standards and the preparation of procedural blanks were performed using Milli-Q water (Millipore Milli-Q, Bedford, MA).

The samples analyzed in this study included FIJI Natural Artesian Water, bottled by Natural Waters of Viti Ltd. (Yaqara, Viti Levu, Fiji Island), a commercially available product with high silica content. This material has been selected for quality control and performance assessment in an ongoing, informal, interlaboratory comparison program. Representative water samples (brackish and stream water) separated in this study were all collected in northern Sweden. The Swedish natural waters exhibited silicon concentrations between 2 and 5 mg L^{-1} and the FIJI water contained, according to the product description, 85 mg L^{-1} silica. The FIJI water sample exhibited low nickel content and was spiked to a concentration of ~250 μg L^{-1} in specific experiments to evaluate the elution profile of this potentially interfering element. This suite of samples was selected for the purpose of testing the separation procedure on different matrixes.

(11) De La Rocha, C. L.; Brzezinski, M. A.; DeNiro, M. J. *Geochim. Cosmochim. Acta* **2000**, *64*, 2467−2477.
(12) Ding, T.; Wan, D.; Wang, C.; Zhang, F. *Geochim. Cosmochim. Acta* **2004**, *68*, 205−216.
(13) Vanhaecke, F.; Moens, L. *Anal. Bioanal. Chem.* **2004**, *78*, 232−240.
(14) Wickbold, R. *Fresenius Z. Anal. Chem.* **1959**, *171*, 81−91.
(15) Rodushkin, I.; Ödman, F.; Olofsson, R.; Axelsson, M. D. *J. Anal. At. Spectrom.* **2000**, *15*, 937−944.
(16) Stenberg, A.; Andrén, H.; Malinovsky, D.; Engström, E.; Rodushkin, I.; Baxter, D. C. *Anal. Chem.* **2004**, *76*, 3971−3978.
(17) Weyer, S.; Schwieters, J. B. *Int. J. Mass Spectrom.* **2003**, *226*, 355−368.

The silicon isotopic reference material IRMM-018, manufactured by the Institute of Reference Material and Measurements (Geel, Belgium), was used as standard during isotopic analyses. Although NBS28 Silica Sand has been proposed as the primary reference material for Si isotopic measurements,[18] Valkiers et al.[19] have shown that NBS28 and IRMM-018 are isotopically indistinguishable. IRMM-018 is readily available and certified for Si isotopic composition and is therefore adequate as a standard for the present method development.

Safety Considerations. Hydrofluoric acid can cause severe burns and must be used with extreme care. It should be neutralized with sodium bicarbonate prior to disposal.

Sample Preparation. Before separation, the water samples were filtered through 0.45-μm polycarbonate filters (Sarstedt, Numbrecht, Germany) to remove highly polymerized colloidal and biogenic silica together with suspended organic matter. Natural water samples were stored in acid-cleaned high-density polypropylene bottles. It is recommended to dilute samples with high levels of dissolved silica to below 60 mg L^{-1} to prevent polymerization during storage. This is especially important for samples containing a high-salt matrix.[1] Dissolved silicon concentrations in the filtered samples were determined using ICP-SFMS.

For samples that were to be loaded onto the column (see below) in $Si(OH)_4$ (in equilibrium with $H_3SiO_3^-$) form, the pH was adjusted to slightly alkaline conditions (pH 7.0−8.5) with 100 mM NaOH. When such solutions are passed through a bed of strong-base cation-exchange resin in the free base form, the silica is ionized in contact with the resin and then retained as silicate ions. Very alkaline solutions are unsuitable because the hydroxide ion behaves as an eluent at high concentrations. For samples to be separated using silicon in SiF_6^{2-} form, pretreatment with 0.025% HF was required; note that the molar ratio F/Si needs to be kept >6 to prevent loss of volatile SiF_4.[1] Silicic acid reacts quantitatively with aqueous HF to form SiF_6^{2-} and H_2O.[1]

The isotopic reference material IRMM-018, received in the form of silica sand, was dissolved by adding 100 μL of HNO_3 to 20 mg of solid material, followed by 150 μL of HF. The sample was then diluted to 10 mL with Milli-Q water when the silica particles were seen to be completely dissolved, which requires only ~5 min for the finely ground IRMM-018 material.

Silicon Separation Using Strong-Base Anion-Exchange Chromatography. The columns were prepared by adding ~0.44 g of resin between small cotton wool plugs in precleaned 5-mL disposable pipet tips. The resin was washed with 10 mL of Milli-Q and thereafter preconditioned with 7.5 mL of freshly prepared 2 M NaOH (the resin changes color from yellow to orange-red). The column was then washed with Milli-Q until the eluent became neutral or weakly acidic (usually after passage of 12.5−15 mL), according to the procedure proposed by Ali et al.[8] The pH value reaches a minimum of ~5. The selected amount of sample (usually 300 μg) was then loaded onto the column in either $Si(OH)_4$ form[8] or SiF_6^{2-} form.[14] It is highly recommended to dilute samples with high levels of dissolved silica to a maximum concentration of 15 mg L^{-1}, to avoid temporary overload of the column. The column was thereafter washed with 30 mL of Milli-Q water to quantitatively remove the matrix elements. Details of the silicon separation scheme are shown in Table 2.

Table 2. Silicon Separation Scheme for Strong-Base Ion-Exchange Chromatography Using Dowex 1 × 8, 100−200 Mesh

separation stage	matrix	no. of fractions	volume/mL
preconditioning	2 M NaOH	1	7.5
wash[a]	Milli-Q	1	15
sample load	pH 7.0−8.5 or 0.025% HF	1	variable[b]
matrix wash	Milli-Q	3	10 + 10 + 10
matrix elution	1.0% HCl + 0.1% HF	1	10 + 10
wash stage	Milli-Q + 0.1% HF	1	5
elution	1.0% HNO_3 + 0.025% HF	3	5 + 8[c] + 5

[a] Milli-Q rinse until pH 7−5 of the eluent was reached. [b] Depending on the concentration of silicon in the sample, usually 20 mL. [c] Denotes the major elution fraction containing >97% of the Si.

Mass Spectrometric Measurements. Silicon isotope ratio measurements were performed by MC-ICPMS using Mg for mass discrimination correction, as discussed in detail below. All samples and standards were diluted to a final Si concentration of 5 ± 0.5 mg L^{-1}, spiked with 2 mg L^{-1} Mg and matrix matched to 0.50% HNO_3. Nitric acid matrix is used due to the fact that the silicon is eluted in 1% HNO_3 matrix and any need for extensive dilution is thus avoided. Typical sensitivities for ^{25}Mg and ^{28}Si in high-resolution mode were 2.0 ± 0.2 and 5.0 ± 0.5 V per mg·L^{-1}, respectively. For ^{28}Si, the sensitivity is superior to that obtained using a Nu Plasma MC-ICPMS device in low-resolution mode with direct solution aspiration (0.45 V per mg·L^{-1})[9] and comparable to that obtained for the same type of instrument with a desolvating nebulizer (6 V per mg·L^{-1}).[20] The blank signal on m/z 28 using the quartz introduction components was as low as 20−40 mV, similar to levels reported using a HF-resistant system[9] or an alumina injector.[20] All samples were analyzed in duplicate giving a total measuring time per sample of 14 min using multidynamic measurements, including takeup and washout times. Duplicate measurements allow the detection of memory effects in the introduction system, which has been claimed to be problematic in some cases.[9]

Silicon isotope abundance ratios are reported according to conventional δ^XSi notation, defined by the relationship[10]

$$\delta^X\mathrm{Si} = \left[\frac{(^X\mathrm{Si}/^{28}\mathrm{Si})_{\mathrm{sample}}}{(^X\mathrm{Si}/^{28}\mathrm{Si})_{\mathrm{reference}}} - 1\right] \times 1000\% \qquad (1)$$

where $X = 29, 30$ and the measured isotope ratios have each been corrected for mass bias using the Mg internal standard in combination with an exponential model in the fashion proposed by Woodhead.[21] Outlier elimination using the 2σ criterion was activated at the integration, cycle, and block levels in the resident Neptune software.

RESULTS AND DISCUSSION

Silicon Recovery and Elution Profile. When the essentially neutral $Si(OH)_4$ solution was passed through the strong-base anion

(18) Carignan, J.; Cardinal, D.; Eisenhauer, A.; Galy, A.; Rehkämper, M.; Wombacher, F.; Vigier, N. *Geostand. Geoanal. Res.* **2004**, *28*, 139−148.
(19) Valkiers, S.; Russe, K.; Taylor, P.; Ding, T.; Inkret, M. *Int. J. Mass Spectrom.* **2005**, *242*, 321−323.
(20) Cardinal, D.; Alleman, L. Y.; de Jong, J.; Ziegler, K.; André, L. *J. Anal. At. Spectrom.* **2003**, *18*, 213−218.
(21) Woodhead, J. *J. Anal. At. Spectrom.* **2002**, *17*, 1381−1385.

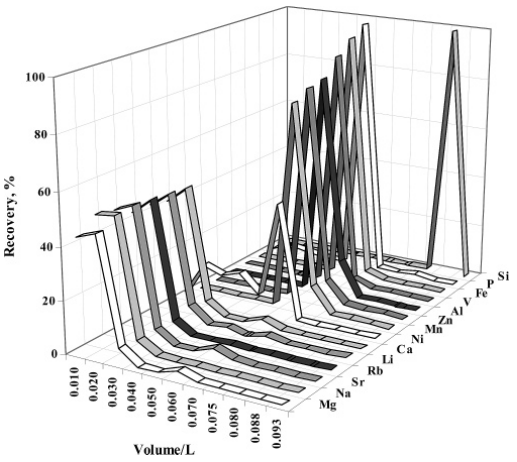

Figure 1. Elution profiles of silicon, as well as potentially interfering and major elements. The sample volume was 20 mL and was collected in the two first 10-mL fractions. The next three 10-mL fractions (to 50 mL) are from the matrix wash stage (see Table 2), followed by two 10-mL matrix elution fractions. HCl is washed from the column in the 70−75-mL fraction, before elution of Si commences in the three final fractions (75−93 mL). The elution profile illustrated was conducted using the SiF_6^{2-} loading form (see text for details). Recoveries of the presented elements range from 96.5 to 103.6% as determined using ICP-SFMS.

resin in hydroxide form, the silicic acid was dissociated to $H_3SiO_4^-$ and quantitatively retained by the column. The elution profile of silicon, as well as of potentially interfering species and major elements, is shown in Figure 1. Note that silicon was the only element that could be detected at significant concentration in the elution stage, with a recovery of 99.3 ± 2.0% (95% confidence interval) for the separation procedure, which excludes the possibility of operationally induced fractionation during sample preparation. To further ensure the absence of induced fractionation, the Si single-element standard was subjected to the proposed procedure (hereafter referred to as separated standard), the results of this experiment being discussed below.

The most critical step in the silicon separation was the matrix elution stage, i.e., the elution of the concomitant metals, such as Al, Fe, Mn, V, and Zn. In the absence of hydrofluoric acid in the eluent, ~60% of the silicon was observed to be lost. This behavior is most likely due to a combination of the relatively low selectivity of the silicate anion compared to the chloride ion (only valid for samples loaded in $Si(OH)_4$ form), silicic acid polymerization under acidic conditions, and the instability of the system when changing from hydroxide to chloride form. Most likely, the addition of hydrofluoric acid to samples loaded in $Si(OH)_4$ form converts the retained silicate ion to SiF_6^{2-}, which exhibits a higher selectivity coefficient due to its doubly charged character. It is very important that this conversion is rapid and quantitative in order to prevent silicon loss at this stage.

According to our observations, the maximum capacity of the 0.44-g column was 300−400 μg of Si in the form of $Si(OH)_4$, but is most likely significantly increased when the dissolved silicon is loaded in SiF_6^{2-} form, due to its greater charge and consequently higher selectivity. A total load of 300 μg of silicon results in a final concentration of ~35 mg L^{-1} in the silicon-containing fraction. The maximum capacity of dissolved silicon is dependent on the presence of other anions and might be reduced for samples exhibiting high levels of competing anions. The equilibrium between monosilicic acid and the silicate ion will be unfavorably altered when the hydroxide ions on the resin surface have been quantitatively exchanged. As a result of this, the pH and subsequently the retention of dissolved silicon will decrease rapidly. Optimization of the system on the matrix of interest is required to be able to operate under capacity-maximized conditions.

Chromatographic Separation of Potential Interferences. The alkali and alkaline earth metals exhibited no affinity for the column and were quantitatively eluted in the first matrix wash step (0−30 mL of Milli-Q water). It was of primary interest to confirm that magnesium was absent from the silicon elution fraction due to the fact that Mg was to be utilized for on-line mass-bias correction. According to our results, remaining impurities in the silicon-containing fraction of the major elements (Ca, Mg, Na) were present at less than 0.05% of their initial concentrations.

Numerous elements, including Al, Fe, Mn, Ni, P, V, and Zn, were retained by the column in hydroxide form but were completely stripped in the matrix elution step (1.0% hydrochloric and 0.1% hydrofluoric acid), as evident from Figure 1. Similar to several other metals, Fe was quantitatively retained by the column and eluted in the matrix elution stage. Nickel, on the other hand, exhibited only partial retention, which resulted in stripping of ~45% during the matrix washing stage. The total recovery of Ni and Fe was >95%. It is particularly gratifying to note that these two elements are quantitatively removed, since ^{56}Fe, ^{58}Fe, ^{58}Ni, and ^{60}Ni present in the silicon elution fraction could deteriorate the accuracy of the measurements by forming doubly charged ions appearing at the same nominal m/z values as the analyte isotopes (Table 3). Using the Saha equation, as well as the ionization temperature and electron number density prescribed by Niu and Houk,[22] the fractions of doubly charged Fe and Ni in the plasma can be estimated as 4×10^{-5} and 2×10^{-6}, respectively. These ions would appear on the low-mass sides of Si isotopes in the high-resolution mass spectra of Figure 2, but the mass resolution of the Neptune is insufficient to discriminate against interferences on both sides of the Si isotopes while simultaneously maintaining flat-topped peaks. Correction for doubly charged ion interferences could be implemented by monitoring $^{57}Fe^{2+}$ and $^{61}Ni^{2+}$ at half-mass positions using additional Faraday cups in a fashion similar to that described by Ramos et al.[23] However, due to the efficiency of the chromatographic separation of Fe and Ni (see Figure 1), and the low levels of formation under the conditions prevailing in the plasma, no signals attributable to doubly charged ions were detected, and so monitoring doubly charged ion formation was deemed unnecessary for the present application.

Instrumental Resolution of Remaining Interferences. The precise measurement of the isotopic composition of Si using MC-ICPMS is hampered by difficulties originating from the sample matrix, mainly the presence of polyatomic ion interferences.[9,20] Therefore, both chemical and instrumental resolution of interfering elements is an absolute requirement for accurate and precise

(22) Niu, H.; Houk, R. S. *Spectrochim. Acta, Part B* **1996**, *51B*, 779−815.
(23) Ramos, F. C.; Wolff, J. A.; Tollstrup, D. L. *Chem. Geol.* **2004**, *211*, 135−158.

Table 3. List of Potential Interferences on the Si Isotopes[a]

isotope	hydrides	nitrogen based	carbon based	doubly charged ions[b]
^{28}Si		$^{14}N_2^+$ (960)[c]	$^{12}C^{16}O^+$ (1560)[c]	$^{56}Fe^{2+}$ (−2960)
^{29}Si	$^{28}SiH^+$ (3510)[c]	$^{14}N^{15}N^+$ (1090)[c]	$^{12}C^{16}OH^+$ (1100)[c]	$^{58}Fe^{2+}$ (−2940)
		$^{14}N_2H^+$ (770)[c]	$^{12}C^{17}O^+$ (1280)[c]	$^{58}Ni^{2+}$ (−3280)
			$^{13}C^{16}O^+$ (1330)[c]	
^{30}Si	$^{29}SiH^+$ (2840)[c]	$^{12}N^{16}O^+$ (1240)[c]	$^{13}C^{17}O^+$ (1044)	$^{60}Ni^{2+}$ (−3580)
		$^{14}N^{15}NH^+$ (810)[c]		
		$^{14}N^{14}ND^+$ (650)		

[a] The approximate resolution, calculated according to the conventional definition,[13] required for separation from the analyte peak is reported in parentheses. [b] Negative value indicates that the interference appears on the low-mass side of the Si isotope. [c] Visible in the high-resolution mass spectra of Figure 2.

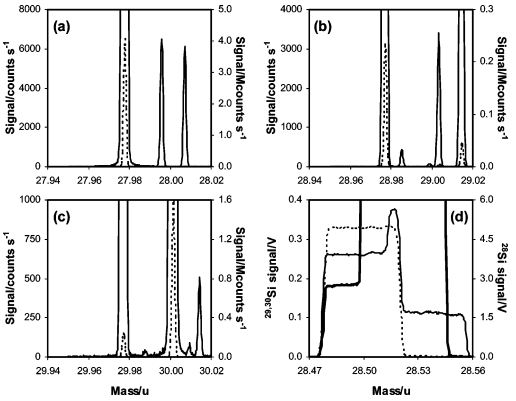

Figure 2. High-resolution mass spectra of m/z (a) 28, (b) 29, and (c) 30 using the working standard solution at a silicon concentration of 1 mg L^{-1} in 1% HNO_3 acquired using the Element2 ICP-SFMS instrument. The solid lines in (a−c) relate to the scale-expanded, left-hand axes, and the dotted spectra to the right-hand axes. Identities of the major polyatomic ions were derived from exact mass measurements and are listed in Table 3. In (d), the flat-topped peaks for ^{28}Si (dotted line), ^{29}Si (solid line), and ^{30}Si (bold line) are shown, together with attendant signal contributions from interfering species on the high-mass sides of the analyte ion plateaus. The mass scan used the working standard at 1 mg L^{-1} Si in 0.5% HNO_3 and was recorded using the Neptune under high-resolution conditions. Note that the abscissa in (d) refers to the mass at the center cup in the Faraday collector array.

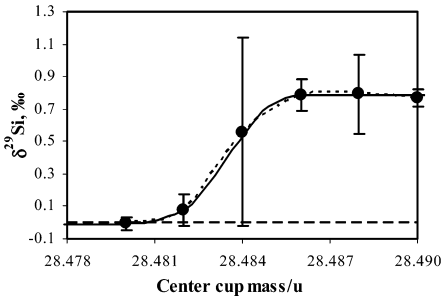

Figure 3. Plateau test for the Neptune MC-ICPMS instrument in high-resolution mode, conducted using center cup mass settings between m/z 28.480 and 28.490 u, revealing the location of the interference-free region for measurement of $^{29}Si^+$. At $m/z > 28.4805$ u, the onset of a second plateau begins to affect the measurement of $^{29}Si^+$. Inspection of the high-resolution spectrum from the Element2 (Figure 2b) suggests that $^{28}SiH^+$ is the source of the second plateau. This was confirmed by using the spectrum from Figure 2b to simulate a mass scan for the Neptune, as depicted by the solid line (see text for details). The data points are measurements made during the plateau test for the Neptune, with associated uncertainty bars drawn at the 2s level. All data have been normalized to $^{29}Si^+$ intensities (lines) or $^{29}Si/^{28}Si$ isotope abundance ratios (data points) corresponding to $m/z = 28.480$, to scale the results in terms of $\delta^{29}Si$; see eq 1.

Si isotope abundance ratio measurements. Potential interferences on the Si isotopes are compiled in Table 3.

High-resolution mass spectra acquired on the Element2 in the m/z regions of 28, 29, and 30 are shown in Figure 2a−c, where several interferences are visible on the high-mass sides of the Si isotopes originating from N-, O-, and C-containing species. These are impossible to remove chemically since they originate from the solvent and entrained atmospheric gases. Since the comparatively minor interferences on $^{28}Si^+$ are attributable to $^{14}N_2^+$ and $^{12}C^{16}O^+$ (Figure 2a), and thus partially derived from entrainment, desolvating nebulizers cannot completely eliminate these potential sources of error in low-resolution instruments.

The spectrum at m/z 29 (Figure 2b) reveals the presence of a nonnegligible isobaric interference on ^{29}Si, which was identified on the basis of its exact mass to originate from $^{28}SiH^+$. The insufficiency of using matrix-matched blanks to correct for spectral interferences becomes particularly evident when dealing with inferences originating from the analyte itself. Preliminary experiments have shown that the level of hydride formation, i.e., the ratio between $^{28}SiH^+$ and $^{28}Si^+$, varies between 6.7×10^{-5} and 15.3×10^{-5} depending on the matrix, type of introduction system, use of the X-cone or standard skimmer, and sample gas flow (data not shown). Despite the minor mass difference between $^{28}SiH^+$ and $^{29}Si^+$ (at 0.0083 u, this constitutes the most demanding of the spectral interferences observed during the course of this work), the high-resolution capabilities of the Neptune are sufficient to perform interference-free determinations, assuming that nickel and iron are chemically removed. The precision and accuracy of the isotope abundance ratio measurement may be substantially deteriorated without instrumental resolution of $^{29}Si^+$ from $^{28}SiH^+$, due to the extensive variations in the level of interference formation.

Figure 3 depicts a more detailed view of the hydride interference in the region of the pure $^{29}Si^+$ plateau. At this juncture, it is relevant to discuss the differences in the calculation of resolution, $R = m/\Delta m$ using single-collector or $R^* = m/\Delta m^*$ using multi-collector mass spectrometers. For the former, Δm is the full width of a peak measured at 5% of the signal maximum. In the case of

multicollector mass spectrometry, Δm^* is defined as the difference between the masses where the analyte intensity is equal to 5 and 95% of the maximum.[13,17] Calculating R^* for both instruments yielded values of 20 000 for the Element2 and 9300 for the Neptune. Using the ratio between these values and the conventional resolution measured for the Element2 of 9300 allows an estimate of $R = 4300$ to be computed for the Neptune. The high-resolution mass spectrum shown in Figure 2b was mathematically converted to $R = 4300$ and subjected to a moving average filter[16] to generate the simulated flat-topped peak included in Figure 3. Clearly, the result of the simulation faithfully reproduces the deviations in the immediate neighborhood of the onset of the $^{28}SiH^+$ interference and serves to confirm the identity of the species responsible for the step in the mass scan recorded using the Neptune. It can also be seen that making measurements on the rising part of the signal (at $m/z = 28.484$ u in Figure 3) is detrimental to precision.

Measured relative deviations in the $^{29}Si/^{28}Si$ ratio vary by up to 0.8‰ as the center cup mass setting is stepped from the region where only $^{29}Si^+$ is collected (the measured ratio was used as the denominator in eq 1) to beyond the point at which $^{28}SiH^+$ also enters the Faraday cup (see Figure 3). Thus, the range of variation during measurements with and without the intensity contribution from the $^{28}SiH^+$ being instrumentally resolved approaches the expected range of fractionation for a variety of sample types.[4−7,10−12,20] Although formation of $^{29}SiH^+$ could also be discerned in high-resolution mass spectra at m/z 30 such as that in Figure 2c, the intensity of the interference was barely significantly separated from the noise (^{29}Si exhibits ∼20 times lower atomic abundance compared to ^{28}Si). The interference arising from the hydride can therefore be confidently considered as negligible during measurement of $^{30}Si^+$.

Extreme difficulties in measuring $^{30}Si/^{28}Si$ isotope abundance ratios by MC-ICPMS instruments, due to the presence of $^{14}N^{16}O^+$ interference at the numerator m/z, have been reported previously.[9,20] The magnitude of the interference (Figure 2c), combined with instability in the level of NO^+ formation in the plasma, severely deteriorates the precision (and, for low-resolution MC-ICPMS instruments, the accuracy as well[9,20]) of the isotope abundance ratio determination. Even using the Neptune, the width of the plateau is somewhat limited due to tailing from the NO^+ interference as apparent from Figure 2d. Despite the huge $^{14}N^{16}O$ ion beam (25 V), the interference-free and largely, though not entirely (as discussed below), tailing-free plateau region for $^{30}Si^+$ exceeds 0.015 u, which makes it possible to achieve high-precision isotope abundance ratio measurements for $^{30}Si/^{28}Si$ with this instrument.

Blank Contribution. The presence of high blank levels may result in an overestimation of the peak intensity and might even alter the resulting isotope abundance ratio in a sample, given that the Si in the blank may be isotopically distinct. Significant silicon contamination may originate from the quartz sample introduction system, reagents, the resin, or the plastic materials. The column's contribution was significantly reduced after one use, resulting in a separation blank of 0.5−0.8 μg of silicon in the elution fraction. Assuming a 300-μg sample load, this corresponds to 0.2−0.3%. Due to the fact that the recovery remained quantitative and that the blank level was significantly reduced after one separation, reutilization of the column is recommended.

Comparison of Separation Approaches. The only element that exhibits elution behavior dependent on the loading form is magnesium. Magnesium behaves like other major elements (Ca, Na, Sr) when it is loaded in 0.025% hydrofluoric acid and elutes quantitatively in the first matrix wash (Milli-Q water) stage. When magnesium was loaded with silicon as $Si(OH)_4$, it was partly retained by the column, most eluting in the matrix wash stage and ∼40% in the matrix elution stage (see Table 2). As previously discussed, quantitative removal of magnesium is a prerequisite for high-precision measurement using the current measurement protocol, both separation approaches fulfilling this goal.

Carbonate-rich waters should preferably be loaded in SiF_6^{2-}(aq) form, to avoid substantial CO_2 (g) formation during the matrix elution stage. Gas formation may deteriorate the chromatographic characteristics and alter the elution times. Controlled formation of CO_2 (g) does not change the position of the silicon-containing fraction and is not a significant problem. If unexpected and extensive formation of gas occurs during the matrix elution stage, it can be countermanded by increasing the volume of eluent by 1−2 mL; if the gas bubbles prevent the eluent flow, it might be necessary to physically press the resin to remove the gas.

Correction for Mass Discrimination. Magnesium, or more specifically the isotope ratio $^{26}Mg/^{25}Mg$, possesses the chemical and physical characteristics required of an internal standard element for on-line mass discrimination correction of Si isotope abundance ratios. Together with the ability to remove magnesium to insignificant impurity levels during the chromatographic isolation of silicon (Figure 1), the facts that the two aforementioned Mg isotopes are virtually interference free, as confirmed by high-resolution mass spectra collected on the Element2, and are present at relatively high abundances (10.00% ^{25}Mg and 11.01% ^{26}Mg),[24] account for the selection as internal standard. Nevertheless, formation of $^{24}MgH^+$ was detectable in the high-resolution mass spectra collected using the Element2 on m/z 25 (data not shown). However, the extent of the hydride formation was on average 10−20 times lower than that of $^{28}SiH^+$. As a consequence, variations in the levels of hydride formation maximally account for deviations in the $^{26}Mg/^{25}Mg$ ratio of ±0.02‰.

To determine the efficiency of the mass discrimination correction of Si isotope abundance ratios using magnesium, isotopic analyses of the Ultra Scientific working standard prepared at varying concentrations or in different matrixes, ranging from 0.05 to 1.00% nitric acid, were conducted. As reference for computation of $\delta^X Si$ values according to eq 1, the same working standard was diluted to a concentration of 5 mg L^{-1} Si in 0.50% nitric acid matrix; all solutions contained 2 mg L^{-1} Mg. As seen in the results of the isotopic analyses presented in Figure 4, measurements of $^{29}Si/^{28}Si$ are fairly tolerant to variations in Si and HNO_3 concentrations over most of the test ranges. The fact that the $\delta^{29}Si$ value exhibits no systematic dependence on the nitric acid concentration demonstrates that complete elimination of N-related interferences by virtue of the use of high-resolution MC-ICPMS is possible, albeit within given limits as may be derived from Figure 4.

(24) De Laeter, J. R.; Böhlke, J. K.; De Bièvre, P.; Hidaka, H.; Peiser, H. S.; Rosman, K. J. R.; Taylor, P. D. P. *Pure Appl. Chem.* **2003**, *75*, 683−800.

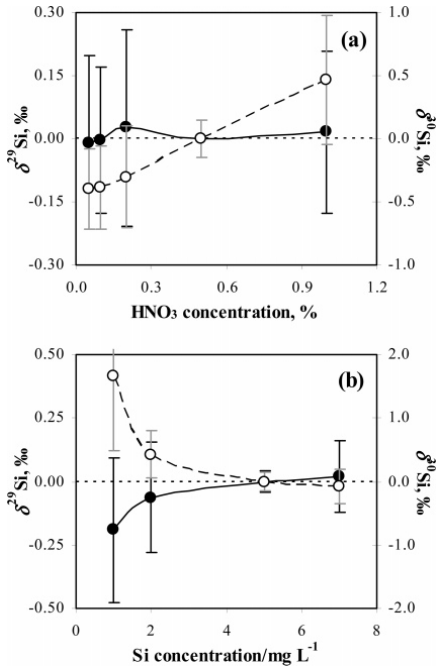

Figure 4. Effects of (a) nitric acid and (b) silicon concentrations on the accuracy of δ^XSi values using Mg for on-line mass-bias correction. Corrected isotope abundance ratios for a solution of 5 mg L^{-1} Si in 0.5% HNO_3 have been utilized as reference values for the computation of δ^XSi values using eq 1. Filled circles with black uncertainty bars (95% confidence intervals) on solid lines plot the data for δ^{29}Si (left-hand axes); open circles with gray uncertainty bars on dashed lines represent δ^{30}Si results.

Table 4. Determined Isotopic Compositions of Selected Samples[a]

sample identification	δ ^{29}Si, ‰	δ ^{30}Si, ‰
working standard	0.70 ± 0.04	1.52 ± 0.22
separated standard	0.71 ± 0.12	1.39 ± 0.32
FIJI Natural Artesian Water	1.34 ± 0.10	2.58 ± 0.13

[a] Normalized using the composition of IRMM-018[19] as reference in eq 1, uncertainty terms expressed as 95% confidence intervals.

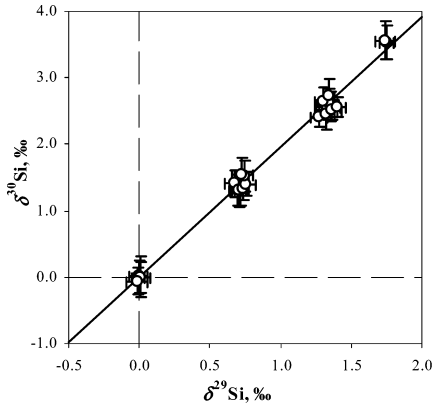

Figure 5. Three-isotope plot of $\delta^{29,30}$Si values (n = 24) graphed according to the relationships proposed by Young et al.[26] Uncertainty bars correspond to 95% confidence limits. Linear regression using weighting of both variables yielded intercept and slope estimates of $a_W = -0.03 \pm 0.11$ and $b_W = 1.96 \pm 0.10$ ($r^2 = 0.9928$), respectively, consistent with a purely mass-dependent process governing fractionation in the samples.

On the contrary, the mass bias corrected $^{30}Si/^{28}Si$ results display pronounced variations across the parameter ranges covered. These results may be interpreted in terms of tailing from the massive $^{14}N^{16}O^+$ interference alluded to above. With increasing nitric acid concentration in the sample matrix (Figure 4a), formation of decomposition products, such as NO^+, will obviously be enhanced. In turn, this leads to greater contributions from $^{14}N^{16}O^+$ tailing at the point on the plateau where the ^{30}Si isotope is monitored (Figure 2d) and, hence, an increase in the calculated δ^{30}Si value when the nitric acid content of the sample exceeds that of the reference solution. Increasing the silicon concentration has the opposite effect, since the relative contribution of the interference to the measured signal becomes attenuated. Thus, a decrease in the calculated δ^{30}Si value would be expected as the silicon concentration increases, which is exactly the pattern seen in Figure 4b. Consequently, it is extremely important to matrix- and concentration-match blanks, samples, and standards with respect to HNO_3 and Si in order to achieve high-quality Si isotope abundance ratios using MC-ICPMS, even when high-resolution measurements can be made, particularly for $^{30}Si/^{28}Si$.

Using an alternative medium, such as HCl, to avoid the difficulties associated with the presence of HNO_3 might be worth pursuing. It must be remembered though, that separation of Si using Dowex 1 × 8 as chromatographic stationary phase necessitates the presence of HNO_3 in the final elution step (Table 2). Variations in acid strength affect the magnitude of mass bias,[25] a problem that would be compounded when trying to match concentrations of both HNO_3 and HCl in a mixture.

Application to the Isotopic Analysis of Si in Natural Water Samples. Although it has already been established that silicon is quantitatively recovered using the developed separation technique, it is prudent to verify that the isotopic composition remains the same. For this reason, isotope abundance ratios were performed on aliquots of a monoelemental solution before (denoted working standard) and after (separated standard) complete preparation according to the protocol presented here. No significant differences were obtained, as seen in Table 4, where our results for FIJI Natural Artesian Water are also specified.

Figure 5 shows a three-isotope plot of the experimentally determined $\delta^{29,30}$Si values constructed using linear regression with weighting of both variables, according to Young et al.[26] The silicon isotope data describe a single mass-dependent fractionation line, demonstrating the robustness of the analytical results. Despite the limited number of samples, the weighted slope (1.96 ± 0.10; 95% confidence interval) is statistically indistinguishable from that

(25) Malinovsky, D.; Stenberg, A.; Rodushkin, I.; Andrén, H.; Ingri, J.; Öhlander, B.; Baxter, D. C. *J. Anal. At. Spectrom.* **2003**, *18*, 687−695.
(26) Young, E. D.; Galy, A.; Nagahara, H. *Geochim. Cosmochim. Acta* **2002**, *66*, 1095−1104.

reported by De La Rocha[9] (1.93) on the basis of a much more extensive data set acquired using laser fluorination and IRMS.[10] It should also be mentioned that the weighted intercept (−0.03 ± 0.11) is within uncertainty of zero, as defined by the assigned composition of IRMM-018, i.e., $\delta^{29}Si = \delta^{30}Si = 0‰$.

The natural water samples exhibited extensive degrees of isotopic variability (Figure 5). Depletion in the lighter isotopes is somewhat expected due to the fractionation during weathering of silicate minerals[11,12] and the enrichment of heavier isotopes in certain plant materials.[7]

CONCLUSION

The proposed chromatographic separation procedure provides quantitative recovery of silicon from natural waters without inducing artificial fractionation (Table 4), and complete removal of potentially interfering matrix components (Figure 1), in a much simpler, safer, and less expensive manner than afforded by fluorination-based methodologies. It must be emphasized that isolation of Si from Fe and Ni is particularly important, even for high-resolution MC-ICPMS measurements, because doubly charged ions would appear at the low-mass sides of the Si ion beams.[17] A further practical advantage of the chromatographic procedure is that the concentration of HF in the Si elution stage is fairly low (0.025%) and further reduced by dilution prior to isotopic analysis. This serves to limit blank levels contributed by the conventional quartz sample introduction system. Additionally, the possibility to adapt the procedure to other sample types is considered to be promising and warrants further study.

Problems associated with spectral interferences (Figure 2) can either be eliminated by chemical purification or by exploiting the high-resolution capabilities of the Neptune MC-ICPMS instrument. However, there is still room for improvement regarding tailing from the abundant $^{14}N^{16}O^+$ interference at the $^{30}Si^+$ plateau. When using conventional solution nebulization, as in the present work, careful matching of the HNO_3 concentration in all standards and samples must be observed, to prevent systematic errors in the $^{30}Si/^{28}Si$ measurement (Figure 4), even when using high resolution. This suggests that a desolvating nebulizer system such as that employed by Cardinal et al.[20] would be beneficial in order to attenuate the major source of the interference, although minor formation would still be expected as a result of air entrainment into the plasma. It should also be mentioned that Cardinal et al.[20] did not detect the $^{28}SiH^+$ interference on $^{29}Si^+$ (Figure 3), although it is unclear whether this resulted from minimization of precursor H-radicals via desolvation or was due to resolution limitations of the mass spectrometer. In either case, it is always beneficial to thoroughly investigate the potential occurrence of spectral interferences during method development for MC-ICPMS using an instrument providing true high-resolution operation, such as the Element2 exploited in this study.

De La Rocha[9] expressed reservations concerning the efficacy of using Mg as an internal standard for mass-bias correction in view of the order of magnitude lower sensitivity for Si on a Nu Plasma MC-ICPMS instrument. Later work by Cardinal et al.[20] using the same type of instrument, and the results of the present study demonstrate that Mg is, in fact, an excellent internal standard element. In combination with the proposed method of sample preparation and utilizing the high-resolution capabilities of the Neptune instrument, it therefore possible to obtain accurate and precise data for all three Si isotopes in water samples by MC-ICPMS (Figure 5).

ACKNOWLEDGMENT

We thank Magnus Land, Stockholm University, for providing IRMM-018 and FIJI Natural Artesian Water. This study was supported by EUs structural fund for Objective 1 Norra Norrland and the Center for Isotope and Trace Element Measurement at Luleå University of Technology. Purchase of the Neptune was made possible by a grant from Kempestiftelsen, and Analytica AB provided technical and financial support. We are also grateful to two anonymous reviewers for constructive comments.

Received for review July 13, 2005. Accepted October 28, 2005.

AC051246V

III

Silicon isotopic composition of boreal forest vegetation in Northern Sweden

Chemical Geology (2007) (submitted)

E. Engström, I. Rodushkin, B. Öhlander, J. Ingri and D. C. Baxter

Silicon isotopic composition of boreal forest vegetation in Northern Sweden

E. Engström [a, *], I. Rodushkin [a, b], B. Öhlander [a], J. Ingri [a] and D. C. Baxter [b]

[a] *Division of Applied Geology, Luleå University of Technology, S-971 87 Luleå, Sweden*

[b] *ALS Laboratory Group, ALS Scandinavia AB, Aurorum 10, S-977 75 Luleå, Sweden*

* Corresponding author. ALS Laboratory Group, ALS Scandinavia AB, Aurorum 10, S-977 75 Luleå, Sweden. Tel: +46 920 289976; fax: +46 920 289940. *E-mail address:* emma.engstrom@alsglobal.com (E. Engström)

Abstract

Thorough characterization of the Si isotopic composition of the terrestrial biogenic pool could potentially allow Si isotope information to be used when assessing the relative contributions from biogenic and mineral sources to soil water, plants and natural waters. In the present study, the Si isotopic compositions of major biomass components in a boreal forest in Northern Sweden were investigated, along with the relative contributions from exogenous Si incorporated in the plant structure. This was achieved using chemical purification and high-resolution multi-collector inductively coupled mass spectrometry (MC-ICPMS) for the precise and accurate determination of the Si isotopic composition of plants. The technique, based on strong-anion exchange chromatography, allows efficient separation of Si from matrix and

interfering elements, while recovering in excess of 99% Si. The long-term instrumental reproducibility, expressed as two standard deviations (2σ), for the isotopic reference material NBS28 (n = 12) was 0.10‰ for δ^{29}Si and 0.25‰ for δ^{30}Si, exceeding 2σ for replicate analyses (including dissolution, separation and isotopic analysis) for plant samples.

Results for the analyses of composite plant samples for the eight most prolific species in the boreal forest yielded a surprisingly homogenous Si isotopic composition, expressed as δ^{29}Si (2σ) and δ^{30}Si (2σ), ranging from (–0.15 ± 0.11)‰ to (0.13 ± 0.06)‰ and (–0.31 ± 0.08)‰ to (0.22 ± 0.13)‰. Isotopic and elemental analyses of local airborne particulate matter suggests that the exogenous Si contribution varies between 0.3 and 73%, indicating that the potential surface contribution must be considered during Si uptake studies. The present study thus provides evidence that thorough appreciation of the forms of Si in plants is an absolute requirement when assessing the plant impact on the Si cycle via the difference in dissolution kinetics for phytoliths and mineral Si.

Keywords: Silicon isotopic composition; Plants; Phytoliths; MC-ICPMS

1. Introduction

Silicon has been proven to increase resistance to abiotic and biotic stress in plants, which has been exploited in the routine application of Si-containing fertilizers to crops (Ma and Yamaji, 2006). Non-ionic dissolved silicic acid is taken up from the soil solution in large amounts by vegetation during the growing season (Alexandre et al., 1997; Derry, 2005; Farmer et al., 2005; Mitani and Ma, 2005; Ma and Yamaji, 2006). Transpiration then concentrates the absorbed silicic acid within the plant until polymerization occurs, forming precipitates of hydrated amorphous silica (opal-A), also known as phytoliths (Ma and Yamaji, 2006). These phytoliths are re-deposited in the soil profile after plant death, and the dissolution of the hydrated amorphous silica returns the silicic acid to the soil solution, where it becomes available for plants once more (Farmer et al., 2005).

The use of vegetal Si isotopic information in the assessment of the relative contributions of Si released from weathering and from dissolution of phytoliths in the soil solution is limited by inhomogeneity in the Si isotopic composition of phytoliths (Basile-Doelsch, 2006). Characterization of the average Si isotopic composition of the biogenic and mineral Si outputs would facilitate determination of their relative impacts on the isotopic signature of the soil solution, assuming that they are initially significantly different. Nevertheless, the number of publications presenting Si isotopic information on plants is still limited (Douthitt, 1982; Ding et al., 2005; Opfergelt et al., 2006*a*, *b*). This might be due to the extensive sample preparation required, consisting of four or more separate steps, for accurate analyses of Si isotopic compositions (Ding et al., 2005; Opfergelt et al., 2006*a*, *b*), combined with the relatively low Si concentrations in terrestrial plants (<0.1% to 10% dry weight), as a result of differences in their capacities to accumulate Si (Ma and Yamaji, 2006).

It should be noted that plants might accumulate silica originating from two different sources. As well as uptake of dissolved silicic acid from the soil solution enriched in heavier isotopes via the root system, surface contamination by exogenous material, partly consisting of Si bearing phases such as SiO_2, silicates and clay minerals (Wyttenbach and Tobler, 1998; Ma and Yamaj, 2006) also occurs, the latter exhibiting average depletion in the heavier isotopes (Ziegler et al., 2005; Basile-Doelsch, 2006). The relative contributions of these sources are dependent on the species, plant part, geographic location, animal disturbance and climatic conditions (Wyttenbach and Tobler, 1998). The Si isotopic composition in plants is therefore a result of the relative mixing between these sources, and the isotopic fractionation during the uptake of silicic acid (Opfergelt et al., 2006*b*).

Existing chemical preparation procedures for silicon isotopic analyses briefly consist of phytolith dissolution following organic matter dissolution (Opfergelt et al., 2006) or fusion (Ding et al., 2005), precipitation of SiO_2 using triethylamine molybdate (Opfergelt et al., 2006) or diluted polyethylene oxide solution (Ding et al., 2005), followed by combustion at 1000 ºC. Conventional methods for phytolith extraction are based on the assumption that there are no silicon losses during organic matter dissolution (Shahack-Gross et al., 1996; Webb and Longstaffe; 2000, Opfergelt et al., 2006) or rinsing of the SiO_2 precipitate (Shahack-Gross et al., 1996; Webb and Longstaffe; 2000; Ding et al., 2005). A chemical purification protocol with no risk of losses of silicon during sample preparation would be advantageous for isotopic analyses of vegetation with low silicon content. Further, a more time- and labour efficient method could potentially increase the interest in performing silicon isotopic analyses of plants.

This study presents the adaptation of an efficient chemical purification procedure, based on anion-exchange chromatography (Engström et al., 2006), to the determination of the Si isotopic

composition of plant and humus samples by high-resolution MC-ICPMS. The method was applied to composite samples of eight different plant species characteristic of a coastal boreal forest in Northern Sweden, as well as humus, in order to survey the Si isotopic composition of the biomass and to provide an estimate of the biogenic Si output.

2. Experimental section

2.1 Sampling site

The plant species have been sampled in the vicinity of a 50-hectare nature reserve in Kalix municipality in Northeast Sweden (Svarthällberget; Lat: N65º 48' 50.80"; Long: E23º 31' 22.11"), comprising a continental promontory with sandy beaches, and located on the coastline of the Bay of Bothnia. The sampling area, 200 m × 50 m, is covered by boreal forest. The region is characterized by bedrock consisting of dolomitic limestone and soil of sandy till with an average grain size of 0.5-1.0 mm (Fromm, 1965), the local till being composed of quartz, feldspar, biotite and amphibole. Further, the area has a well-developed podzol profile and a high permeability due to the large grain size. The bedrock is exposed in the forest area and along the coastline.

2.2 Samples and sampling

Materials from the following species were collected at the end of August 2006; Norway spruce (*Picea abies*), European larch (*Larix decidua*), downy birch (*Betula pubescens*), rowan (*Sorbus aucuparia*), goat willow (*Salix caprea*) and lingonberry (*Vaccinium vitis-idaea*). The collected spruce needles were one-year old parts only. Leaf blades from lyme grass (*Leymus arenarius*) were harvested from the sandy beaches in the spring (May 31) and in the autumn (August 25) of 2006. Additional sampling of step moss (*Hylocomium splendens*) and humus was

performed in the autumn. Sand and brackish water was collected from the beaches along the coastline of the Bay of Bothnia.

Leaves and needles were sampled at a height of approximately 1-2 m above the ground. The number of individuals per species sampled is detailed in Table 3. The humus samples consisted of eight sub-samples per area. Additional sampling of lichens (*Alectoria sarmentosa*) was performed for the purpose of establishing the elemental ratios Si/Al and Si/Ti of the exogenous Si surface contamination.

All the samples were stored in airtight 'zip-lock' plastic bags during transport and storage, after ascertaining that no contamination resulted in this way.

2.3 Reagents

The hydrofluoric (40% HF, Suprapure grade; Merck) and hydrochloric (30% HCl, analytical plus grade; Fluka, Steinhem, Germany) acids, as well as granular NaOH (analytical grade; Merck, Darmstadt, Germany), were used as supplied. The analytical-reagent grade nitric acid (65% HNO_3; Merck) was additionally purified by sub-boiling distillation.

Distilled Milli-Q water (Millipore Milli-Q, Bedford, MA) was used for preparation of all measurement solutions including standards, samples and procedural blanks, and solutions for the separation. The calibration and internal standard solutions were prepared by diluting single-element standards from Ultra Scientific (North Kingstown, U. K.)

Dowex 1×8 strong base anion-exchange resin (Serva Feinbiochemica, Heidelberg, Germany), mesh 100-200, was used for the silicon separation.

Reference material 8546, NBS28 Silica sand, supplied by National Institute of Standards and Technology (NIST; Gaithersburg, MD 20899), was used as standard during the isotopic

measurements (δ^{29}Si and δ^{30}Si). IRMM-018, manufactured by the Institute of Reference Material and Measurement (IRMM; Geel, Belgium), was included in the study for quality assurance during the isotopic analyses.

2.4 Preparation procedure

Brackish water from the Bay of Bothnia was prepared for analysis as described by Engström et al. (2006). For other sample types, a modified procedure was developed, as described below.

2.4.1 Dissolution procedure. All plants were thoroughly washed with deionized water to remove exogenous material from the plant material. The samples were thereafter heated to 50 ºC until dryness, followed by overnight ashing at 550 ºC, and gravimetric determination of the ash content (in %) after the samples had cooled down to room temperature in a dessicator.

The determination of Na, Mg, Al, Si, K and Ca in the biological ashes was performed prior to the final dissolution of the material using HF. Knowledge of the total concentrations of Al and carbonates formed during the ashing procedure at 550°C is necessary for determining the amount of HF required for the final dissolution. The dissolution of biological ashes using HNO_3 and HF is not applicable in the silicon separation procedure described for natural waters (Engström et al., 2006), since the NO_3^- anion exhibits high selectivity during the separation and therefore negatively affects the retention of dissolved Si species during the sample-loading step.

Prior to the determination of the elemental content, the biological ashes were dissolved by adding 1 ml concentrated HNO_3 (sp) and 20 µl HF (sp) acid to approximately 10-20 mg biological ash. The samples were left to react over night at room temperature and were thereafter diluted to 10 ml. For ICP-SFMS analysis, the digests were additionally diluted 10-fold and internal standard (In) was added to a final concentration of 25 µg l^{-1}. All samples and standards

were matrix matched to a HNO_3 concentration of 0.7 M. The elemental concentrations were determined by external calibration combined with internal standardization.

The amount of HF to be added to the samples was calculated using the elemental concentrations of Na, Mg, Al, Si, K and Ca in the biological ashes. Firstly, Na and K carbonates were estimated using the elemental concentrations obtained from the ICP-SFMS analysis. The carbonates will consume stoichiometric amounts of hydrogen ions (H^+) to produce CO_2 (g). If the added amount of H^+ is not sufficient for quantitative transformation the solution will remain neutral, resulting in non-quantitative recovery of silicon. The consumed amount of HF (mol) can be considered as neutralized and therefore not reactive. Secondly, since the insoluble compound AlF_3(s) is formed when Al_2O_3 is treated with HF, the consumption of F^- during its formation must be considered (Greenwood and Earnshaw, 2001). Formation of further insoluble precipitates, consisting of MgF_2 and CaF_2 (K_{sp} = $5.3 \cdot 10^{-9}$ and $3.7 \cdot 10^{-8}$; Petrucci and Harwood, 1997), also consumes F^-.

The molar ratio between F and Si has to be kept above six to ensure formation of soluble SiF_6^{2-}, since losses of silicon as volatile SiF_4(g) might otherwise introduce isotopic fractionation during the dissolution step. In fact it has previously been proposed that the molar ratio F:Si needs to exceed 68.5 to yield quantitative recovery (De La Rocha and Brzezinski, 1996). For this reason, the target molar ratio F:Si has been set to 100 during this study.

The amount of HF (mol) required for the quantitative recovery of silicon during the dissolution of biological ashes is therefore calculated according to:

$$n_{HF} = 2 \cdot n(\Sigma\ Na_2CO_3) + 2 \cdot n(\Sigma\ K_2CO_3) + 3 \cdot n(Al^{3+}) + 2 \cdot n(Ca^{2+}) + 2 \cdot n(Mg^{2+}) + 100 \cdot n(Si) \quad (1)$$

where *n* represents the number of moles of the indicated species. It should be noted that Mg and Ca are also available as carbonates in the samples. However, the amount of H^+ required for the transformation of CO_3^{2-} to CO_2 (g) is equivalent to the consumption (mol) of F^-.

The dissolution was performed by adding 50-200 mg of biological ash and 300 µl Milli-Q to a 10 ml pre-cleaned tube to form a slurry. The calculated amount of HF was then added and the samples left to react for 3-7 days. Silicon is transformed to the divalent SiF_6^{2-} anion during dissolution, which exhibits high selectivity during separation and is therefore quantitatively retained by the column (see following section).

The Si isotopic reference materials IRMM-018 and NBS28, as well as the sand sample, were dissolved using a combination of HNO_3 and HF. The samples were left to react until the silica particles were completely dissolved and thereafter diluted to 10 ml. The time required for complete dissolution of NBS28 was 7-20 days depending on the size of the silica grains, whereas IRMM-018 was ready in less than 24 h.

2.4.2 Silicon separation using anion-exchange chromatography. Anion-exchange columns were prepared by adding approximately 1 g Dowex 1×8 resin, mesh 100-200, between two cotton wool plugs in 5 ml disposable plastic pipette tips. Prior to pre-conditioning using 10 ml freshly prepared 2 M NaOH, the columns were washed with approximately 15 ml Milli-Q. After the addition of NaOH, the columns were rinsed with Milli-Q until the eluent reached a pH-value of ~ 5 (Ali et al., 2004). The digested samples were left to sediment overnight and thereafter diluted to a final Si concentration of 15-400 mg l^{-1} in 20 ml with Milli-Q prior to loading on the anion-exchange columns. The loaded amount of Si therefore varied between 120 and 8000 µg in 20 ml depending on the content of the original plant material.

The matrix was then removed by adding 30 ml Milli-Q water in three portions of 10 ml, and two fractions of 10 ml 95 mM HCl + 23 mM HF, followed by a fraction of 5 ml 23 mM HF. Silicon was eluted with 15 ml 0.14 M HNO_3 + 5.6 mM HF after 10 ml had been allowed to pass through the column. In comparison to the separation scheme for natural waters (Engström et al. 2006), the pre-conditioning and Si elution stages have been modified due to the use of an increased amount of resin.

2.5 Instrumentation

The single-collector, double-focusing, sector field ICP-MS used in this study for determining the elemental concentrations of the plant materials and in the separation fractions was the Element2 (*Thermo Fisher Scientific*, Bremen, Germany). The Element2 was also used for acquiring high-resolution spectra of ^{25}Mg, ^{26}Mg, ^{28}Si, ^{29}Si and ^{30}Si. Typical operating conditions and measurement parameters are given in Table 1.

The silicon isotopic analyses were performed by MC-ICP-MS using the Neptune (*Thermo Fisher Scientific*, Bremen, Germany) in high-resolution mode (Weyer and Schwieters, 2003). A platinum guard electrode (CD-system activated) and Ni skimmer X-cone served to maximize the ion transmission. Instrumental operating conditions and measurement parameters are detailed in Table 2. After igniting the plasma, the instrument was left to stabilize for approximately 2 h before making any measurements. The instrumental sensitivity and resolution were optimized on a daily basis.

Since the mass difference between ^{25}Mg and ^{30}Si slightly exceeds 17%, which is the maximum allowed by the detector array of the Neptune (Weyer and Schwieters, 2003), the isotopic analyses were conducted in multi-dynamic mode, changing the magnet setting between measurement of the Mg and Si isotopes (the cup configurations are presented in Table 2). A

plateau test (Weyer and Schwieters, 2003) of the measured $^{29}Si/^{28}Si$ and $^{30}Si/^{28}Si$ ratios using only the main cup configuration was conducted prior to each measurement session to locate the exact position of the interference-free plateau.

Table 1
ICP-SFMS (Element2) instrumental operating conditions and measurement parameters.

Parameters	
Rf power / W	1400
ICP torch	Fassel torch, 1.5 mm id
Spray chamber	Scott-type (double pass), water cooled
Sampler cone	Nickel 1.1 mm orifice diameter
Skimmer cone	Nickel 0.8 mm orifice diameter
Argon gas flow rates/ l min^{-1}	
Coolant	15
Auxiliary	0.85
Nebulizer	0.80-1.00 (optimized daily)
Multielemental determination	
Scan type	E-scan
No. of scans	9 for each resolution
Isotopes	
Low, medium and high resolution mode	(Engström et al., 2004)
Acquisition window (% of peak width)	50 in LRM; 120 in MRM and HRM
Search window (% of peak width)	50 in LRM; 80 in MRM and HRM
Integration window (% of peak width)	50 in LRM; 60 in MRM and HRM
Acquiring high-resolution spectra	
Isotopes	
High resolution mode	^{24}Mg, ^{25}Mg, ^{26}Mg, ^{28}Si, ^{29}Si and ^{30}Si
Acquisition window (% of peak width)	1000 in HRM

Table 2

Instrumental operating conditions and measurement parameters for multi-collector ICP-MS (Neptune).

Parameters	
Rf power/W	1200
Accelerating voltage/V	-10000
Sampler cone	Nickel 1.1 mm orifice diameter
Skimmer cone	Nickel X-cone 0.8 mm orifice diameter
Spray chamber (tandem arrangement)	Cyclone + Scott type double pass
Nebulizer	Low-flow PFA microconcentric
Sample uptake rate / µl min^{-1}	250
Argon gas flow rates/ l min^{-1}	
Coolant	16
Auxiliary	0.60
Nebulizer	~1.1
Main configuration	
Isotopes (cup)	^{28}Si (L1), ^{29}Si (H1) and ^{30}Si (H2)
Sub configuration	
Isotopes (cup)	^{25}Mg (L2) and ^{26}Mg (C)
Magnet setting / u	28.486-28.491 (centre cup)
Number of integrations	4
Integration time / s	1.049
Number of blocks	5
Number of cycles	5

2.6 Mass spectrometric measurement

The chromatographic elution fractions were analyzed by single-collector ICP-MS (Element2) prior to the isotopic analyses in order to obtain accurate concentrations of Si and Mg, as well as to assure the absence of remaining matrix and interfering elements. Samples and standards were then diluted to a Si concentration of 5 mg l^{-1} before spiking to 5 mg l^{-1} Mg and matrix matching to 0.07 M HNO_3 in the measurement solution. A typical sensitivity of 5 V per mg l^{-1} for ^{28}Si using a conventional solution introduction system during this study is comparable with, or

superior to that obtained using a NuPlasma equipped with a desolvating nebulizer (Cardinal et al., 2003). However, sensitivity of up to 13 V per mg l^{-1} has been reported for the NuPlasma 1700 high-resolution MC-ICP-MS device (Georg et al., 2006). The ^{28}Si blank level was about 80 mV, corresponding to a silicon concentration of approximately 2 μg l^{-1}.

The resulting silicon isotope abundance ratios ^{29}Si/^{28}Si and ^{30}Si/^{28}Si are expressed according to conventional δ-notation using NBS28 as the standard, i.e.

$$\delta^{29}Si = \left[\frac{\left({}^{29}Si/{}^{28}Si \right)_{\text{sample}}}{\left({}^{29}Si/{}^{28}Si \right)_{\text{standard}}} - 1 \right] \cdot 1000\,‰ \qquad (2)$$

$$\delta^{30}Si = \left[\frac{\left({}^{30}Si/{}^{28}Si \right)_{\text{sample}}}{\left({}^{30}Si/{}^{28}Si \right)_{\text{standard}}} - 1 \right] \cdot 1000\,‰ \qquad (3)$$

where the experimental ratios have been corrected for mass bias according to an exponential model using Mg as internal standard (Baxter et al., 2006). Outliers were eliminated at the integration, cycle and block levels using the 2σ criterion in the Neptune software. All Si fractions have been analyzed in duplicate. The instrumental long-term reproducibility, expressed as twice the standard deviation (2σ), for the reference material NBS28 (n = 12) measured on three different days was 0.10‰ for δ^{29}Si and 0.25‰ for δ^{30}Si.

When the amount of material was sufficient, the entire sample preparation procedure, as well as the isotopic analysis, was performed in duplicate in a balanced experimental design (Ramsey, 1998). The average difference in δ^{29}Si between the two replicates, where the complete sample preparation procedure was repeated, was 0.03‰, with minimum and maximum deviations of 0.02 and 0.04‰, respectively. The corresponding values for δ^{30}Si were 0.08‰ (average), 0.03‰ (min) and 0.09‰ (max). It should be noted that the δ^{29}Si-difference between

two replicates is comparable to, or even less than, the instrumental standard deviation. The method reproducibility for δ^{29}Si is at least 3 times improved in comparison to previously reported values of 0.10-0.16‰ for samples exhibiting, in extreme cases, 100 times higher silicon concentrations (Opfergelt et al., 2006*b*). Unfortunately we cannot make a similar comparison of method reproducibility with the results of silicon isotopic analyses of rice plants from the Zhejiang province, China, since no such data were reported (Ding et al., 2005).

Robust analysis of variance (ANOVA) was applied to the data for the six duplicates in order to separate the three components of variability in the data, attributed to the different species, the sub-sampling of the test material in the laboratory, and the instrumental determination. For δ^{29}Si and δ^{30}Si the robust estimates of sub-sampling standard deviation were 0‰ and 0.041‰, respectively. These values were combined with the corresponding standard deviations for duplicate analyses (by summing as variances) to yield estimates of combined measurement uncertainty (Ellison et al., 2000) for results of single digests (see Table 3).

Quality control of the Si isotope data included analyses of IRMM-018 in each session, yielding average δ^{29}Si and δ^{30}Si values of (-0.85 ± 0.07)‰ and (-1.73 ± 0.11)‰, respectively. Results for additional Si isotope reference materials analyzed during the course of this study are reported in Reynolds et al. (2007). A three-isotope plot was also constructed from the mass bias corrected δ-values for all sample data collected according to the method proposed by Young et al. (2002). Linear regression using weighting of both axes resulted in a slope of 1.94 ± 0.05, which encompasses the theoretical slopes calculated for both equilibrium (1.931) and kinetic (1.964) mass dependent fractionation processes. Consequently, the resulting Si isotopic data represent a single mass-dependent fractionation line, demonstrating the robustness of the data, but with insufficient precision to delineate the mechanism.

3. Result and discussion

3.1 Silicon recovery and elution profile

The separation efficiency was evaluated by determining elemental concentrations in eluates from the separation of samples of vegetation, using single-collector ICP-SFMS. The elution profiles for Si and representative matrix elements from step moss (*Hylocomium splendens*) are presented in Fig. 1. It can be seen that the column quantitatively retains Si, purportedly in the form of SiF_6^{2-}, during the sample load stage, and that there are no losses during the matrix wash stages.

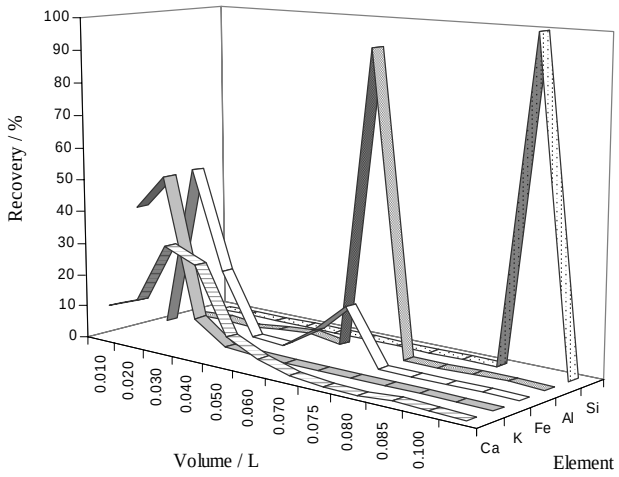

Figure 1 Elution profiles of matrix- and potential interfering elements, as well as Si, during the separation procedure based on anion-exchange chromatography. The separated sample consisted of step moss (*Holycomium splendens*) exhibiting a SiO_2-content of 1.18 % (approximately 7500 μg Si was loaded on the column). The volumes 0-20 ml, 20-50 ml, 50-75 and 85-100 ml represent the sample load stage, MQ wash, matrix wash and Si-containing fraction elution, respectively.

The alkali metals (Na, K, Li and Rb), as well as Cr, Mn and Zn, (all represented by K in Fig. 1) displayed little or no affinity for the resin, whereas the alkaline earths (Sr, Ca, Ba and Mg, represented by Ca) and Al exhibited partial or quantitative retention, respectively, during the sample load stage. These latter elements (alkaline earths and Al) were quantitatively eluted during the matrix wash using a mixture of 95 mM HCl + 23 mM HF. Compared to the elution profiles observed for natural water samples (Engström et al., 2006), fewer elements were found to be retained during the sample load stage. In fact, elements such as Fe, P, Zn and Mn (represented by Fe in Fig. 1) that were quantitatively retained from natural water samples were largely lost during sample loading. It should be noted that Si was the only element present in high concentrations (>mg l^{-1}) in the elution fraction. Furthermore, the method allows efficient separation of silicon hexafluoride and chloride anions, since the latter is eluted in the fraction before silicon.

The average silicon recoveries for the separation and the hydrofluoric acid dissolution were in excess of 99 %, excluding the possibility of induced artificial fractionation during the separation procedure. The capacity of the columns was determined to be 8000 μg Si for the digests of vegetal material, which opens up the possibility to use the developed separation procedure for soil and sediment samples as well. In comparison to methods based on cation-exchange chromatography (Georg et al. 2006), potential matrix effects during the isotopic analyses are minimized, since both anions and cations are removed from the sample matrix as demonstrated by Fig. 1.

High-resolution spectra of ^{28}Si, ^{29}Si and ^{30}Si acquired using ICP-SFMS (not shown) were virtually identical to those obtained using Si working standard solutions (Engström et al., 2006), demonstrating the efficiency of the analyte purification. Nevertheless, instrumental resolution of

the remaining N-, O-, C-, and $^{28}SiH^+$ interferences is still an absolute requirement for achieving accurate and precise determination of the Si isotopic composition. In addition, exact matching of the measurement solution, with respect to matrix and Si concentration, is required due to tailing from $^{14}N^{16}O^+$ at the $^{30}Si^+$ plateau.

The removal efficiency of magnesium (Mg) during the separation of the solutions containing dissolved Si was essentially quantitative, resulting in a residual Mg content of <0.05% in the Si elution fraction. Interference from $^{24}MgH^+$ on $^{25}Mg^+$ is not visible in high-resolution spectra (not even in unseparated ash digests; not shown), verifying the low level of hydride formation expected since the bond dissociation energy of MgH^+ is only 1.94 ± 0.06 eV (Dalleska et al., 1993), whereas that for SiH^+ is 3.23 ± 0.04 eV (Elkind and Armentrout, 1984). Quantitative removal of Mg is of paramount importance given its intended use for internal standardization, having previously been concluded to possess the physical, as well as the chemical properties required of an internal standard for Si isotopic analyses (Cardinal et al., 2003; Engström et al., 2006).

However, it should be noted that Mg contamination of the Si elution fraction has been detected twice during the purification of botanical ashes, most probably originating from partial dissolution of precipitated MgF_2, transferred to the columns in the sample load stage, during the Si elution. It is therefore highly recommended to separate the particulate matter from the dissolved phase by gravitational settling prior to sample loading. For the same reason, re-utilization of the columns should be avoided. It has also been observed that the isotopic composition of silicon in the separated samples is not stable over time and thus it is therefore mandatory to perform the isotopic analyses within four weeks after the separation stage is completed to avoid introducing systematic errors.

3.2 Blank contribution

Assuming that the Si-containing fraction has a volume of 15 ml and that the sample has to be diluted two-fold prior to the analysis to yield a desired concentration of 5 mg l^{-1} Si, then a minimum sample load of 150 μg is required. To avoid loading suspended precipitates of CaF_2, MgF_2 or AlF_3 present in the sample solution, it is recommended to load no more than 9.5 of 10 ml (diluted to 20 ml), resulting in a sample load of approximately 160 μg Si. The blank contribution from the separation procedure has been quantified as 0.5-0.8 μg Si (Engström et al., 2006), and that from the HF dissolution corresponds to approximately 0.5-2.0 μg Si. Assuming that the difference in the Si isotopic composition, δ^{29}Si, between the blank and the sample is equal to 2‰, a blank contribution of 5% imposes a bias of 0.1‰, roughly corresponding to 2σ for replicate analyses of NBS28. Since the blank contribution is actually less than 2% of the minimum amount of Si loaded on the column (160 μg), the resulting method detection limit can be estimated as 0.004-0.017 % SiO_2 in the plant sample on a dry weight basis, assuming 2-10% ash content and dissolution of 200 mg ash. This corresponds to the lowest reported method detection limit for the determination of the Si isotopic composition of plant material. It should be noted that it is possible to reduce the blank contribution significantly by using HF with lower levels of Si impurities if necessary.

3.3 Elemental concentrations in the plant materials

Selected elemental and ash contents of each plant sample are detailed in Table 3. It is interesting to note that the ash content of lyme grass (*Leymus arenarius*) decreased from the spring to the autumn, indicating a high level of mass dilution or in situ leaching during the growing season (Wolterbeek, 2002). The silica concentration varied between 0.03 (*Betula*

pubescens) and 0.6% (*Hylocomium splendens*) in the plant samples, while the humus samples exhibited higher levels of up to 1.53 %, indicating an enrichment of phytoliths or Si-containing primary and secondary minerals in this material. The concentrations of Na and Mg are relatively constant for the studied species, while the concentration of Al exhibits significant variations between the phanerogams and the step moss, indicating high levels of surface contamination in the latter. Furthermore, the calculated concentration of Na in the ash of lyme grass (*Leymus arenarius*) displays an increase of 100% from spring to autumn, indicative of a successive enrichment of sea spray.

Additional sampling of lichens (*Alectoria sarmentosa*) was performed for the purpose of establishing the elemental ratio Si/Al of the exogenous Si surface contaminations or soil dust. Since, unlike vascular plants, lichens do not have a root system, they are dependent on the atmospheric supply of essential nutrients (Loppi et al., 1999). The total amount of Si and Al in lichens therefore originates from soil dust. According to Wyttenbach and Tobler (1998), and Loppi et al. (1999), elements that originate from surface contamination can be identified by positive correlation with terrogenic elements such as Al, Ti and Sc. The total concentration of Al in the biological samples can therefore be used to estimate the terrogenic contribution of Si in plants, using the elemental ratio Si/Al in lichens (Reimann et al., 2001). The results of our calculations of the surface Si contribution (in %), as well as the underlying Si/Al elemental ratios, are presented in Table 3 and discussed below.

Table 3

Determined ash and elemental contents (dry weight), calculated Si/Al elemental ratios and surface contamination contribution, and Si isotopic compositions of plant species

	Norway spruce (*Picea abies*)	European larch (*Larix decidua*)	Downy birch (*Betula pubescens*)	Rowan (*Sorbus aucuparia*)	Goat willow (*Salix caprea*)	Lingonberry (*Vaccinium vitis-idaea*)	Lyme grass (*Leymus arenarius*)		Step moss (*Hylocomium splendens*)	Lichen (*Alectoria sarmentosa*)	Humus horizon
							Spring [b]	Autumn [c]			
n [a]	>5	1	9	>5	4	>200	4	4	-	-	-
Ash content (%)	2.0	5.1	4.9	7.2	8.7	2.9	7.5	3.0	4.1		8.5
Na (mg kg^{-1})	27.6	108	31.6	67.5	191	48.8	218	169	262	-	378
Mg (mg kg^{-1})	437	1790	3700	3080	2110	1420	1540	1640	1420	-	1340
Al (mg kg^{-1})	9.5	71.1	19.7	25.8	25.2	55.9	1.0	7.6	660	-	2050
Si (mg kg^{-1})	258	1843	124	207	204	334	972	1240	2780	-	7140
K (mg kg^{-1})	4910	16300	5890	14500	13200	6280	28800	8340	4860	-	1340
Ca (mg kg^{-1})	1840	1370	9710	12000	19700	5810	1640	2010	4080	-	16800
SiO_2 (%) [d]	0.06	0.40	0.03	0.04	0.04	0.07	0.21	0.27	0.60	-	1.53
SiO_2 (%) [e]	2.81	7.73	0.55	0.62	0.50	2.50	2.80	8.81	14.5	-	17.9
Elemental ratio Si/Al	27.2	25.9	6.3	8.0	8.1	6.0	970	163	4.2	3.1	3.5
Surface contribution (%)	11	12	49	39	38	52	0.3	1.9	74	100	89 [f]
$\delta^{29}Si$ [g]	0.12 (0.01) [h]	0.13 (0.06)	-0.07 (0.04) [h]	-0.01 (0.01)	-0.15 (0.11)	-0.05 (0.03) [h]	-0.05 (0.11) [h]	0.34 (0.08)	-0.08 (0.18)	-0.08 (0.07) [i]	-0.15 (0.05)
$\delta^{30}Si$ [g]	0.20 (0.08) [h]	0.22 (0.13)	-0.22 (0.13) [h]	-0.10 (0.10)	-0.31 (0.08)	-0.18 (0.10) [h]	-0.15 (0.28) [h]	0.56 (0.13)	-0.24 (0.14)	-0.14 (0.13) [i]	-0.27 (0.06)

Footnote Table 3

[a] Number of individuals per species combined in composite sample. [b] Sampled on May 31, 2006. [c] Sampled on August 25, 2006. [d] Silica content reported on dry weight basis (%). [e] Silica content reported on ash basis (%). [f] Estimated non-biogenic Si contribution. [g] Expanded uncertainty calculated using a coverage factor of 2 (Ellison et al., 2000) for duplicate analyses of each of two separately digested and purified aliquots of a single or a composite sample, unless otherwise noted. [h] For duplicate analyses of a single digested and purified aliquot the uncertainty contribution from sampling as estimated by robust ANOVA (Ramsey, 1998) has been factored into the expanded uncertainty calculation. [i] Data for sand.

It should be mentioned that the presence of co-deposits of Al and Si in conifers have been suggested (Hodson and Sangster, 1998, 1999), implying that the estimated surface contribution using Al as normalizing element could be overestimated. However, solid Al was mainly found in the epidermis of the needles, implying that the observed Al could be of exogenous origin. The interactions between Si and Al have attracted substantial interest, since it has been proposed that Si might have a detoxifying effect against Al that has been mobilized during events of acid precipitation (Hodson and Sangster, 1998, 1999). Due to the carbonaceous bedrock in this area, the soil is expected to be well buffered and it is therefore unlikely that Al toxicity will occur (Hodson and Sangster, 1999). Nevertheless, for the purpose of verifying the resulting surface contributions, corresponding calculations were preformed using Ti (Wyttenbach and Tobler, 1998; Reimann et al., 2001), yielding equivalent results ($R^2 = 0.9648$).

3.4 Silicon isotopic composition of boreal forest

Table 3 and Fig. 2 present data for the Si isotopic composition of representative plant species from a boreal forest in Northern Sweden. Correlation detected previously between the silica content and δ^{29}Si, δ^{30}Si in different parts of the same plant (Ding et al., 2005; Opfergelt et al., 2006*a*, *b*) is not reflected between the species included in Fig. 2. Instead, the Si isotopic compositions of the species collected in the forest area are surprisingly homogeneous, with δ^{29}Si (δ^{30}Si) ranging from -0.15‰ (-0.31‰) for goat willow to 0.13‰ (0.22‰) for European larch.

It has been proposed that the accumulated Si in plants originates from the soil solution and from local airborne particulate matter (Wyttenbach and Tobler, 1998; Loppi et al., 1999; Reimann et al., 2001), although previous studies of the Si isotopic composition have focused on the root uptake. Any in situ fractionation during uptake of dissolved silicic acid may be difficult to evaluate due to the existence of particulate matter incorporated in the leaf structure. This

might also appear to be a plausible explanation for the lack of variation in the determined Si isotopic compositions (Table 3).

Since the sampling area consists of a continental promontory with sandy beaches, it is likely that the airborne particulate matter, to a large extent, consists of sand originating from the coastline. For that reason, sand was sampled and analyzed, and the resulting Si isotopic data included in Fig. 2. It is evident that the δ^{29}Si of the sand is similar to the isotopic composition of plant material with potentially high surface contributions from exogenous silica, i.e. *Betula pubescens*, *Salix caprea* and *Hylocomium splendens*. By assuming that the isotopic composition of each plant species results from two-component mixing of incorporated airborne sand with Si taken up from the soil solution, it is possible to recover the uncontaminated biogenic Si signature. The results of these calculations, based on the estimated species-specific surface Si contribution (Table 3), are depicted in Fig. 2. It can be seen that, despite substantial proportions of surface Si contamination on several sample types (Table 3), only the Si isotopic composition of humus appears to be significantly altered, see below.

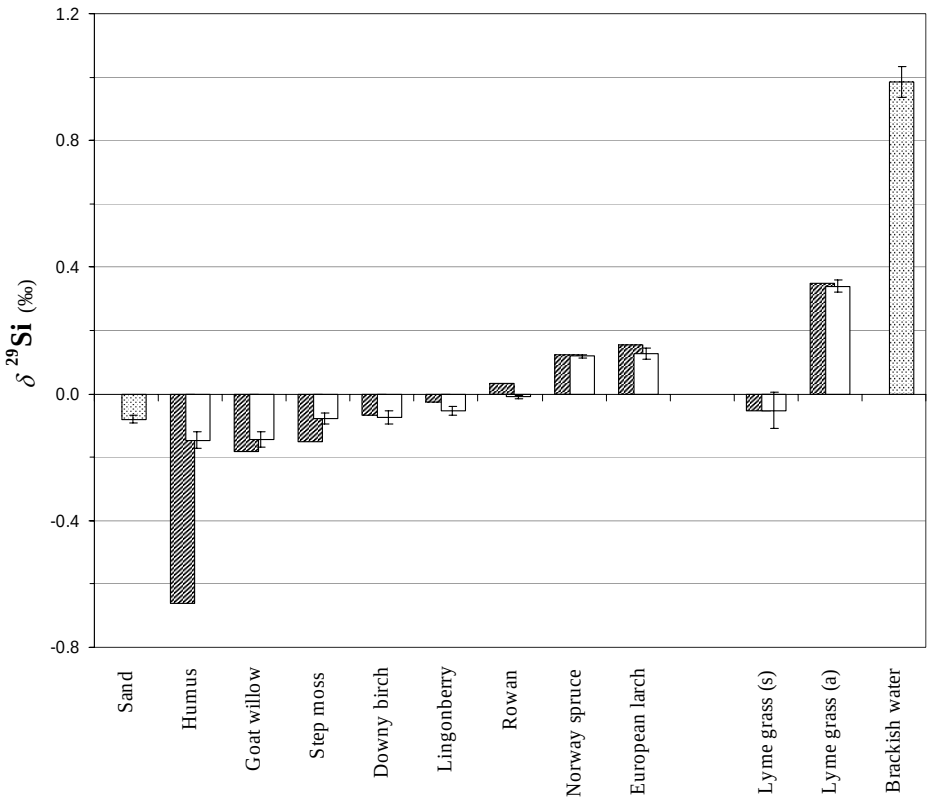

Figure 2 Results of the Si isotopic analyses of plant material and humus from the boreal forest, where the species are arranged according to increasing δ^{29}Si. The uncertainty bars are drawn at the 2σ level, where σ represents either the standard deviation for two measurements on each of two sub-samples, where available, or the sum of the sampling and analytical uncertainty components (see section 2.6). Samples in the latter category are *Vaccinium vitis-idea*, *Betula pubescens*, *Leymus arenarius* (s) and *Picea abies*. Results for samples collected in the spring and autumn are denoted by (s) and (a), respectively. Also shown are δ^{29}Si -values for coastal sand and brackish water (dotted bars). Hatched bars show δ^{29}Si-values recalculated to recover the biogenic component, assuming that the samples have been contaminated with coastal sand (see text for details).

Since leaves of downy birch have a sticky surface for the first weeks of the growing season, and those of goat willow have a constantly hairy surface, higher levels of surface contamination compared to other plant structures are expected. Furthermore, lingonberry leaves have a well-developed wax layer and grow approximately 10-20 cm above the ground, undoubtedly increasing the potential for accumulating exogenous material on leaf surfaces. In fact, the isotopic compositions of the leaf structures with high levels of surface Si contributions are, indeed, very similar to the sand sample included in the study, while those of needles are isotopically heavier, reflecting the greater impact of depletion of ^{28}Si in the available silicic acid in the soil solution in comparison to the surface contribution. The estimated high levels of surface contribution indicate that speciation of Si in plants is required in the assessment of the relative contributions of biogenic and mineral Si in the secondary silicon pool, since the dissolution kinetics are different for phytoliths and the exogenous material incorporated in the leaf structure.

The isotopic signature of the humus layer, consisting of partly decomposed biological material, should theoretically exhibit a Si isotopic composition representing the average biomass, assuming that in situ leaching of silicic acid does not induce fractionation. However, as is often the case, the humus layer contains inorganic particles, which most probably dominate the Si isotopic composition. This is confirmed by the high concentration of Al in this horizon, since the average plant-to-soil concentration ratio is very low (Wyttenbach and Tobler, 1998). The total content of Si in the humus layer is most probably the result of mixing between plant phytoliths and Si containing primary and secondary minerals, rather than sand. Therefore the calculated composition of biogenic Si in humus is likely erroneous (see Fig. 2), being incorrectly based on the assumption that the surface contribution is entirely from coastal sand.

It is interesting to note that the Si isotopic composition of lyme grass (*Leymus arenarius*) significantly varies between the spring and the autumn, indicating that the sampling time is of the utmost importance. A potential explanation for this phenomenon might be that this plant species grows in the sandy borders between the forest and the sea, and that the bioavailable dissolved silicic acid in July and August is mainly of marine origin and thus exhibits enrichment in the heavier isotopes (De La Rocha et al., 1998), as reflected in the data for brackish water in Fig. 2. Since the snow melts in May-June, the soil profile is over-saturated with melted snow during this period, resulting in an increased water pressure from the forest area reducing the level of brackish water accessible to the lyme grass. The silicic acid available to the lyme grass and the forest vegetation is therefore most probably of the same origin in May, which is shown by the similar isotopic compositions.

The Si isotopic composition of brackish water in the Bay of Bothnia is assumed to exhibit temporal variations, due to the seasonal utilization of dissolved silicic acid by diatoms, as well as seasonal variations in the Si isotopic composition of river water (Georg et al., 2006). Since diatoms preferentially take up ^{28}Si (De La Rocha et al., 2000), the δ-values of the dissolved phase are expected to increase during spring and summer. Moreover, lyme grass has leaf blades with distinct prominent adaxial ribs, the specific surface area corresponding to approximately five times the measurable leaf area. This increases the risk of a pronounced Si contribution from surface contamination consisting of sea spray, as verified by the increased concentration of Na in the autumn sampling (Table 3), exhibiting enrichment of the heavier isotopes. Preliminary data for the δ^{29}Si of the local brackish water have been added to Fig. 2 for reference. Further, the isotopic differences between the pseudostem, young midribs and petioles of banana and the

source, reported by Opfergelt et al. (2006), are comparable to the difference between the isotopic composition in the local brackish water and the leaf blades of autumnal lyme grass.

The plants included in this study can be considered to be representative biomass for a boreal forest in Northern Sweden, allowing estimation of the silicon isotopic composition of the biological output, which potentially can be used for assessing the relative contributions from biogenic and mineralogenic silicon in the soil solution, plants and natural waters. The plant parts represent the biological matter accumulated in the humus horizon during the autumn litter fall, and therefore the biogenic output. The relative proportions of plant species in Northeast Sweden vary depending on the geographic co-ordinates, altitude and geology. Isotopic analyses of the biological materials yielded a surprisingly homogeneous silicon isotopic composition, expressed as δ^{29}Si (2σ) and δ^{30}Si (2σ), ranging from (–0.15 ± 0.11)‰ to (0.13 ± 0.06)‰ and (–0.31 ± 0.08)‰ to (0.22 ± 0.13)‰.

4. Conclusion

Previous studies of the Si isotopic composition of plant materials (Ding et al., 2005; Opfergelt et al., 2006*a*, *b*) have been focused on the Si uptake mechanism, and therefore only include one plant species, which eliminates the possibility to investigate the homogeneity of the biological Si pool. The present study, including plant material encompassing the bulk of the biomass in a boreal forest in Northern Sweden, reveals relatively homogenous δ-values, ranging from –0.15 to 0.13‰ per u. Leaf blades of lyme grass (*Leymus arenarius*) collected in the sandy border between the forest area and the brackish water of the Bay of Bothnia exhibited δ^{29}Si values ranging from (–0.05 ± 0.10)‰ in the spring to (0.34 ± 0.04)‰ in the autumn, possibly indicating preferential enrichment of the heavier isotopes during the growing season or a shift in the source of the assimilated Si. The present study also indicates that the presence of Si

containing exogenous material on the surface of vegetation must be considered during uptake studies. Thus the isotopic composition of plant material from Northern Sweden is determined by that of the available dissolved silicic acid, fractionation during root uptake and the existence and isotopic signature of surface contamination.

Acknowledgements

We would like to thank Dieke Sörlin, Frauke Ecke and Tommy Sörlin for fruitful discussions. This study was supported by EU's structural fund for Objective 1 Norra Norrland and the Centre for Isotope and Trace Element Measurement at Luleå University of Technology. Purchase of the Neptune was facilitated by a grant from Kempestiftelsen. The staff of ALS Scandinavia AB is gratefully acknowledged for technical support.

References

Alexandre, A., Meunier, J.-D., Colin, F., Koud, J.-M., 1997. Plant impact on the biogeochemical cycle of silicon and related weathering processes. Geochim. Cosmochim. Acta 61, 677-682.

Ali, M.B.S., Hamrouni, B., Bouguecha, S., Dhahbi, M., 2004. Silica removal using ion-exchange. Desalination 167, 273-279.

Basile-Doelsch, I., 2006. Si stable isotopes in the Earth´s surface: A review. J. Geochem. Explor 88, 252-256.

Baxter, D.C., Rodushkin, I., Engström, E., Malinovsky, D., 2006. Revised exponential model for mass bias correction using an internal standard for isotope abundance ratio measurements by multi-collector inductively coupled plasma mass spectrometry. J. Anal. At. Spectrom. 21, 427-430.

Cardinal, D., Alleman, L.Y., De Jong, J., Ziegler, K., André, L., 2003. Isotopic composition of silicon measured by multicollector plasma source mass spectrometry in dry plasma mode. J. Anal. At. Spectrom. 18, 213-218.

Dalleska, N.F., Crellin, K.C., Armentrout, P.B., 1993. Reactions of alkaline earth ions with H_2, D_2 and HD. J. Phys. Chem. 97, 3123-3128.

De La Rocha, C.L., Brzezinski, M.A., 1996. Purification, recovery and laser-driven fluorination of silicon from dissolved and particulate silica for the measurement of natural stable isotope abundances. Anal. Chem. 68, 3746-3750.

De La Rocha, C.L., Brzezinski, M.A., DeNiro, M.J., Shemesh, A., 1998. Silicon-isotope composition as an indicator of past oceanic change. Nature 395, 680-683.

De La Rocha, C.L., Brezezinski, M.A., DeNiro, M.J., 2000. A first look at the distribution of the stable isotopes of silicon in natural waters. Geochim. Cosmochim. Acta 64, 2467-2477.

Derry, L.A., Kurtz, A.C., Ziegler, K., Chadwick, O.A., 2005. Biological control of terrestrial silica cycling and export to watersheds. Nature 433, 728-730.

Ding, T.P., Ma, G.R., Shui, M.X., Wan, D.F., Li, R.H., 2005. Silicon isotope study on rice plants from the Zhejiang province, China. Chem. Geol. 218, 41-50.

Douthitt, C.B., 1982. The geochemistry of the stable isotopes of silicon. Geochim. Cosmochim. Acta 46, 1449-1458.

Elkind, J.L., Armentrout, P.B., 1984. Threshold behaviour for chemical reactions: Line-of-centers cross section for $Si+(^2P) + H_2 \rightarrow Si + H$. J Phys. Chem. 88, 5454-5456.

Ellison, S.L.R., Rosslein, M., Williams, A., 2000. Quantifying uncertainty in analytical measurement, 2nd edition. EURACHEM/CITAC Guide number 4, QUAM2000-1. http://www.eurachem.org/guides/QUAM2000-1.pdf (August 24, 2007).

Engström, E., Stenberg, A., Senioukh, S., Edelbro, R., Baxter, D.C., Rodushkin, I., 2004. Multi-elemental characterization of soft biological tissues by inductively coupled plasma-sector field mass spectrometry. Anal. Chim. Acta 521, 123-135.

Engström, E., Rodushkin, I., Baxter, D.C., Öhlander, B., 2006. Chromatographic purification for the determination of dissolved silicon isotopic compositions in natural waters by high-resolution multicollector inductively coupled plasma mass spectrometry. Anal. Chem. 78, 250-257.

Farmer, V.C., Delbos, E., Miller, J.D., 2005. The role of phytolith formation and dissolution in controlling concentrations of silica in soil solutions and streams. Geoderma 127, 71-79.

Fromm, E., 1961. Beskrivning av jordartskartan over norrbotten län, nedanför lappmarksgränsen. SGU Serie CA 39, (in Swedish with English summary).

Georg, R.B., Reynolds, B.C., Frank, M., Halliday, A.N., 2006. New sample preparation technique for the determination of Si isotopic compositions using MC-ICPMS. Chem. Geol. 235, 95-104.

Georg, R.B., Reynolds, B.C., Frank, M., Halliday, A.N., 2006. Mechanisms controlling the silicon isotopic composition of river water. Earth Planet. Sci. Letter 249, 290-306.

Greenwood, N.N., Earnshaw, A., 2001. Chemistry of the elements, 2nd edition, Reed Educational and Professional Publishing Ltd, Oxford. pp. 233-234.

Hodson, M.J., Sangster A.G., 1998. Mineral deposition in the needles of white spruce [*Picea glauca* (Moench.) Voss]. Ann. Bot. 82, 375-385.

Hodson, M.J., Sangster A.G., 1999. Aluminium/silicon interactions in conifers. J. Inorg. Biochem. 76, 89-98.

Loppi, S., Pirintsos, S.A., De Dominicis, V., 1999. Soil contribution to the elemental composition of epiphytic lichens (Tuscant, Central Italy). Environ. Monit. Assessm. 58, 121-131.

Ma, J.F., Yamaji, N., 2006. Silicon uptake and accumulation in higher plants. Trends Plant Sci. 11, 392-397.

Mitani, N., Ma, J.F., 2005. Uptake system of silicon in different plant species. J. Exp. Bot. 56, 1255-1261.

Opfergelt, S., Cardinal, D., Henriet, C., André, L., Delavaux, B., 2006 *a*. Silicon isotope fractionation between plant parts in banana: In situ vs. in vitro. J. Geochem. Explor. 88, 224-227.

Opfergelt, S., Cardinal, D., Henriet, C., Draye, X., André, L., Delvaux, B., 2006 *b*. Silicon isotopic fractionation by banana (Musa spp.) grown in a continuous nutrient flow device. Plant Soil 285, 333-345.

Petrucci, R.H., Harwood, W.S., 1997. General chemistry, Principles and Modern Applications, 7th edition, Prentice Hall, Inc, New Jersey, p. A26.

Ramsey, M.H., 1998. Sampling as a source of measurement uncertainty: techniques for quantification and comparison with analytical sources. J. Anal. At. Spectrom. 13, 97-104.

Reimann, C., Koller, F., Frengstad, B., Kashulina, G., Niskavaara, H., Engmaier, P., 2001. Comparison of the element conposition in several plant species and their substrate from a 1 500 000-km^2 area in Northern Europe. Sci. Tot. Environ. 278, 87-112.

Reynolds, B.C., Aggarwal, J., André, L., Baxter, D., Beucher, C., Brzezinski, M.A., Engström, E., Georg, B., Land, M., Leng, M.J., Opfergelt, S., Rodushkin, I., Sloane, H.J., van den Boorn, S.H.J.M., Vroon, P.Z., Cardinal, D., 2007. An inter-laboratory comparison of Si isotope reference materials. J. Anal. At. Spectrom. 22, 561-568.

Shahack-Gross, R., Shemesh, A., Yakir, D., Weiner, S., 1996. Oxygen isotopic composition of opaline phytoliths: Potential for terrestrial climatic reconstruction. Geochim. Cosmochim. Acta 60, 3949-3953.

Webb, E.A., Longstaffe, F.J., 2000. The oxygen isotopic compositions of silica phytoliths and plant water in grasses: Implication for the study of paleoclimate. Geochim. Cosmochim. Acta 64, 767-780.

Weyer, S., Schwieters, J.B., 2003. High precision Fe isotope measurements with high mass resolution MC-ICPMS. Int. J. Mass Spectrom. 226, 355-368.

Wolterbeek, B., 2002. Biomonitoring of trace element air pollution: Principles, possibilities and perspectives. Environ. Pollut. 120, 11-21.

Wyttenbach A., Tobler, L., 1998. Effect of surface contamination on results of plant analysis. Commun. Soil Sci. Plant Anal. 29, 809-823.

Young, D.E., Galy, A., Nagahara, H., 2002. Kinetic and equilibrium mass dependent isotope fractionation laws in nature and their geochemical and cosmochemical significance. Geochim. Cosmochim. Acta 66, 1095-1104.

Ziegler, K., Chadwick, O., Brzezinski, M.A., Kelly, E.F., 2005. Natural variations of $\delta\ ^{30}Si$ ratios during progressive basalt weathering. Geochim. Cosmochim. Acta 69, 4597-4610.